ADENOSINERGIC MODULATION OF HIPPOCAMPAL GAMMA OSCILLATIONS: FROM SINGLE CELL TO WHOLE ANIMAL

By

Alexander Nicolaas Johannes Pietersen

A thesis submitted to

The University of Birmingham

for the degree of

DOCTOR OF PHILOSOPHY

Neuronal Networks

School of Clinical and Experimental Medicine

College of Medicine and Dental Sciences

University of Birmingham

March 2010

UNIVERSITY OF BIRMINGHAM

University of Birmingham Research Archive

e-theses repository

ABSTRACT.

Gamma oscillations, synchronous network activity between 30 and 100 Hz, have been linked to higher cognitive functions. Adenosine receptor modulation has been shown to alter cognitive function in animals and humans. In this thesis the effects of adenosine receptor modulation on *in* vitro and *in vivo* hippocampal gamma oscillations were investigated as well as the underlying mechanisms.

A_1-receptor activation selectively decreased gamma oscillations while blocking A_1-receptors and activating A_{2A}-receptors increased gamma oscillations. Increasing endogenous adenosine levels suppressed gamma oscillations while decreasing endogenous adenosine levels facilitated gamma oscillations *in vitro*. Sharp electrode current clamp and whole-cell voltage clamp experiments showed that A_1-receptor activation hyperpolarised resting membrane potential, reduced firing rate and EPSP amplitude and shifted the IPSC reversal potential to more negative potentials. Blocking A_1-receptors increased pyramidal cell excitability and increased excitatory synaptic transmission. The results *in vivo* were more ambiguous but A_1-receptor activation decreased power in all frequency bands indicating that adenosine receptors can modulate hippocampal gamma oscillations *in vivo*. A_1-receptor blockage had no consistent effect on *in vivo* hippocampal gamma oscillations.

Adenosine receptors modulate gamma oscillations in rodent hippocampal slices but are difficult targets for developing treatments that have cognitive benefits because of their ambiguous effects *in vivo*.

ACKNOWLEDGEMENTS

TABLE OF CONTENTS

LIST OF ILLUSTRATIONS

Chapter 1: Introduction

Chapter 2: Modulation of gamma oscillations through adenosine receptors

Chapter 3: Endogenous adenosine levels modulate gamma oscillations

Chapter 4: Adenosine receptor modulation of cellular and synaptic

        properties

Chapter 5: Adenosine receptor modulation of mono-synaptic IPSCs

Chapter 6: Adenosinergic modulation of hippocampal gamma oscillations

       in vivo

LIST OF TABLES

Chapter 5: Adenosine receptor modulation of mono-synaptic IPSCs

Chapter 6: Adenosinergic modulation of hippocampal gamma oscillations

   in vivo

LIST OF ABBREVIATIONS

5'-AMP	- 5'-adenosine monophosphate
5-IT	- 5-iodotubericidin
8-CPT	- 8-cyclopentyl-1,3-dimethylxanthine
AC	- adenylyl cyclase
aCSF	- artificial cerebrospinal fluid
ADA	- adenosine deaminase
ADP	- adenosine diphosphate
AHP_{angle}	- slow afterhyperpolarisation fitted angle
AHP_{amp}	- slow afterhyperpolarisation amplitude
AHP_{max}	- maximum slow afterhyperpolarisation amplitude
AHP_{slow}	- slow afterhyperpolarisation
AHP_{tau}	- slow afterhyperpolarisation time constant
AMP	- adenosine monophosphate
$AP_{slope\ down}$	- action potential downward slope
$AP_{slope\ up}$	- action potential upward slope
AP_{thres}	- action potential firing threshold
ATP	- adenosine triphosphate
CA	- Cornu Ammonis
cAMP	- cyclic adenosine monophosphate
CCH	- carbachol
C_m	- membrane capacitance
CPA	- N^6-Cyclopentyladenosine
DG	- dentate gyrus
ENT-1	- equilibrative nucleoside transporter 1

EPSP	- excitatory postsynaptic potential
$EPSP_{max}$	- maximum fitted EPSP upward slope
$EPSP_{slope\ up}$	- EPSP upward slope
ES_{50}	- stimulus strength at half maximum
GABA	- gamma-aminubutyric acid
GIRK channel	- G-protein Inward Rectifying K^+-channel
I	- current
I_h	- hyperpolarisation-activated cation current
i.p.	- intraperitoneal
IPSC	- inhibitory postsynaptic current
$IPSC_{max}$	- fitted maximum IPSC amplitude
IPSP	- inhibitory postsynaptic potential
$IPSP_{max}$	- maximum fitted IPSP amplitude
I_h	- hyperpolarisation-activated cation current
KA	- kainate
LTD	- long-term depression
LTP	- long-term potentiation
NBTI	- S-(4-nitrobenzyl)-6-thioinosine
PDE	- cAMP phosphodiesterase
R	- resistance
SAH	- S-adenosyl homocysteine
SLM	- stratum lacunosum moleculare
SO	- stratum oriens
SP	- stratum pyramidale
SR	- stratum radatum
Tau_m	- membrane time constant

V   - voltage

V_m - resting membrane potential

tau_m - membrane time constant

CHAPTER 1: INTRODUCTION.

1.1. Caffeine and cognition.

Caffeine is the world's most widely used psychoactive substance, but unlike most other psychoactive substances caffeine is legal and readily available. Caffeine is present in a variety of foods people ingest every day, like coffee, tea, energy drinks and chocolate. Caffeine is best known for its stimulatory effects and warding off drowsiness and restoring alertness. At concentrations associated with normal coffee consumption (1-10 µM) caffeine increases cortical activation and sensory information processing (Fredholm et al., 1999). At concentration reached during normal coffee consumption, caffeine is a non-specific adenosine receptor antagonist. Blocking adenosine receptors has been shown to enhance cognitive function and skill performance during football (Foskett et al., 2009), increase memory retention through blockage of A_{2A}-receptors (Kopf et al., 1999), facilitate memory through A_1-receptors in the posterior cingulate cortex (Pereira et al., 2002) and prevent memory impairment after a convulsive episode in early life (Cognato et al., 2010). Caffeine has also been shown to alter dopaminergic transmission and locomotor behaviour in laboratory animals, positively affect mood in humans, change sleep patterns in laboratory animals and humans, and increase activity in neocortical areas and the hippocampus in laboratory animals and humans. For a review of all the effects see (Fredholm et al., 1999). The cognitive benefits of caffeine are more pronounced in aged humans (Ryan et al., 2002).

1.2. Age-induced cognitive changes and synaptic plasticity.

Physiological ageing is associated with changes in the brain. A well described effect of the ageing brain is the appearance of memory deficits often involving the hippocampus (Lynch, 2004;Rosenzweig and Barnes, 2003). Older mammals have particular trouble with spatial information processing (Bach et al., 1999;Lynch, 2004;Rosenzweig and Barnes, 2003). The decreased performance of aged mammals is most likely not due to general cell loss in the hippocampus (Rasmussen et al., 1996). Thus more subtle neuronal and network changes are likely to be responsible for age-induced memory deficits. Memory formation in the brain almost certainly involves some form of synaptic modification. The two main processes by which memory is thought be formed are long-term potentiation (LTP) and long-term depression (LTD). For a review on how LTP and memory are linked see Lynch, 2004. With ageing there is not a total loss of LTP but rather a reduction in LTP when low-intensity protocols are used (Rosenzweig and Barnes, 2003). At the same time aged rats have a lower threshold for induction of LTD (Rosenzweig and Barnes, 2003). Taking both findings together it seems that aged rats have an increased threshold for LTP making it more difficult to encode a memory. At the same time aged rats' decreased threshold for LTD could potentially make it easier to erase a memory (Rosenzweig and Barnes, 2003). There is a negative correlation between the performance of animals in spatial learning tasks and the amount of LTP that could be induced *in vitro* in slices made from the same animal (Bach et al., 1999). One of the ways to increase the performance of aged animals in memory tasks is treatment with the cyclic adenosine monophosphate (cAMP) phosphodiesterase inhibitor rolipram. This suggests that a decrease in cAMP and/or cAMP induced signalling is one of the mechanisms contributing to the age-related change in memory processes (Lynch, 2004). Most likely one of the main reasons aged mammals show cognitive decline is change in network connectivity and function. In the hippocampus there is not a loss of cells but a change in the amount of

functional synapses each axon makes (Rosenzweig and Barnes, 2003). Aged animals have reduced network function possibly affecting cognition (Vreugdenhil and Toescu, 2005).

Aged animals show an increase in endogenous adenosine levels that tonically activate adenosine receptors (Sebastiao et al., 2000). This increase is most likely a result of altered localised synaptic modification of extracellular adenosine metabolism (Cunha, 2001;Sebastiao et al., 2000). Increased adenosine A_1-receptor activation through elevated ambient adenosine levels will suppress neuronal activity and decrease the efficiency of synaptic transmission. Adenosine is considered a suppressor of neuronal activity (Dunwiddie and Masino, 2001). Adenosine A_1-receptor activation has been negatively linked to cognitive performance in rodent models (Corodimas and Tomita, 2001;Fredholm et al., 1999;Von Lubitz et al., 1993). Adenosine A_1-receptor activation reduces cAMP levels through inhibiting adenylyl cyclase (AC) activity (Fredholm et al., 2001). This indicates that the age-related reduction in cAMP levels could partly be due to increased adenosine A_1-receptor activation through increased ambient adenosine levels. This would fit well with the increased beneficial effect caffeine has on cognition in aged humans (Ryan et al., 2002).

1.3. Regulation of adenosine levels in the brain.

Adenosine is considered a neuronal activity suppressant substance and the adenosine levels in the brain are tightly regulated. The ambient adenosine levels in the rat brain are estimated to be around 40 nM in the extracellular space with elevation up to 460 nM (Ballarin et al., 1991). In hippocampal brain slices the ambient adenosine levels fall within the physiological range between 140 and 200 nM (Dunwiddie and Diao, 1994).

1.3.1. Adenosine sources.

Adenosine can reach the extracellular space through two main mechanisms: formation through dephosphorylation of adenine nucleotides by ecto-nucleotidases, and release from the intracellular space through (equilibrium) transporters (see Figure 1.1). Virtually any adenine nucleotide can be dephosphorolated to 5'-adenosine monophosphate (5'-AMP) by ecto-nucleotidases, ecto-phosphodiesterases and apyrases. Subsequently 5'-AMP is dephysphorelated by 5'-nucleotidase to adenosine. The ecto-enzymes involved in converting adenine nucleotides to adenosine are widespread throughout the brain and have a broad specificity (Dunwiddie and Masino, 2001). The process of converting adenine nucleotides to adenosine is generally rapid and takes less than a second (Dunwiddie et al., 1997). There are many mechanisms by which adenine nucleotides are released into the extracellular space. One of such mechanisms is the co-release of adenosine triphosphate (ATP) with neurotransmitters, like acetylcholine, dopamine, serotonine and norepinephrine. The second mechanism by which adenosine can reach the extracellular space is by facilitated diffusion through equilibrium transporters (see Figure 1.1). In the brain the main transporter adenosine flows through in the equilibrative nucleoside transporter 1 (ENT-1) (Cunha, 2001;Latini and Pedata, 2001). The ENT1 is widespread throughout the rat brain but has a relatively high density in the hippocampal region (Guillen-Gomez et al., 2004). These transporters are passive and equilibrate the adenosine concentration across cellular membranes. Due to the relatively high activity of the intracellularly located adenosine kinase the flow of adenosine is usually inwards. Adenosine can be formed intracellularly from adenosine monophosphate (AMP) by cytosolic 5'-nucleotidase (see Figure 1.1). Under normal physiological conditions basal cytosolic AMP concentrations (0.1-0.5 mM) are not high enough to serve as a substrate for 5'-nucleotidase (K_m 1-14 mM) (Latini and Pedata, 2001). The intracellular concentration of adenosine triphosphate (ATP) is about 50 times

higher than AMP. A small change in ATP catabolism can therefore induce a large increase in AMP concentration, which is then converted into adenosine.
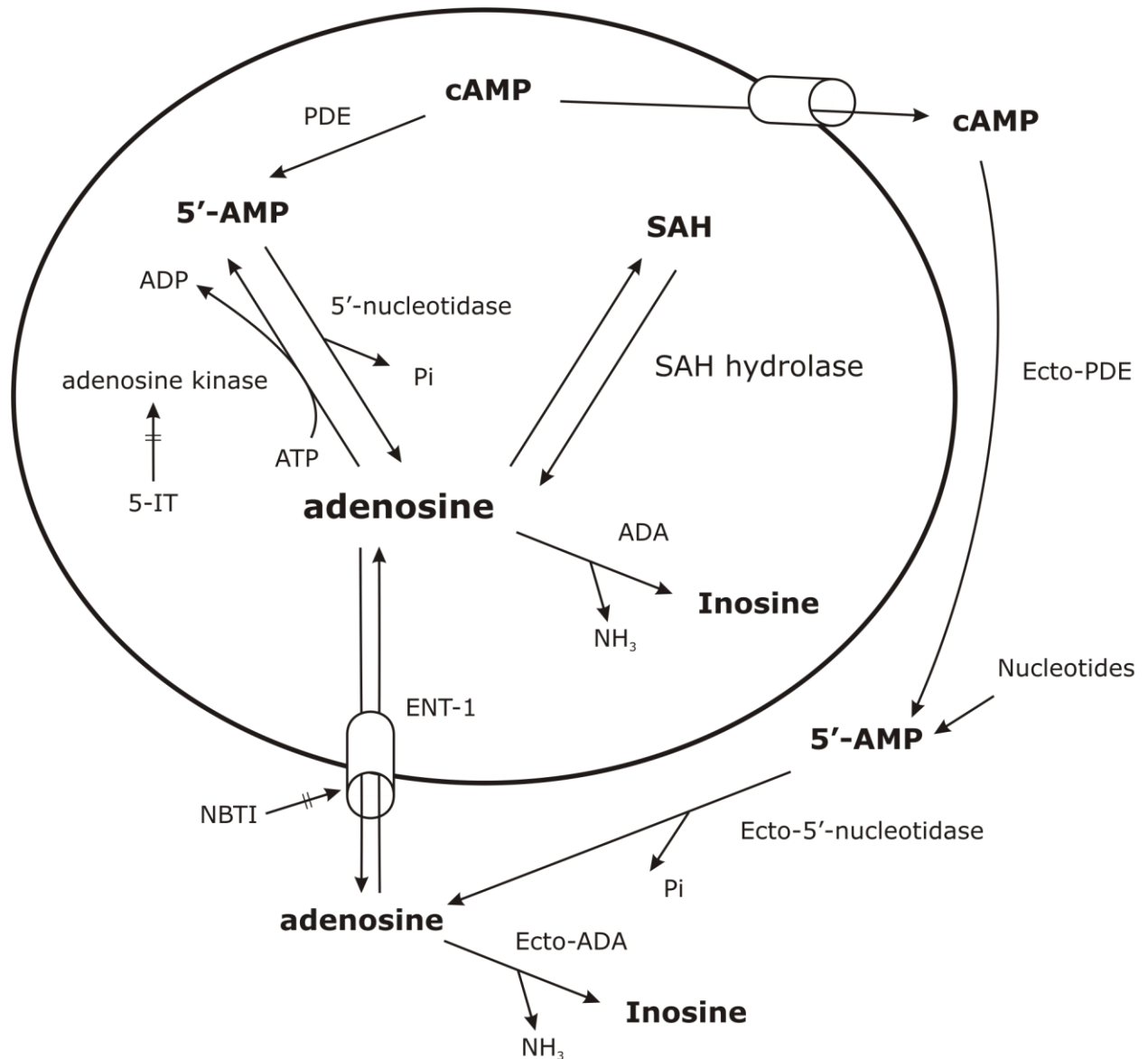
Figure 1.1. Overview of the most important pathways of adenosine production and metabolism. Adenosine kinase is the most active enzyme in metabolizing adenosine. Adenosine can be formed intra- and extracellular by 5'-nucleotidases. Two inhibitors are indicated that are used in this thesis (see chapter 3). Abbreviations: 5-IT, 5-iodotubericidin; ADA, adenosine deaminase; ADP, adenosine diphosphate; ATP, adenosine triphosphate; cAMP, cyclic adenosine monophosphate; ENT-1, equilibrative nucleoside transporter 1; NBTI, S-(4-nitrobenzyl)-6-thioinosine; PDE, cAMP phosphodiesterase; SAH, S-adenosyl homocysteine. Figure inspired by Latini 2001.

The intracellular formation of adenosine from catabolism of cytosolic ATP can be seen as a very sensitive signal of metabolic rate or metabolic stress (Latini and Pedata, 2001). Under metabolic challenging conditions like hypoxia or ischemia extracellular adenosine levels increase rapidly (Dale et al., 2000;Latini et al., 1999;Winn et al., 1981). This increase in extracellular adenosine is due to increased formation of intracellular adenosine subsequently transported through equilibrative transporters to the extracellular space. This process is linked to the balance of energy supply and demand and thus cytosolic ATP degradation (Latini and Pedata, 2001).

Another source of extracellular adenosine is released cAMP. Neurons can release cAMP through a non-specific energy dependent transporter. The released cAMP is then converted to 5'-AMP by ecto-phosphodiesterase and subsequently to adenosine by 5'-nucleotidase (see Figure 1.1). This suggests that neurotransmitters acting on metabotropic receptors coupled to AC could regulate extracellular adenosine levels by changing intracellular cAMP levels. Increased activity of metabotropic receptors can, through increased AC activity, increase cAMP levels which will be converted into adenosine eventually (Latini and Pedata, 2001). This process is not very rapid and unlikely to be the source of adenosine in acute metabolic challenging conditions like hypoxia, but prolonged neurotransmitter release could induce slow changes in intra- and/or extracellular cAMP and adenosine levels. This process could act as a fail-safe to keep neuronal activity from becoming excessive through suppressing neuronal activity by increasing adenosine levels.

1.3.2. Adenosine metabolism.

The main mechanism by which adenosine is removed is through conversion by cytosolic adenosine kinase to 5'-AMP (see Figure 1.1). When adenosine levels increase substantially adenosine deaminase (ADA) helps to clear adenosine by converting it to inosine. Under normal physiological conditions adenosine concentrations are in the nanomolar range which makes adenosine kinase the main adenosine sink. ADA will only start to help clear adenosine once levels rise to the micromolar range (Fredholm et al., 1999;Latini and Pedata, 2001). Adenosine kinase is the most important enzyme in clearing adenosine. Blocking adenosine kinase has a much bigger effect on adenosine release compared to ADA blockage (Lloyd and Fredholm, 1995).

Another enzyme of importance in adenosine metabolism is S-adenosylhomocysteine hydrolase (SAH hydrolase). SAH hydrolase guards the equilibrium between S-adenosylhomocysteine and adenosine + L-homocysteine. The activity of this enzyme does not depend on the adenosine concentration but rather the amino acid concentration. When L-homocysteine levels are low new amino acids are formed thereby also releasing adenosine. The reverse is also true, when L-homocysteine levels are high adenosine can be trapped inside the cell because it is converted to S-adenosylhomocysteine (Fredholm et al., 1999;Latini and Pedata, 2001).

1.4. Adenosine receptors.

So far four distinct adenosine receptors have been cloned and characterised in the brain: A_1-receptors, A_{2A}-receptors, A_{2B}-receptors and A_3-receptors (Fredholm et al., 2001). All four receptors subtypes are seven transmembrane domain receptors and G-protein coupled (see Table 1.1). The A_1-receptor has the highest affinity for adenosine (~70 nM) and the A_{2A}-

receptor has an affinity for adenosine still in the nanomolar range (~150 nM). The A_{2B}-receptor and A_3-receptor have an affinity for adenosine in the micromolar range (see Table 1.1). With adenosine concentrations being between 40 and 460 nM *in vivo* (Ballarin et al., 1991), ambient adenosine levels are high enough to activate both A_1- and A_{2A}-receptors. The effects of minor changes in ambient adenosine levels will therefore be dependent on the distribution of A_1- and A_{2A}-receptors within different brain structures. When adenosine levels rise substantially during pathological conditions the A_{2B}- and A_3-receptors will also be activated. Thus the A_1- and A_{2A}-receptors will be the most likely targets to prevent cognitive decline or boost cognitive function in similar ways as caffeine does.

1.4.1. Adenosine receptor distribution within the brain and periphery.

Adenosine receptors are prevalent throughout the central nervous system (see Table 1.1). Adenosine receptors are so common that you could almost say they are present on every cell. The A_1-receptor is the most abundant receptor of all adenosine receptors in the brain. A_1-receptors are present in virtually all brain areas with the highest levels in the hippocampus, cerebral and cerebellar cotex and certain thalamic nuclei (Fredholm et al., 1999;Ochiishi et al., 1999). A_{2A}-receptors are especially found in dopamine receptor (D_1 and D_2) rich regions of the brain (Fredholm et al., 2001). The highest concentration of A_{2A}-receptors is found in the caudate putamen, nucleus accumbens and the olfactory bulb. In the rest of the brain A_{2A}-receptor mRNA is expressed in very low quantities but functional studies do show A_{2A}-receptors are present in other brain areas. Most likely A_{2A}-receptors are present in the hippocampus and cortex on neurons that project to these areas. A_{2A}-receptors have been shown to exist on the terminals of striatopallidal GABAergic projections. The A_{2B}-receptor and the A_3-receptor are expressed in low levels in most of the brain. There is an

intermediate expression of A_3-receptors in the cerebellum and hippocampus (Fredholm et al., 2001).

Adenosine receptors are also expressed in other organs besides the brain. The peripheral distribution of receptors can have important implication when it comes to possible side effects when using adenosine receptor acting drugs. A_1-receptors are highly expressed in the heart, eye and adrenal glands, and also present in muscle tissue, the liver and colon. A_{2A}-receptors are highly expressed in the spleen and leukocytes, and also present in the heart and blood vessels. Data on the A_{2B}- and A_3-receptors is less clear because of the lack of specific ligands. A_{2B}-receptors are thought to be present in the bladder and colon, and also present on blood vessel and in the eye. A_3-receptors are expressed in the testis and mast cells and also present in the liver and thyroid. Some of the physiological effects of adenosine receptors are: reduced hart rate, decreased renal blood flow, immunosuppression, vasodilatation and alteration of pain perception (Fredholm et al., 2001;Fredholm, 2010). Though this is far from a complete list of physiological effects, it is clear that adenosine receptors can influence many processes in the body.

1.4.2. Adenosine receptor distribution in the hippocampus.

The hippocampal formation consists of three main subfields (see Figure 1.2): the dentate gyrus, the cornu ammonis 3 region (CA3) and the cornu ammonis 1 region (CA1). The CA2 region is less well defined in the rat and will therefore not be mentioned any further in this thesis. The hippocampus is very structured with all the cell bodies arranged in one line (stratum pyramidale, see Figure 1.2). The CA3 area has excitatory projections to the CA1 area (Schaffer-Collaterals). Where the CA3a and CA3b project to both the CA1 stratum

radiatum and stratum oriens the CA3c area projects only to the stratum radiatum (blue lines in Figure 1.2) (Freund and Buzsaki, 1996).
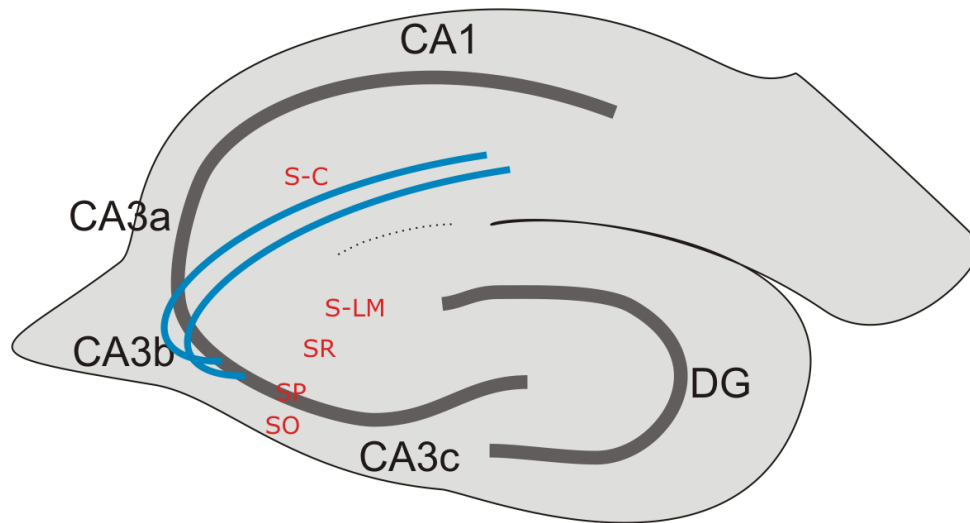
Figure 1.2. Schematic representation of the hippocampus. The cellular layers are indicated by the thick grey lines. The excitatory projections from the CA3 area to the CA1 area (Schaffer-Collaterals) are depicted in blue.
Abbreviations: CA1 = Cornu Ammonis 1, CA3 = Cornu Ammonis 3, DG = dentate gyrus, S-C = Schaffer-Collaterals, S-LM = Stratum Lacunosum Moleculare, SO = Stratum Oriens, SP = Stratum Pyramidale, SR = Stratum Radiatum.

Because the experiments in this thesis are done in the hippocampus the adenosine receptor distribution within the hippocampus will be looked at in more depth in this section. The A_1-receptor has been studied most intensively and is most abundant within the hippocampus (see Table 1.1). Studies using mRNA show the highest A_1-receptor expression in the granular layer of the dentate gyrus (DG) and the stratum pyramidale (SP) of the Cornu Ammonis (CA) (Swanson et al., 1995).

In contrast to mRNA binding studies specific ligand binding studies showed higher density staining in the stratum oriens (SO), stratum radiatum (SR), and stratum lacunosum moleculare (SLM) (Ochiishi et al., 1999;Swanson et al., 1995). Both the cell bodies of

pyramidal cells and interneurons express in A_1-receptors with no apparent discrimination between interneuron subtypes (Ochiishi et al., 1999). Even though staining of the cell bodies is less dense compared to axonal staining, individual neurons can be identified. One important difference between interneurons and pyramidal cells is that on inteneurons there are no A_1-receptors present on axons (Ochiishi et al., 1999) while on pyramidal cells the axons show the highest density of A_1-receptors (Swanson et al., 1995). The axons from and to the hippocampus express A_1-receptors in varying densities. Figure 1.2.A gives a schematic overview of A_1-receptor distribution in the hippocampus including the main incoming and outgoing hippocampal inputs colour coded for adenosine A_1-receptor density. Projections from the DG to the CA3 area express A_1-receptors in high density. The axons from CA3 pyramidal cells passing through the SP projecting to the CA1 (Schaffer-collaterals) have a high A_1-receptor density which is maintained in the SR of the CA3 area but expression diminishes in the SR of the CA1 area. The axons going out of the CA1 also express A_1-receptors abundantly, but not as dense as axons originating in the CA3 area. Radially oriented fibres in CA1, most likely fibres from the temporoammonic pathway, have a moderate A_1-receptor density. Projections from the entorhinal cortex (perforant path) ending in the molecular layer of the dentate gyrus have a moderate density of A_1-receptors, with projections ending in the outer molecular layer having a slightly higher density than projections ending in the inner molecular layer (Swanson et al., 1995). In the hippocampus adenosine receptors are not present on the dendritic tree (Ochiishi et al., 1999;Rebola et al., 2003). A_1-receptors are enriched in the active zone of the synaptic cleft on both the pre- and post-synaptic membrane (Figure 1.2.B). The plasma membrane outside the synaptic zone has some A_1-receptor expression on the pre-synaptic membrane but not as much as along the axon or in the active zone of the synapse. On the post-synaptic membrane there is no further expression of A_1-receptors (Ochiishi et al., 1999;Rebola et al., 2003).

The A_{2A}-receptors mRNA expression pattern is strikingly similar to the expression of A_1-receptor mRNA in the hippocampus (Cunha et al., 1994;Sebastiao and Ribeiro, 1996). The biggest difference is the amount of expression between the two different receptors. Where A_1-receptors are expressed abundantly A_{2A}-receptors are rather sparse. Though A_{2A}-receptors are sparse in the hippocampus they are functional and shown to oppose A_1-mediated effects (Cunha et al., 1994;Sebastiao and Ribeiro, 1996).

Adenosine receptors can also for heteromers with other receptor types. The A_1-receptor and the A_{2A}-receptor have been shown to form heteromers with group-I metabotropic glutamate receptors (Tabata et al., 2007). The A_{2A}-receptor can also form heteromers with dopamine receptors and the expression patterns of dopamine receptors and A_{2A}-receptors are strikingly similar (Fredholm et al., 1999;Tabata et al., 2007).

1.4.3. Signalling through adenosine receptors.

The A_1-receptor is coupled to the pertussis toxin-sensitive G-Proteins ($G_{i1/2/3}$ and G_o). The A_{2A}-receptor is coupled to G_s and G_{olf} G-proteins. Thus much of the effects of adenosine receptor activation can be predicted from what is known about G-protein signalling. The A_{2B}-receptor and A_3-receptor are also G-protein coupled (see Table 1.1) but because their affinity for adenosine in very low and their distribution in the brain is sparse the focus in this thesis will be on the effects of A_1- and A_{2A}-receptors.
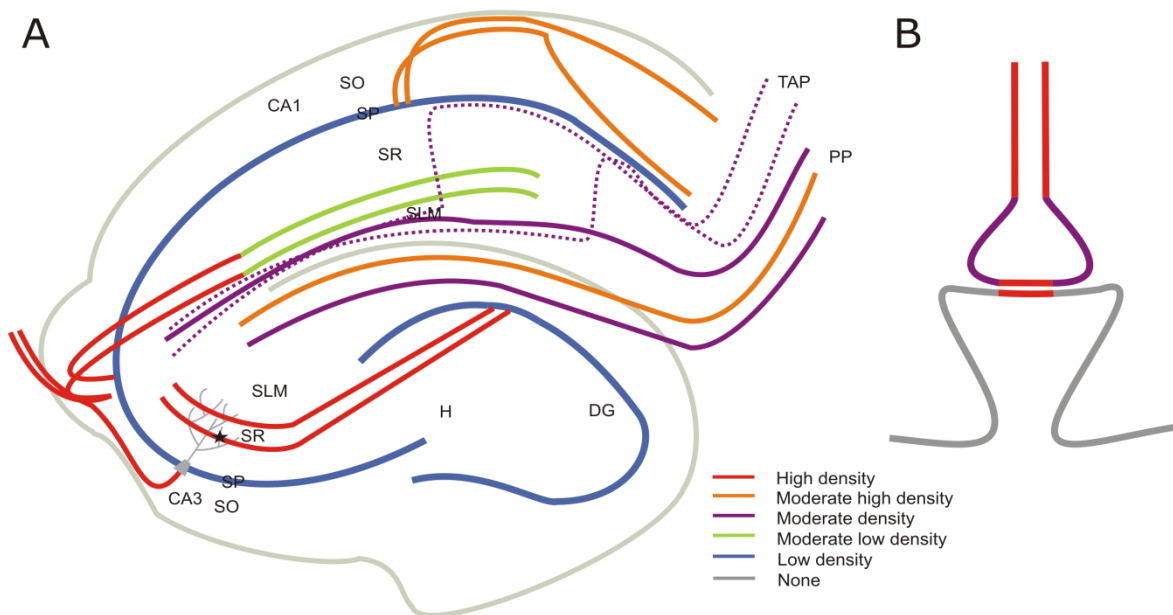
Figure 1.2. A1-receptor density in the hippocampal formation. **A.** Overview of axonal projections with known A1-receptor distribution from receptor labelling techniques. The cellular layer is indicated by the blue line and has a low density of A1-receptors. Projections from the entorhinal cortex ending in the molecular layer of the dentate gyrus (ML-DG) display A1-receptors with projections ending in the outer ML-DG having a higher density than projections ending in the inner ML-DG. The granule cell layer of the dentate gyrus (GC-DG) has a low A1-receptor density which is confined to the fibres passing through the GC-DG. Fibres from the DG projecting to the CA3 area through the Hilus have a high A1-receptor density. The CA3 area shows high density A1-receptor in the stratum radiatum (SR) and stratum oriens (SO). In the stratum pyramidale (SP) the cell bodies have a low density A1-receptor while the fibres passing through the SP are dense in A1-receptor. The Schaffer-collatterals projecting from CA3 to CA1 have a much lower A1-receptor density in the SR of the CA1 than the mossy fibre projections to the CA3 molecular layer. The radially oriented fibres showing moderate density of A1-receptor are most likely projections from the temporoammonic Pathway. The axons projecting from the CA1 SO are moderately high in A1-receptor density. Hippocampal A1-receptors seem to be confined mostly to axons and there is no evidence that A1-receptors are also displayed along the dendritic tree in any area of the hippocampus (Swanson et al., 1995) **B.** Schematic high magnification of the star in panel A. Though A1-receptors are not found on dendritic fibres they are enriched in nerve terminals on the pre and post synaptic membrane in the active zone. The pre-synaptic end of the synapse which comes from the axons also has A1-receptors on the rest of the terminal although not as dense as in the synaptic cleft. The display of A1-receptors on the post-synaptic membrane of the nerve terminal is confined only to the active zone and there are no A1-receptors on the rest of the dendrite (Rebola et al., 2003). Abbreviations: CA1 = Cornu Ammonis 1, CA3 = Cornu Ammonis 3, DG = Dentate Gyrus, H = Hilus, PP = Perforant Path, SLM = Stratum Lacunosum Moleculare, SO = Stratum Oriens, SP = Stratum Pyramidale, SR = Stratum Radiatum, TAP = Temporoammonic Pathway.

A_1-receptor activation: inhibits AC activity thereby reducing cAMP levels; enhances several K^+-channels function; inhibits several types of Ca^{2+}-channels (N and Q type); and is positively coupled to phospholipase C and phospholipase D. A_{2A}-receptor activation increases AC function thereby increasing cAMP levels and activates some voltage sensitive Ca^{2+}-channels (especially L-type channels) (Fredholm et al., 1999;Fredholm et al., 2001). Especially clear in the effect on cAMP levels A_1- and A_{2A}-receptors have partly opposing effects on a cellular level. This is important to keep in mind because both receptors are often co-expressed in the same brain areas and cells. The effect of non-specific agonists or antagonists can therefore depend on receptor distribution and possibly cellular location of the receptors.

A_1-receptors can also inhibit receptors directly through heteromer formation. In cerebellar Purkinje cells A_1-receptors inhibit metabotropic glutamate receptors through a G-Protein independent pathway (Tabata et al., 2007).

1.5. Effects of adenosine receptors on the brain function.

Adenosine is not considered a neurotransmitter because it is not released in a classical Ca^{2+}-dependent fashion or stored in vesicles. There is also no evidence for synapses with adenosine as their primary neurotransmitter (Dunwiddie and Masino, 2001). Therefore adenosine is considered to have a neuromodulatory role. Adenosine receptors have been shown to alter the release of virtually every neurotransmitter system including, glutamate, gamma-aminubutyric acid (GABA), acetylcholine, norepinephine, 5-hydroxytryptamine (5-HT), dopamine and others.

Though adenosine is not considered a neurotransmitter there is evidence that adenosine is released in an activity-dependent matter which is sensitive to TTX and Ca^{2+} (Wall and Dale, 2007).

1.5.1. Synaptic effects of adenosine receptors.

Adenosine A_1-receptors activation blocks neurotransmitter release in mainly excitatory synapses (Haas and Selbach, 2000;Yoon and Rothman, 1991). Inhibitory (GABAergic) synapses are not affected when monosynaptic stimulation is used, but polysynaptic inhibition is almost completely blocked by A_1-receptor activation (Thompson et al., 1992). The reduction in synaptic signalling by A_1-receptors is due to prevention of vesicles releasing their content. Adenosine receptors are perfectly placed to quickly and efficiently alter vesicular transmitter release because of their enrichment in the active part of the synapse (see Figure 1.2.B). Vesicular transmitter release is most likely inhibited via a direct effect on N-type Ca^{2+}-channels through G-proteins independent from cAMP levels (Cunha, 2001;Wu and Saggau, 1994). Even though this process seems most important other effects of adenosine receptors on vesicle release have also been described. A_1-receptors could also directly affect the affinity of the release apparatus for calcium (Scanziani et al., 1992), or directly affect the release apparatus itself (Capogna et al., 1996).

Adenosine A_{2A}-receptor activation has the opposite effect and facilitates synaptic transmission. An A_{2A}-receptor antagonist facilitates GABA release from hippocampal axonal endings (Cunha and Ribeiro, 2000). As A_{2A}-receptors are also G-protein coupled many pathways could be activated. Facilitated synaptic transmission through A_{2A}-receptor activation is dependent on protein kinase C but not protein kinase A activation (Cunha and Ribeiro, 2000). Adenosine A_{2A}-receptors also increase cAMP levels (Table 1.1) through

affecting AC activity. AC activation has also been shown to increase neurotransmitter release from excitatory synapses in the rat hippocampus (Chavez-Noriega and Stevens, 1994). A_{2A}-receptors can also facilitate synaptic transmission through activating P-type Ca^{2+}-channels, thereby enhancing vesicle release (Cunha, 2001;Mogul et al., 1993).

Adenosine receptors can influence synaptic transmission through changing vesicular transmitter release by influencing Ca^{2+}-channel activity, and by cAMP dependent pathways. The effect of adenosine (non-specific agonist) will depend on receptor distribution as A_1- and A_{2A}-receptors have opposite effects on synaptic transmission.

1.5.2. Cellular effects of adenosine receptors.

One of the clearest effects of adenosine A_1-receptor activation is a hyperpolarisation of the resting membrane potential in pyramidal cells (Greene and Haas, 1985), many other neurons and astrocytes (Hosli et al., 1987) and interneurons (Li and Henry, 2000). The A_1-receptor induced hyperpolarisation is caused by increased K^+-current across the membrane (Alzheimer and ten Bruggencate G., 1991). As adenosine receptors signal through G-proteins it is no surprise G-protein-coupled inwardly rectifying K^+ (GIRK) channels are responsible for the A_1-receptor induced hyperpolarisation (Chen and Johnston, 2005;Takigawa and Alzheimer, 2002). Interestingly A_1-receptor antagonists seem to not have any effect on resting membrane potential (Luscher et al., 1997).

A_1-receptor activation also increases accommodation of action potential firing during a prolonged depolarizing stimulus in CA1 pyramidal cells (Greene and Haas, 1985;Haas and Selbach, 2000). Also the slow afterhyperpolarization (AHP) is prolonged during adenosine application (Greene and Haas, 1985;Haas and Selbach, 2000). Both processes are under the control of AC activity which makes it likely adenosine receptors can influence them.

1.6. Gamma oscillations.

Neuronal networks in the brain sometimes display patterns of oscillatory activity. Some structures in the brain generate these rhythms and can therefore be studied *in vitro*. Of particular interest are oscillations within the gamma frequency band (30-100 Hz). Gamma oscillations are linked to a variety of cognitive functions including sensory processing (Engel and Singer, 2001;Singer, 1993), memory (Fell et al., 2001;Herrmann et al., 2004) and selective attention (Fries et al., 2001). The strength of gamma oscillations may affect cognitive performance (Fuchs et al., 2007). In rodents gamma oscillations are prominent during explorative behaviour (Buzsaki et al., 2003;Csicsvari et al., 2003) and thought to contribute to encoding and retrieval of memory (Bauer et al., 2007;Montgomery and Buzsaki, 2007). Gamma oscillations are thought to transfer information between different brain areas. To transfer information from one area to another coupling and synchronization of the different areas seems very important (Fell et al., 2001;Jutras et al., 2009). To code information within a gamma oscillation two main mechanisms are proposed: spike timing and phase encoding. The discussion of these two mechanisms is outside the scope of this introduction but discussed in (Fries et al., 2007).
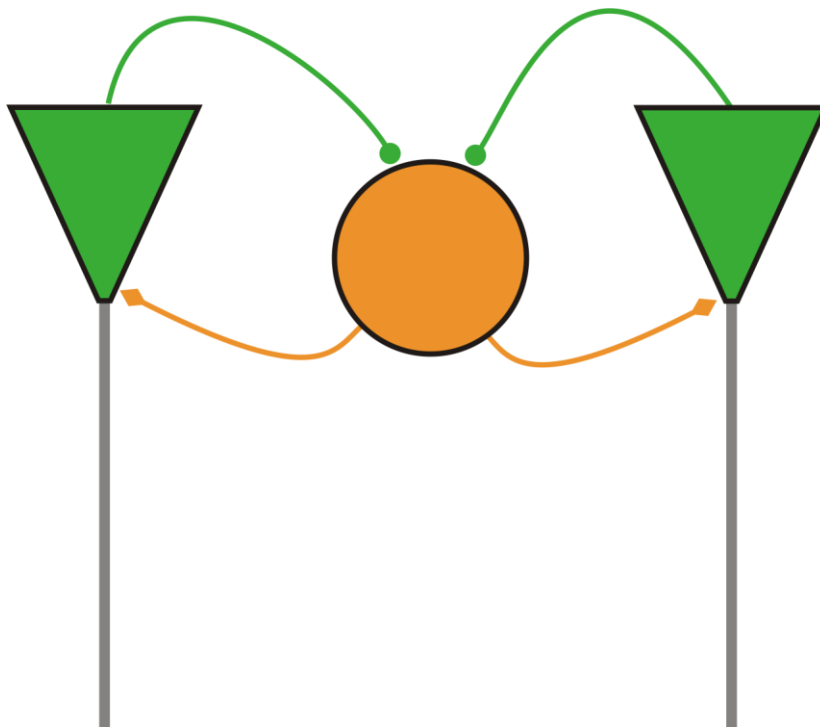
Figure 1.3 Simplified schematic drawing of a CA3 hippocampal network. The green triangular cells are principal cells and the orange round cell represents an interneuron.

1.7. Hippocampal gamma oscillations.

The hippocampus is an area involved in memory processing. Because of the distinct laminar cellular organization within its networks the hippocampus is a perfect area to study network oscillations. The hippocampus has a relatively simple neuronal organization where the cell bodies of principal cells are aligned in one layer (stratum pyramidale, SP, see Figure 1.2.A), with axons originating from one end (stratum oriens, SO) and the dendrites extending towards the other side (stratum radiatum, SR). The axons from the CA3 area project to ipsi-

and contra-lateral CA3 and CA1 cells, targeting both principal cells as well as GABAergic interneurons (Hajos and Paulsen, 2009). The principal cells are very uniform of character within the hippocampus, while there are a variety of GABAergic interneurons (Freund and Buzsaki, 1996). For gamma rhythm generation the perisomatic inhibitory interneuron (basket cells and axo-axonic cells) seems most important (Hajos and Paulsen, 2009). Figure 1.3 is a schematic simplified drawing of how pyramidal cells and perisomatic interneurons are connected within the hippocampus. The key characteristic for a network to be able to generate gamma oscillations is the convergent input onto interneurons from pyramidal cells and the divergent output from interneurons to pyramidal cells. Because the network is organised in this way excitatory input from any pyramidal cell will cause the interneurons to inhibit all pyramidal cells. Thus any excitatory input onto pyramidal cells will only be effective during the time window of fading inhibition. Interneurons fire with a slight phase delay compared to principal cells after which the whole network is silenced and a new gamma cycle can be started (Hajos and Paulsen, 2009). The majority of the extracellular recorded signal is the rhythmic inhibitory post-synaptic potentials (IPSPs) caused by interneuron firing. This might seem slightly contradictory as the pyramidal cells are the main driving force behind the oscillatory activity. But because only a small portion of the pyramidal cells are active during a cycle their contribution to the extracellular field is rather small (Hajos and Paulsen, 2009).

1.7.1. Different models to study hippocampal gamma oscillations *in vitro*.

Gamma oscillations revolve around principal cells that recurrently activate interneurons whereby the interneurons can synchronise the network. Most *in vitro* models increase excitatory drive to pyramidal cells which would lead to a more effective start of a gamma cycle. One way to increase excitatory drive to principal cells in the hippocampus is by activating cholinergic muscarinic receptors through carbachol (CCH) application (Fisahn et al., 1998). In making slices, cholinergic inputs from the medial septum/diagonal band are cut off. Adding CCH is a pharmacological way of restoring that input and is quite effective in generating gamma oscillations.

Another way to induce gamma oscillations in the hippocampus is through activation of kainate receptors, possibly mimicking the loss of glutamatergic tone after slicing. Kainate receptors are widely expressed in the hippocampus. The GluR6 subunit is crucial for oscillation induction and increases excitatory drive to pyramidal cells and interneurons (Fisahn, 2005).

Gamma oscillations can also be induced by activation of metabotropic glutamate receptors (Boddeke et al., 1997). This model differs slightly from the CCH model but also relies on increased activity of pyramidal cells (Boddeke et al., 1997).

The last model discussed here is the spontaneous gamma oscillations in hippocampal slices. If slice quality is very high, hippocampal slices can display gamma oscillations without any pharmacological induction (Pietersen et al., 2009b;Trevino et al., 2007). Even though all previous models reliably induce gamma oscillations, there are differences between the involvement of different subsets of interneurons (Hajos et al., 2004;Middleton et al., 2008;Palhalmi et al., 2004) and different contribution of recurrent excitation (Bartos et al., 2007).

The different models could represent different *in vivo* processes within the hippocampus dependent on the input received. For instance, the spontaneous gamma oscillation could represent gamma oscillations found during rapid eye movement sleep (Montgomery et al., 2008), while kainate (KA) and CCH models could be more a model for behaviour that increases glutamatergic or cholinergic receptor activation (e.g. exploration). In this thesis the spontaneous and KA-induced models of hippocampal gamma oscillations are used predominantly, but also some work is done in the CCH-induced model.

1.8. Adenosinergic modulation of hippocampal gamma oscillations: from single cell to whole animal.

This thesis will look at how adenosine receptors can influence hippocampal gamma oscillations *in vitro*, *in vivo* and look at the underlying cellular and network changes responsible for adenosine receptor modulation changes in hippocampal gamma oscillations.

1.8.1. Can adenosine receptor modulation alter hippocampal gamma oscillations *in vitro*?

In the first part of this thesis the role of adenosine receptor modulation on different *in vitro* models of hippocampal gamma oscillations will be investigated. Gamma oscillation strength has been linked to memory performance (Fuchs et al., 2007). The adenosine receptor antagonist caffeine has also been linked to increased memory performance (Fredholm et al., 1999;Pereira et al., 2002). Taking both these facts together adenosine receptors could possibly affect memory performance through gamma oscillation strength modulation. Adenosine receptors are well placed to influence network activity through its various cellular and synaptic effects (see Table 1.1). Caffeine has been shown to increase KA-induced

hippocampal gamma oscillations *in vitro* (Pietersen et al., 2009a). Caffeine is a non-specific adenosine receptor antagonist and will activate both A_1- and A_{2A}-receptors in the hippocampus. A_1-receptors are more abundant within the hippocampus than A_{2A}-receptors (see Table 1.1) and caffeine has a higher affinity for A_1-receptors (Fredholm et al., 1999). Thus it is more likely that the caffeine induced increase in gamma oscillations is an effect mediated through A_1-receptor antagonism. A_{2A}-receptors have the opposite effect on many signalling pathways (see Table 1.1) and can inhibit A_1-receptor function directly (Cunha, 2001). Therefore it is likely that drugs specific for the A_{2A}-receptor have opposite effects compared to A_1-receptor acting drugs.

In chapter 2 the effects of specific and non-specific adenosine receptor acting drugs on different models of hippocampal gamma oscillations (spontaneous, KA-induced and CCH-induced) will be described. It is hypothesised that the non-specific A_1-receptor agonist adenosine will decrease gamma oscillation strength and the non-specific A_1-receptor antagonist caffeine will increase gamma oscillation strength in all models. The specific A_1-receptor antagonist 8-CPT and specific A_{2A}-receptor agonist CGS21680 are expected to increase gamma oscillation strength.

To be able to say anything about whether or not natural fluctuations in ambient adenosine levels can influence cognitive function, endogenous adenosine levels are modulated in chapter 3. Intracellular adenosine breakdown is decreased by inhibiting adenosine kinase (see Figure 1.1) and expected to increase adenosine levels and thereby suppress hippocampal gamma oscillations. Because ambient adenosine levels in hippocampal slices are high enough to tonically activate adenosine receptors (Dunwiddie and Diao, 1994), reducing the extracellular adenosine concentration, by blocking the ENT-1 transporter and adding ADA, is expected to increase hippocampal gamma oscillations.

1.8.2. What cellular and synaptic changes underlie adenosinergic modulation of hippocampal gamma oscillation?

After establishing the effects of adenosine receptor modulation on hippocampal gamma oscillations (chapter 2 and 3) the cellular and synaptic changes underlying these effects are explored. In chapter 4 and 5 the effects of A_1-receptor agonists and antagonists on CA3c pyramidal neurons will be investigated. It is expected that A_1-receptor activation will hyperpolarise neurons (Greene and Haas, 1985;Li and Henry, 2000) and inhibit excitatory input (Haas and Selbach, 2000;Yoon and Rothman, 1991). A_1-receptor blockage will probably increase excitation but not depolarise the resting membrane potential (Luscher et al., 1997). Because gamma oscillations are mainly recorded IPSPs a closer look will be taken at polysynaptic and monosynaptic inhibition. A_1-receptor agonists are expected to decrease polysynaptic inhibition but not mono-synaptic inhibition (Thompson et al., 1992).

1.8.3. Does adenosinergic modulation have the same effect *in vivo*?

To be able to say anything about whether or not adenosine receptors are a good target for prevention of cognitive decline or enhancement of cognitive function the results obtained *in vitro* have to be verified *in vivo*. Chapter 6 will look at the effects ventricular injected A_1-receptor acting drugs have on gamma oscillations in anaesthetised animals. It is expected that A_1-receptor modulation will have similar effects on gamma oscillations *in vivo*. Because adenosine receptors are so widespread throughout the brain (see Table 1.1) other brain areas can have unexpected influences on the hippocampus.

Finally in the last chapter (chapter 7) the most important results will be summarised and discussed in relation to cognition.

Receptor subtype	A$_1$-receptor	A$_{2A}$-receptor	A$_{2B}$-receptor	A$_3$-receptor
Adenosine affinity	~70 nM	~150 nM	~5100 nM	~6500 nM
G-protein coupling	G$_{i1/2/3}$ / G$_o$	G$_s$ / G$_{olf}$ /G$_{15/16}$	G$_s$ / G$_{q/11}$	G$_{i2/3}$ / G$_{q/11}$
Effect of G-protein coupling	AC ↓ → cAMP ↓, K$^+$-channel function ↑, Phospholipase C and D ↑, Ca^{2+}-channel (N, Q type) ↓	AC ↑ → cAMP↑, Ca^{2+}-channel (L-type) ↑	AC ↑ → cAMP↑, phospholipase C ↑	AC ↓ → cAMP ↓, phospholipase C ↑, intracellular Ca^{2+} ↑
Distribution in the brain	High density: Hippocampus, cerebral and cerebellar cortex, certain thalamic nuclei Intermediate levels: other brain regions	High density: caudate putamen, nucleus accumbens, tuberculum olfactorium), olfactory bulb Low density: Rest of the brain	Low density: brain	Intermediate density: cerebellum, hippocampus Low levels: most of the brain
Synaptic effects	Inhibits neurotransmitter release	Facilitates neurotransmitter release	Possibly facilitates neurotransmitter release	Possibly inhibits neurotransmitter release
Cellular effects	Hyperpolarises resting membrane potential	Depolarises resting membrane potential (in the presence of an A$_1$-receptor blocker	Unknown	unknown

Table 1.1. Relevent facts of adenosine receptors . Abbreviations: AC, adenylyl cyclase; cAMP, cyclic adenosine monophosphate.

CHAPTER 2: MODULATION OF GAMMA OSCILLATIONS THROUGH ADENOSINE RECEPTORS.

2.1. Introduction.

In this chapter the effects of adenosine receptor acting drugs on hippocampal gamma oscillations *in vitro* will be investigated. Of the possible ways to investigate hippocampal gamma oscillations *in vitro*, three models were chosen: carbachol-induced (CCH), kainate-induced (KA) and spontaneous.

Local networks can generate rhythmic activity in interneurons at frequencies in the gamma band (30-100 Hz) through increased principal cell activity (Bartos et al., 2007). Multiple pyramidal cells converge their input onto interneurons, while the output of interneurons diverges onto multiple principal cells (see Figure 1.3). Because the network is setup in that way interneurons can synchronise principal cell activity, causing sustained rhythmic activity (Fisahn et al., 1998). Increases in gamma oscillations are seen during exploration behaviour in rodents (Buzsaki et al., 2003). Also higher cognitive processes like memory (Herrmann et al., 2004) and sensory information processing (Engel and Singer, 2001) have been linked to gamma oscillations. The strength of gamma oscillations may affect cognitive performance (Fuchs et al., 2007).

Gamma oscillations can occur naturally in hippocampal slices (Pietersen et al., 2009b;Trevino et al., 2007), and can be evoked by activation of muscarinic receptors (Fisahn et al., 1998) or activation of kainate receptors

(Hajos et al., 2003). Gamma oscillations can be modulated by neurotransmitters like norepinephrine (Hajos et al., 2003).

Adenosine is a neuroprotective agent that increases strongly in extracellular concentration during pathological conditions like hypoxia (Frenguelli et al., 2003;Winn et al., 1981) and ischemia (Latini et al., 1999;Lloyd and Fredholm, 1995). Adenosine has been shown to reduce glutamate and acetylcholine neurotransmitter release through adenosine A_1-receptor activation (Haas and Selbach, 2000).

Caffeine is a non-specific adenosine receptor antagonist (Fredholm et al., 1999) and has been described to have cognitive enhancing effects in rodents and humans (Fredholm et al., 1999;Hogervorst et al., 2008). One of the possible mechanism by which caffeine can enhance cognitive function is by increasing brain synchronicity within the gamma range.

Caffeine has been shown to increase KA-induced gamma oscillations within the hippocampus *in vitro* (Pietersen et al., 2009a). First the effect of caffeine and adenosine on CCH-induced gamma oscillations will be investigated. The effect of different doses of adenosine on KA-induced hippocampal gamma oscillations will be investigated. One dose of adenosine will be used in both other models as well. Further receptor specificity will be determined in KA-induced gamma oscillations. We predict that caffeine will increase CCH-induced gamma oscillations and that adenosine will decrease gamma oscillations in all models in a dose dependent manner. The effect of the non-specific agonist adenosine is expected to mainly come from adenosine A_1-receptor modulation, because the affinity for the A_1-receptor is higher than for the other adenosine receptors (see introduction Table 1.1). As adenosine A_{2A}-receptors oppose the effects of adenosine A_1-receptors ((Fredholm et al., 2001), introduction Table 1.1) it is predicted that a specific adenosine A_{2A}-receptor agonist will increase gamma oscillations.

2.2. Materials and methods.

All experiments complied with the University of Birmingham ethical committee and all procedures were performed under the UK Animals (Scientific Procedures) Act 1986.

2.2.1. Tissue preparation.

Male C57BL/J6 mice (2-5 months) were anaesthetised by an intra-peritoneal injection of a ketamine (75 mg/kg) and medetomidine (1 mg/kg) mixture, and killed by cervical dislocation. Mice were used because work where this thesis is based on was done in mouse hippocampal slices. The brain was removed and chilled in an oxygenated sucrose based cutting solution containing (in mM): sucrose, 189; KCl, 2.5; $NaHCO_3$, 26; NaH_2PO_4, 1.25; D-glucose 10; $MgCl_2$, 5; $CaCl_2$, 0.1; pH 7.4. Using an Integraslicer (Campden Instruments, Loughborough, UK) 400 μm thick horizontal slices were made from the ventral hippocampus and put either in a Haas-type recording chamber at the interface between moist carbogen (95%, O_2, 5% CO_2) and artificial cerebrospinal fluid (aCSF, containing (in mM): D-glucose, 10; $NaHCO_3$, 26; NaCl, 125; KCl, 3; NaH_2PO_4, 1.25; $CaCl_2$, 2; $MgCl_2$, 1) at 32°C, or stored in a static interface type chamber containing aCSF at room temperature for later use. Fluid levels were kept relatively high in the recording chamber using a perfusion rate of 8±1 ml/min minimizing gravitational pull onto the mesh but not submerging the slices. Slices were allowed to recover for 50 minutes before recordings started.

2.2.2. Electrophysiological recordings.

Local field potentials were recorded with aCSF-filled glass pipette recording electrodes (4-5 MΩ) from stratum radiatum of the CA3c hippocampal area (Figure 2.1.A). Recordings were

amplified with Neurolog NL104 AC-coupled amplifiers (Digitimer Welwyn Garden City, UK) and band-pass filtered at 3-500 Hz. Noise locked to the powerline frequency 50 Hz was removed with Humbug noise eliminators (Digitimer Welwyn Garden City, UK). Subsequently the signal was digitised and sampled at 2 kHz using a CED-1401 interface (Cambridge Electronic Design, Cambridge, UK) and analyzed using Spike-2 software (Cambridge Electronic Design, Cambridge, UK).

After one hour of recovery in the interface chamber, slices were selected for spontaneous, KA-induced or CCH-induced gamma oscillation experiments. Slices selected for spontaneous gamma oscillations had to fulfil the criteria: peak power in the gamma range > average power in the beta range. Figure 2.1.B shows a typical power spectrum of a KA-induced singular oscillation. The light grey area is the gamma range. The gamma band was set between 20 and 60 Hz (Fisahn et al., 1998) because recordings were made at 32°C, which shifts the frequency bands to lower frequencies compared to recordings at body temperature (Dickinson et al., 2003). To calculate the power within the gamma range, the power underneath the curve is averaged (shown for the gamma range). In spontaneous gamma oscillation experiments modulating drugs were added 60 minutes after slices were placed into the recording chamber.

In slices not selected for spontaneous gamma oscillation experiments, gamma oscillations were induced by adding KA (50 nM) or CCH (5 µM) to the aCSF. The best predicable development for KA-induced and CCH-induced gamma oscillations was between 1h and 2h after application (Pietersen 2009 supplement). Adenosine receptor acting drugs were added to the aCSF 60 minutes after KA or CCH application. All modulating drugs were added for 20 minutes.

Drugs used were diluted from the following stock solutions: kainate (50 µM stock in water), carbachol (10 mM stock in water), caffeine (100 mM stock in water), adenosine (10 mM

stock in aCSF, or directly dissolved in aCSF at high concentrations), 8-cyclopentyl-1,3-dimethylxanthine (8-CPT; 50 mM stock in dimethyl sulfoxide (DMSO)) and 4-[2-[[6-Amino-9-(*N*-ethyl-*b*-d-ribofuranuronamidosyl)-9H-purin-2-yl]amino]ethyl]benzenepropanoic acid hydrochloride (CGS21680; 100 mM stock in DMSO). In experiments where drugs were dissolved in DMSO care was taken to add equal amounts of DMSO to the aCSF solution before and after drug application. CGS21680 was obtained from Tocris (Bristol, UK), all other drugs were purchased from Sigma (Poole, UK).
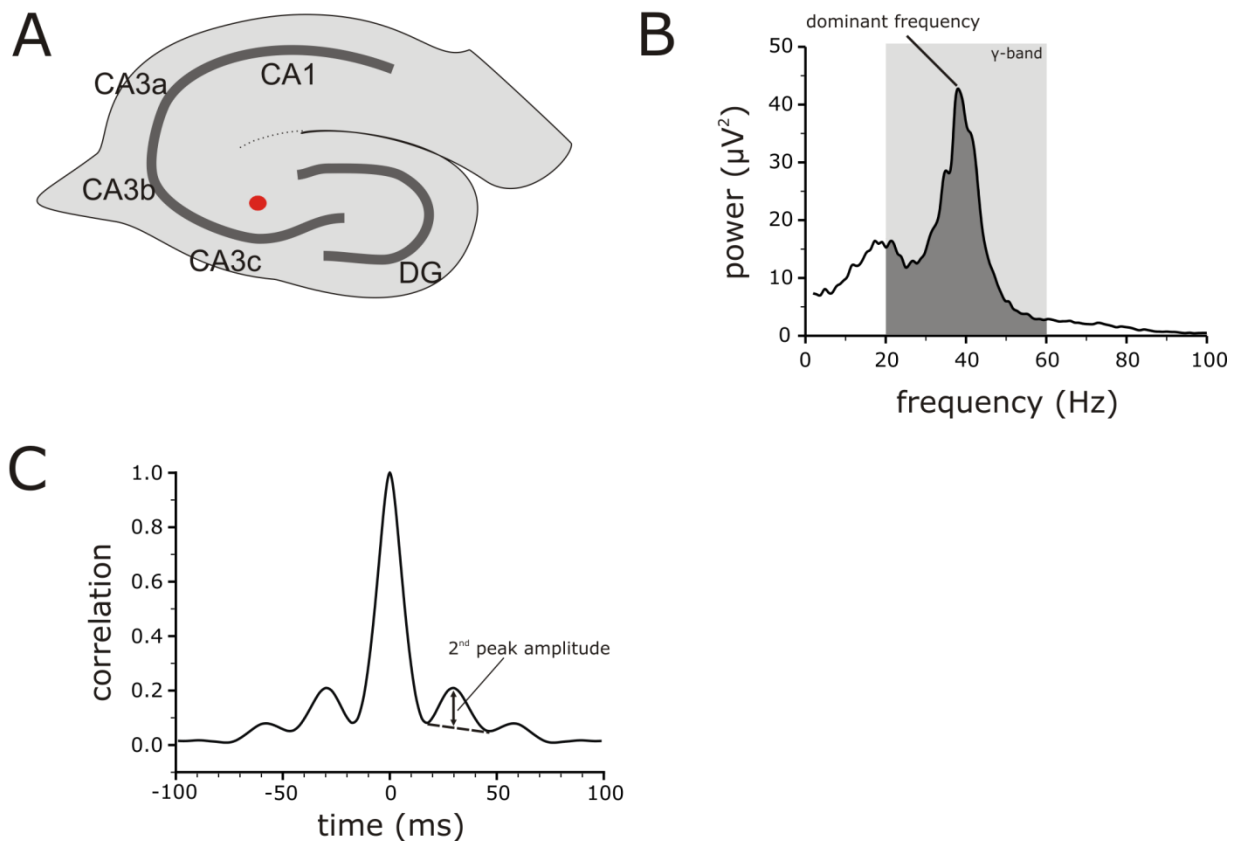
Figure 2.1. Methods chapter 2. **A.** Schematic representation of the mouse hippocampus. The red dot indicates where field recordings were made. **B.** Power spectrum of a KA induced network oscillation. The light grey area indicates the gamma range. The dark grey area is the area under the curve from which the average is used as a measure of power within frequency bands. The dominant frequency is determined by the frequency which has the most power. **C.** Example of how autocorrelation was analyzed. Second peak amplitude was measured by taking the maximum deviation between the straddling troughs.

2.2.3. Analysis and statistics.

Oscillation power was calculated from the recordings for four frequency bands (slow: 3-8 Hz, beta: 8-20 Hz, gamma: 20-60 Hz, fast: 60-100 Hz) using fast fourier transform (1 Hz bin size). Data was analyzed in 30 seconds epochs. A power spectrum was made using a fast fourier transformation for every 30 seconds and used for further analysis. Due to the large variability of absolute power between individual slices, data was normalised to 5 minutes prior the start of modulating drug application or corresponding time in controls (see Figure 2.2). The effect of adenosine receptor acting drugs was compared with time matched controls because the baseline progressively increased in the KA-induced and CCH-induced models. In the spontaneous model the baseline decreased over time.
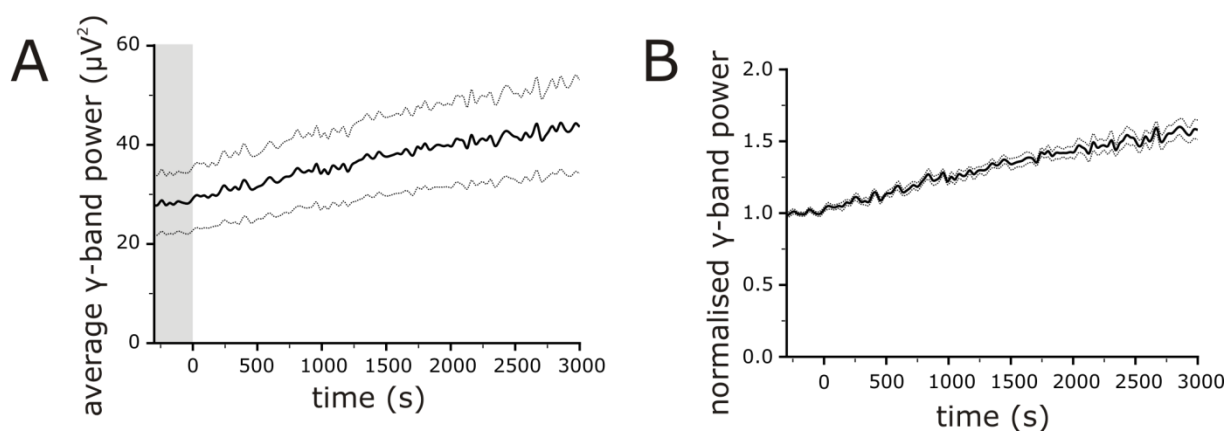
Figure 2.2. Effect of normalisation on gamma band power. There is a large variability between slices in the absolute gamma band power resulting in large error bars (dotted lines) in the average development over time (A). By normalising the gamma band power to five minutes before the point of drug injection (time = 0) the error bars are reduced (B). Even though the absolute power has a large variability the growth over time is very similar from slice to slice. The grey area in A indicates the data points used to normalise the average gamma band power.

Dominant frequency within the gamma range was determined from the power spectra (see Figure 2.1.B). If drug modulation caused the dominant frequency to shift outside the gamma range data was corrected and the peak in the beta range was taken as the dominant frequency.

Autocorrelation is a measure of the regularity of an oscillation. The waveform is compared to itself and the better you can predict the value of the next cycle the bigger the value for the second peak will be. If a waveform is a perfect sinusoid the autocorrelation will be maximal. As a measure of autocorrelation the amplitude of the second peak in the autocorrelogram was calculated. The maximum deviation from an imaginary line between the straddling troughs was taken as the amplitude of the second peak (see Figure 2.1.C).

For frequency band power and the amplitude of the second peak in the autocorrelogram statistical comparisons were made 20 minutes after drug application on the normalised drug induced changes and the normalised change over time in controls. Data acquired by undergraduate students Nisha Patel (8-CPT data) and Dominic Lancaster (CGS21680 data) were compared to their matched controls. Data acquisition done by Dominic Lancaster was co-supervised by me. For all other parameters statistical comparisons were made between the change after 20 minute of drug application and the time matched change in controls. All parameters were checked for normality using the Kolmogorov-Smirnov test in SPSS 15.0, and if data was normally distributed statistical comparison was made using a Student's *t*-test. If data was not normally distributed the non-parametric Mann-Whitney U test was used. Data are expressed as means±standard error of the mean (s.e.m.). If the significance criterion was below 0.05, data were considered significantly different from controls. Numbers of observations (n, number of slices) are quoted in the Tables 2.1, 2.2 and 2.3.

2.3. Results

2.3.1. The effect of caffeine and adenosine on CCH induced gamma oscillations.

At concentrations reached through normal coffee consumption (1-10 μM) caffeine can antagonise adenosine A_1-receptors and adenosine A_{2A}-receptors (Fredholm et al., 1999). Caffeine has been shown to increase KA induced gamma oscillations in the hippocampus at similar concentrations (Pietersen et al., 2009a). To make sure this increase is not model specific the effects of 50 μM caffeine on CCH-induced gamma oscillations were investigated. Caffeine (50 μM) increased oscillation power in all frequency bands (see Table 2.1), example in Figure 2.3.A. The power spectrum (Figure 2.3.B) shows that caffeine increases the power before and around the dominant frequency. Also visible is an increase in power around 63 Hz. This is double the dominant frequency and considered a harmonic. This is also visible in the raw traces as the trace recorded in the presence of caffeine has a more saw tooth like character than before caffeine was added. Oscillations induced by CCH have a very regular character, visible in the sharp peak in the power spectrum and the large second peak amplitude in the autocorrelogram. The average second peak amplitude was 0.80±0.05 (n=18). There was no difference between controls and caffeine in the normalised second peak amplitude after 20 minutes of drug application (see Table 2.1). The average gamma band power was 76.2±16.8 μV^2 (n=18), for the average of all other frequency bands see Table 2.1. Caffeine significantly increased the power in all frequency bands. The gamma band power increased to 3.08±0.28 (n=5) times the starting value (Figure 2.3.D), while controls only increased to 1.20±0.09 (n=6) times the starting value (Student's *t*-test, $t_{4.9}$=-6.8, *p*=0.002). Caffeine increased the beta band power
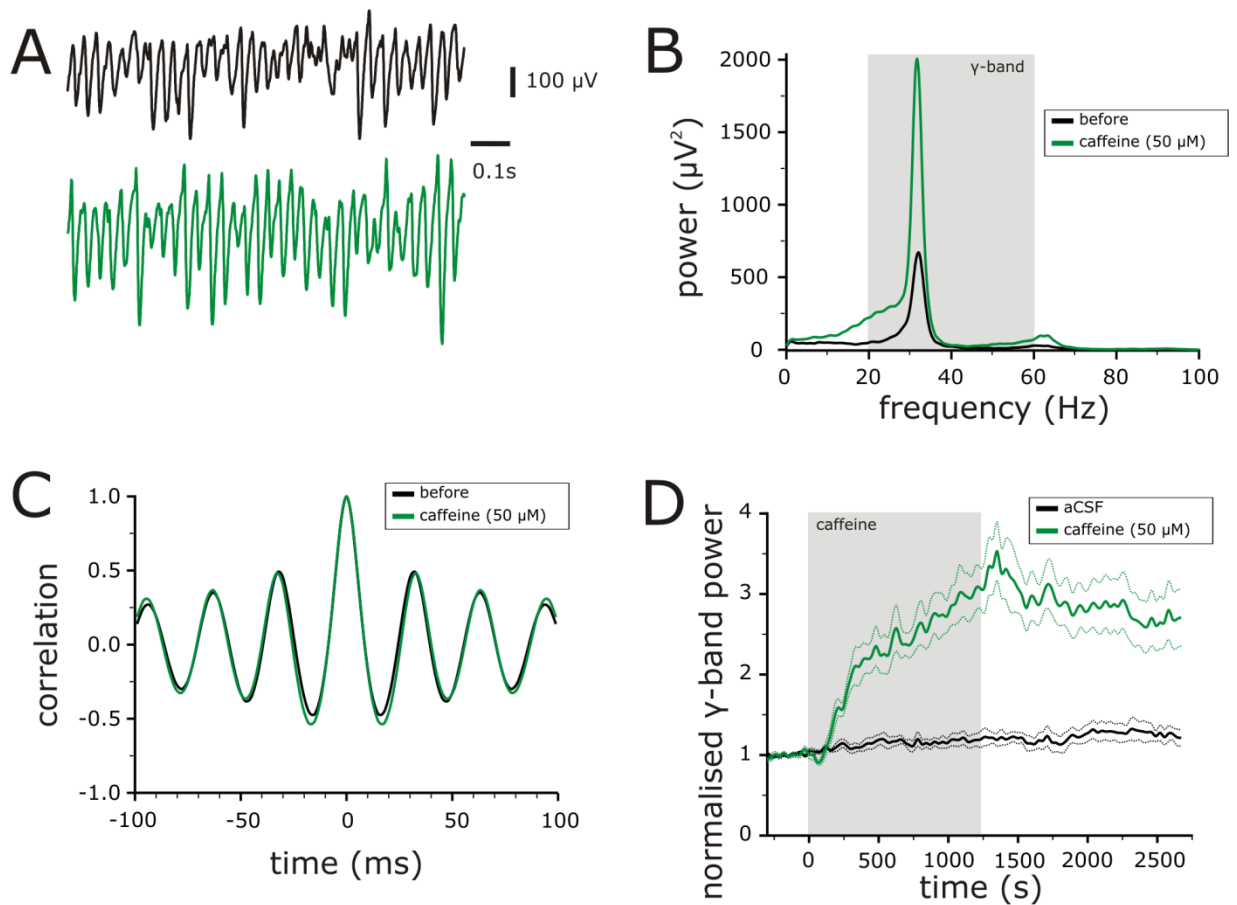
Figure 2.3. Effect of caffeine on CCH-induced gamma oscillations. **A.** Example traces before (black) and during caffeine (50 μM) application (20 minutes). Caffeine increased synchronous network activity **B.** Power spectrum before and after 20 minutes of caffeine application. Caffeine increased power in all frequency bands but mostly in the gamma band. **C.** Autocorrelogram from the same data as the power spectrum. Caffeine slightly increases the second peak amplitude. **D.** Normalised development of CCH-induced gamma band power in aCSF (black lines, n=6) and in the presence of caffeine (green lines, n=5). Caffeine significantly increased normalised gamma power after 20 minutes (p=0.002) compared to controls.

to 2.31±0.28 (n=5) times the starting value (Student's *t*-test, $t_{4.3}$=-4.7, *p*=0.011), slow band power to 1.56±0.12 (n=5) times the starting value (Student's *t*-test, t_9=-4.6, *p*=0.001) and fast band power to 3.06±0.20 times the starting value (Student's *t*-test, t_9=-8.8, *p*=0.000001), see Table 2.1 for control values. To test how the change in the gamma

range compares to the change in the beta range, the gamma/beta ratio is calculated by dividing the power in the gamma range by the power in the beta range. The gamma/beta ratio for CCH induced oscillations was 1.84±0.18 (n=18) before drug application. Caffeine increased the power in the gamma range increased more than the power in the beta range, but there was no significant difference between in change in gamma/beta ratio between controls and caffeine (see Table 2.1). The average dominant frequency in CCH-induced oscillations was 34.8±0.05 Hz (n=18). Caffeine shifted the dominant frequency down slightly (-1.38±0.66 Hz, n=5), but that shift was not significantly different from the shift in controls (-1.11±0.31 Hz, n=6).

To find out if non-selective adenosine receptor agonists can decrease network oscillations, the effects of adenosine (50 µM) on CCH induced hippocampal gamma oscillations was investigated. Adenosine decreased oscillatory activity 20 minutes after application (Figure 2.4.A). The power spectrum (Figure 2.4.B) shows a decrease in power specifically around the dominant frequency. Also notice the disappearance of the harmonic around 65 Hz after 20 minutes of adenosine application. In contrast to caffeine adenosine does affect the regularity of the oscillation and decreases the second peak amplitude in the autocorrelogram (Figure 2.4.C). Striking is how quickly adenosine exerts its effects on gamma oscillations (Figure 2.4.D). Within one to two minutes after adenosine application the normalised average power in the gamma range decreased rapidly to a new steady level. Adenosine decreased the power within the gamma range to 0.61±0.12 (n=7) times starting values (Student's t-test, t_{11}=3.8, p=0.003) after 20 minutes. The power in the fast band decreased to 0.60±0.11 (n=7) times the starting values (Student's t-test, t_{11}=3.5, p=0.005). The normalised power within the beta and slow bands did decrease slightly but not significantly compared to the change in aCSF controls (see Table 2.1). The decrease in power was most

specific for the gamma range. Adenosine significantly decreased the gamma/beta ratio by -

0.59±0.29 (n=7),
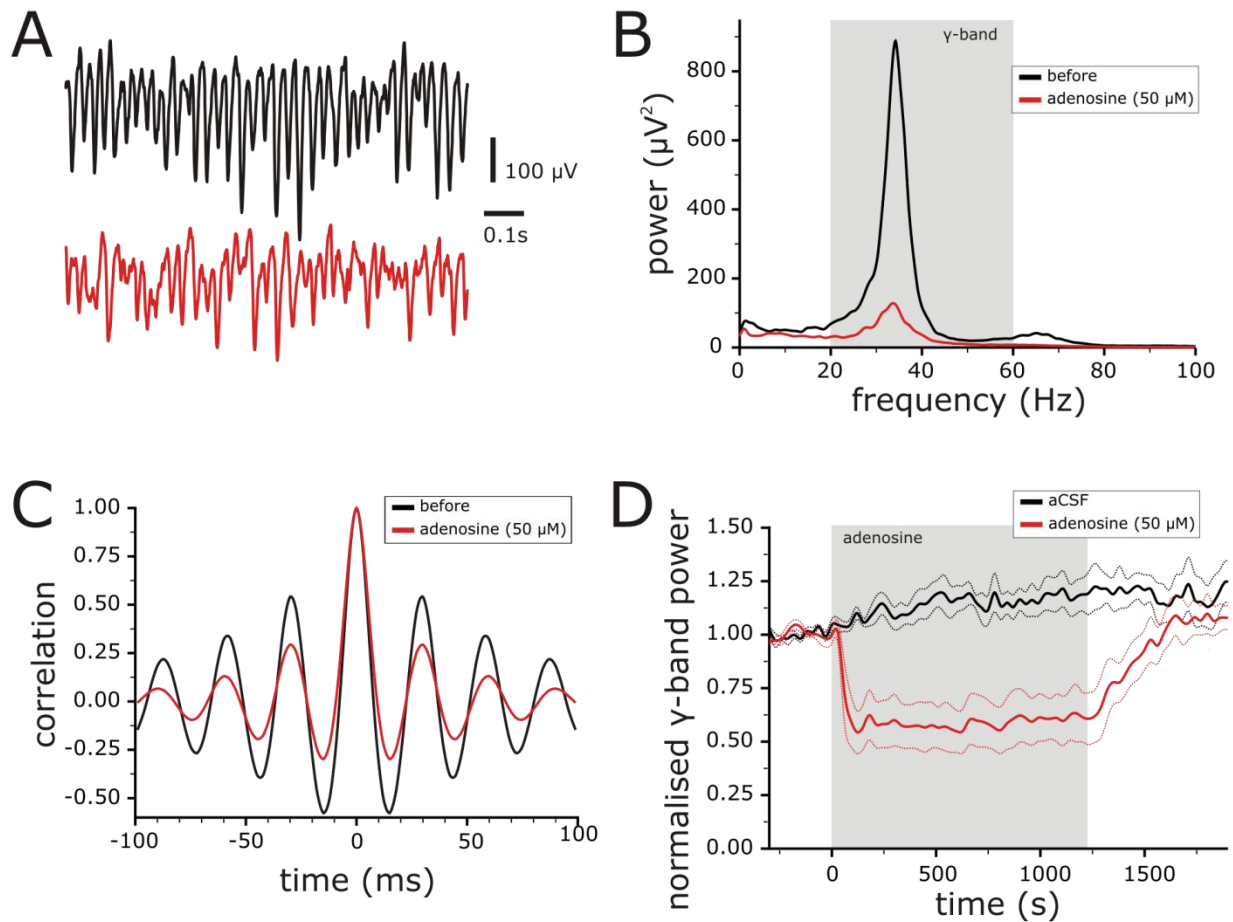
Figure 2.4. Effect of adenosine (50 uM) on CCH-induced gamma oscillations. **A.** Example traces before (black) and during adenosine (50 μM) application (20 minutes). **B.** Power spectrum before and after 20 minutes of adenosine application. Adenosine decreased power in the gamma range. **C.** Autocorrelogram from the same data as the power spectrum. Adenosine decreases the second peak amplitude significantly (p=0.001). **D.** Normalised development of CCH-induced gamma band power in aCSF (black lines, n=6) and in the presence of adenosine (red lines, n=7). Adenosine significantly decreased normalised gamma power after 20 minutes (p=0.003) compared to controls.

while in aCSF controls specificity increased slightly, 0.19±0.10 (n=6) (Student's t-test, t_{11}=2.4, p=0.035). The dominant frequency did shift down a little but the shift was not different from the change in control (see Table 2.1). Adenosine reduced the regularity of the oscillation, visible through decreased amplitude of the second peak in the autocorrelogram. The second peak amplitude decreased significantly to 0.69±0.03 (n=7) times the starting values (Student's t-test, t_{11}=4.8, p=0.001).

The non-selective adenosine receptor antagonist caffeine and the non-selective adenosine receptor agonist adenosine modulate CCH induced hippocampal network oscillations most powerfully within the gamma range.

2.3.2. The effect of different adenosine concentrations on KA induced hippocampal network oscillations.

To check if the reduction in CCH-induced hippocampal gamma oscillations is model-specific, the same adenosine concentration (50 μM) was also applied to KA-induced hippocampal gamma oscillations. Adenosine decreased KA induced gamma oscillations in a similar way as CCH induced gamma oscillations. Figure 2.5.A shows a reduction in signal amplitude 20 minutes after adenosine application. The power spectrum shows a loss of power mostly within the gamma range (Figure 2.5.B) and a shift of the dominant frequency to lower values. The shift in dominant frequency is also visible within the autocorrelogram (Figure 2.5.C) where the time to the second peak is increased. The amplitude of the second peak is reduced indicating a loss of regularity of the oscillation. The average power in the gamma band before drug application was 43.7±7.1 μV^2 (n=30). Adenosine significantly decreased the power within the gamma band to 0.90±0.08 (n=9) times starting values (see Figure 2.5.D). In aCSF controls the power in the gamma band increased to 1.42±0.03 (n=10)

times the starting values (Student's *t*-test, $t_{17}=6.5$, *p*=0.000005). Adenosine also significantly decreased the power in the fast band to 0.92±0.06 (n=9) times starting values (Student's *t*-test, $t_{17}=7.0$, *p*=0.000002). There was no significant difference between adenosine and controls for the slow and beta bands (see Table 2.2). The average gamma/beta ratio in KA induced gamma
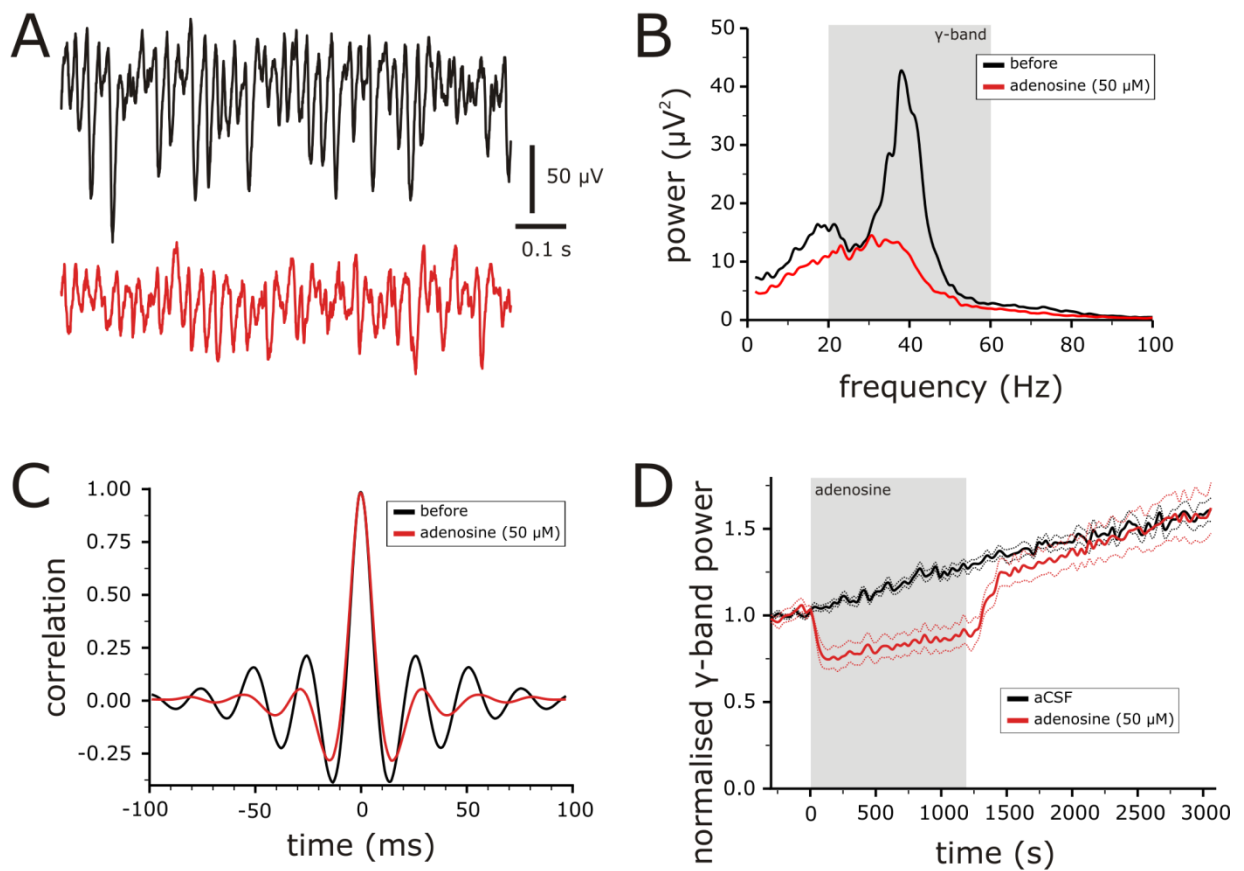

Figure 2.5. Effect of adenosine (50 µM) on KA-induced gamma oscillations. **A.** Example traces before (black) and during adenosine (50 µM) application (20 minutes). **B.** Power spectrum before and after 20 minutes of adenosine application. Adenosine decreased power in the gamma range. **C.** Autocorrelogram from the same data as the power spectrum. Adenosine decreases the second peak amplitude significantly (p=0.0002). **D.** Normalised development of KA-induced gamma band power in aCSF (black lines, n=10) and in the presence of adenosine (red lines, n=9). Adenosine significantly decreased normalised gamma power after 20 minutes (p=0.000005) compared to controls.

oscillations was 0.98±0.05 (n=30). While there was hardly any change in gamma/beta ratio in controls (0.03±0.03, n=10) adenosine decreased gamma/beta ratio by -0.28±0.06 (n=9) (Student's t-test, $t_{10.7}$=4.6, p=0.001). The dominant frequency before drug application was 36.0±0.8 Hz (n=30). Adenosine significantly shifted the dominant frequency by -6.0±1.2 Hz (n=9), while in aCSF controls there was a slight increase by 0.5±0.9 Hz (n=10) (Student's t-test, t_{17}=4.5, p=0.0003). The average second peak amplitude in the autocorrelogram was 0.34±0.02 (n=30). Adenosine significantly decreased the second peak amplitude to 0.45±0.04 (n=9) times starting values (Mann-Whitney U-test, U=0.0, p=0.0002). All effects were reversed when adenosine was washed out.

A very high concentration of 200 μM adenosine almost completely and reversibly blocked oscillatory activity within the hippocampal network in KA induced network oscillations (example in Figure 2.6.A). Where 50 μM adenosine decreased power mostly in the gamma band, a high dose of 200 μM adenosine wipes out almost all oscillatory activity. Strong reductions in power in the fast, gamma and beta bands (see power spectrum Figure 2.6.B) are observed. The oscillation is decreased so much that in 200 μM adenosine the autocorrelogram does not have a second peak within 100 ms. This indicated that the oscillation has a dominant frequency of below 10 Hz or that there was no dominant frequency at all. Adenosine decreased power in the gamma band to 0.13±0.07 (n=3) times starting values (Mann Whitney U-test, U=0.0, p=0.011), in the fast band to 0.28±0.12 (n=3) times starting values (Mann Whitney U-test, U=0.0, p=0.011) and the beta band to 0.56±0.04 (n=3) times starting values (Mann Whitney U-test, U=0.0, p=0.011). The power in the slow band did not change significantly different from controls (see Table 2.2). The oscillation became less specific for the gamma band as the specificity dropped by -0.54±0.11 (n=3) (Mann Whitney U-Test, U=0.0, p=0.011). As there was no, or hardly any, second peak to measure in the autocorrelogram it is no surprise that adenosine decreased

the second peak amplitude to 0.02±0.02 (n=3) times starting values (Mann Whitney U-Test, U=0.0, p=0.011). In experiments where no second peak was visible in the autocorrelogram the peak amplitude was set to zero. With losing almost all power in the gamma and beta bands, adenosine shifted the dominant frequency by -13.5±2.4 Hz (n=3) (Mann Whitney U-Test, U=0.0, p=0.011).
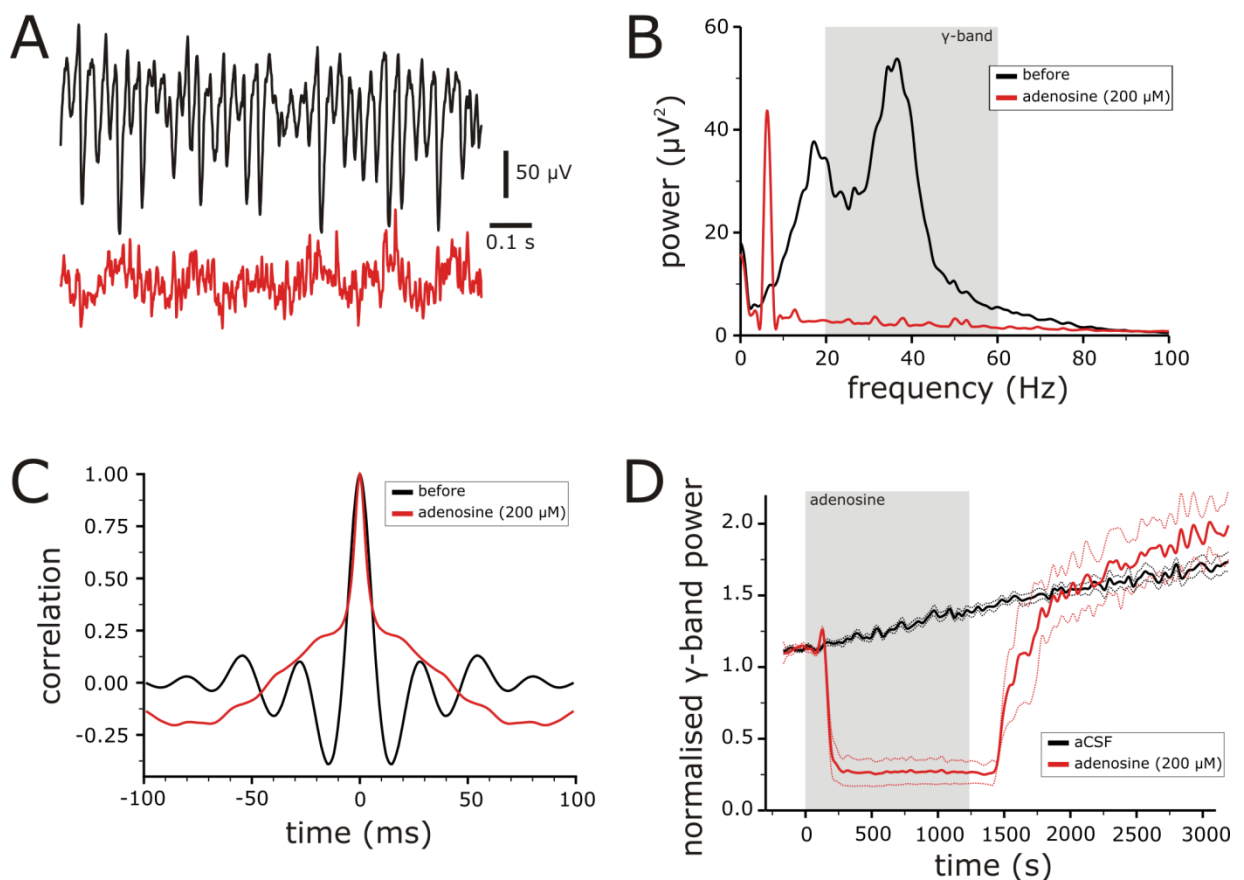

Figure 2.6. Effect of adenosine (200 µM) on KA-induced gamma oscillations. **A.** Example traces before (black) and during adenosine (200 uM) application (20 minutes). **B.** Power spectrum before and after 20 minutes of adenosine application. Adenosine decreased power in the fast, gamma and beta bands. **C.** Autocorrelogram from the same data as the power spectrum. Adenosine decreases the second peak amplitude significantly (p=0.011). **D.** Normalised development of KA-induced gamma band power in aCSF (black lines, n=10) and in the presence of adenosine (red lines, n=3). Adenosine significantly decreased normalised gamma power after 20 minutes (p=0.0011) compared to controls.

With a high dose adenosine completely blocking all activity in the gamma range, the effects of a low dose (10 µM) of adenosine were investigated next. A low dose of adenosine (10 µM) decreased signal amplitude slightly (Figure 2.7.A). In the power spectrum a small decrease in power in the gamma band is visible (Figure 2.7.B). After 20 minutes of adenosine (10 µM) application the power hardly changed from starting values 1.00±0.04 (n=8), the power in aCSF controls increased to 1.42±0.03 (n=10) times starting values. Thus at 20 minutes after adenosine application 10 µM adenosine decreased gamma oscillations significantly (Student's t-test, U_{16}=7.9, p=0.0000007). The fast band showed the same development as the gamma band (1.02±0.05, n=8) 20 minutes after drug application (Student's t-test, U_{16}=6.7, p=0.000005). The slow and beta bands did not show any significant differences with the change in controls (see Table 2.2). With the power in the gamma range decreasing and the power in the beta range following the aCSF controls development, the specificity significantly decreased by -0.22±0.04 (n=8) (Student's t-test, U_{16}=5.3, p=0.00007). The dominant frequency shifted significantly by -4.2±1.6 Hz (n=8) (Student's t-test, U_{16}=2.7, p=0.015). Just like with the high and moderate dose of adenosine, 10 µM significantly decreased the second peak amplitude in the autocorrelogram to 0.56±0.05 (n=8) time the starting values (Mann Whitney U-test, U=1.0, p=0.001).

Different doses of adenosine (10, 50 and 200 µM) decreased KA induced hippocampal network oscillations. Where the highest dose almost completely blocked all activity the lower doses were more specific for the gamma range.
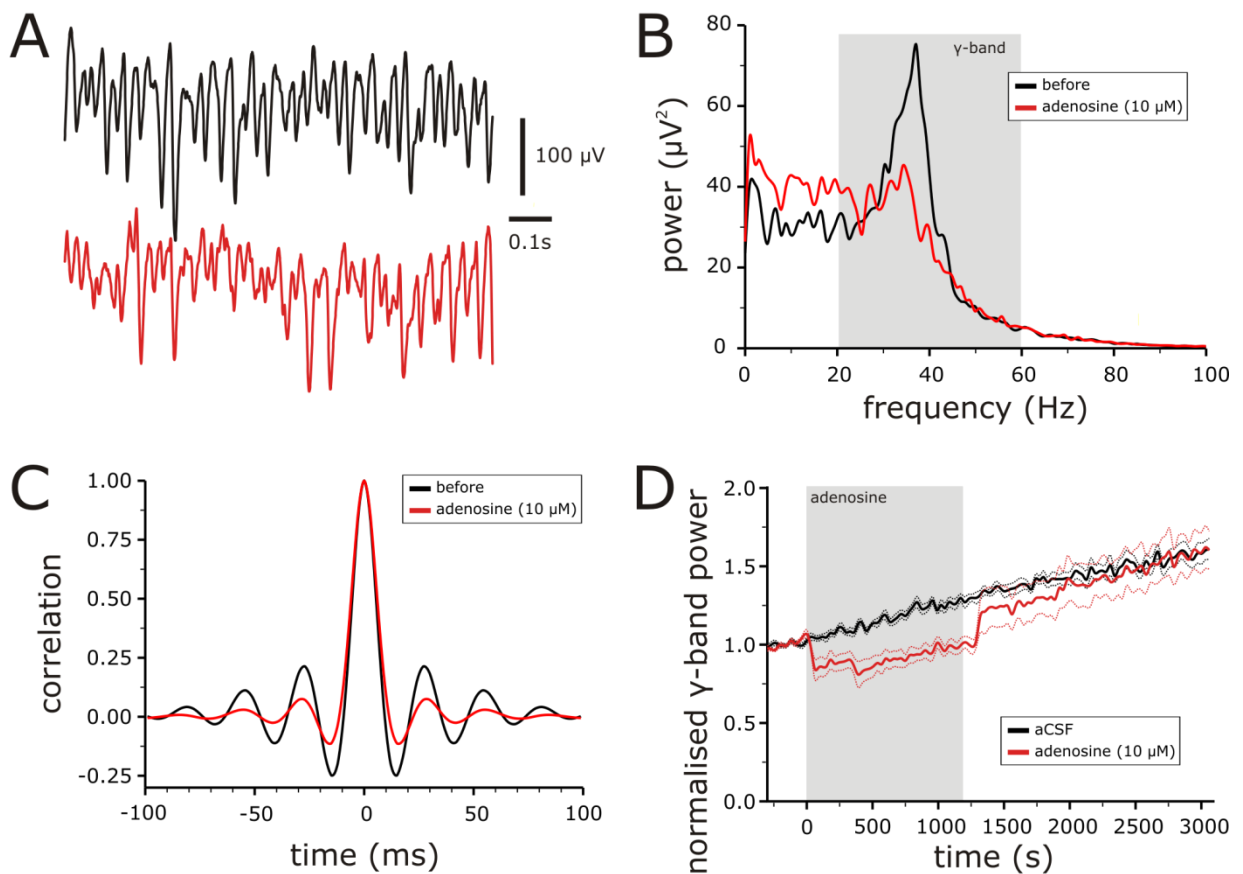
Figure 2.7. Effect of adenosine (10 µM) on KA-induced gamma oscillations. **A.** Example traces before (black) and during adenosine (10 µM) application (20 minutes). **B.** Power spectrum before and after 20 minutes of adenosine application. Adenosine decreased power in the fast and gamma bands. **C.** Autocorrelogram from the same data as the power spectrum. Adenosine decreases the second peak amplitude significantly (p=0.001). **D.** Normalised development of KA-induced gamma band power in aCSF (black lines, n=10) and in the presence of adenosine (red lines, n=8). Adenosine significantly decreased normalised gamma power after 20 minutes (p=0.0000007) compared to controls.

2.3.3. The effect of A_1- and A_{2A}-receptor modulation on KA induced hippocampal gamma oscillations.

Caffeine is a non-selective adenosine receptor antagonist that powerfully increases gamma oscillations in the hippocampus. Adenosine A_1-receptors are more abundant within the hippocampus than adenosine A_{2A}-receptors (see introduction Table 1.1). This means that a

non-selective antagonist will activate both receptors but the effects seen are most likely caused by the A_1-receptor. It is therefore expected that antagonizing the adenosine A_1-receptor will increase gamma oscillations.

The selective adenosine A_1-receptor antagonist 8-CPT (5 µM) increased KA-induced gamma oscillations in a similar way as caffeine. There is an increase in the oscillatory activity (Figure 2.8.A). The power spectrum (Figure 2.8.B) there is an increase in power within the gamma range. The increase in the gamma range is mainly around the dominant frequency creating a sharp peak. Also visible is the appearance of a harmonic at double the dominant frequency (around 68 Hz) which increases the power in the fast frequency band. The power in the lower frequency bands also increases but not as much as in the gamma range. The appearance of a sharp peak in the gamma band already indicates that the oscillation became more regular. The increase in regularity is also visible through the increased second peak amplitude in the autocorrelogram (Figure 2.8.C). After 20 minutes 8-CPT significantly increased gamma band power to 3.96±0.91 (n=6) times starting values while aCSF controls only increased to 1.21±0.05 (n=10) times starting values (Student's t-test, U_{14}=-5.0, p=0.013). The specific adenosine A_1-receptor agonist N6-(2-phenylisopropyl)adenosine (PIA) has the opposite effect of 8-CPT and decreases KA-induced hippocampal gamma oscillations (Pietersen et al., 2009a).

Adenosine A_{2A}-receptors are less abundant in the hippocampus than A_1-receptors but they are located at similar sites (see introduction, (Cunha et al., 1994;Sebastiao and Ribeiro, 1996). Adenosine A_{2A}-receptors have been shown to have the opposite effect of adenosine A_1-receptors partly due to direct inhibition of A_1-receptors (Lopes et al., 1999). To test whether adenosine A_{2A}-receptors can modulate KA-induced gamma oscillations the
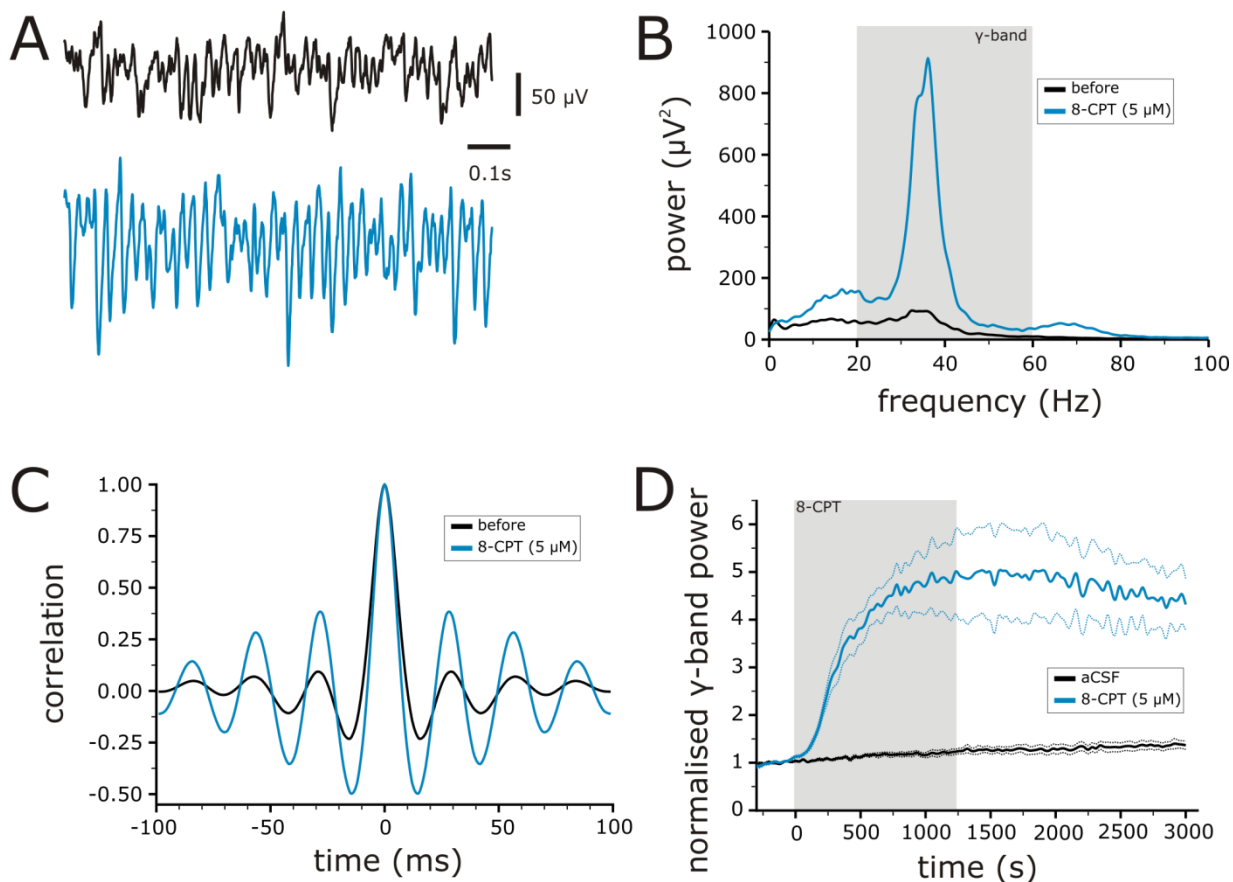
Figure 2.8. Effect of 8-CPT (5 µM) on KA-induced gamma oscillations. The data for this experiment were acquired by Nisha Patel. **A.** Example traces before (black) and during 8-CPT (blue, 5 uM) application (20 minutes). 8-CPT increased synchronous network activity. **B.** Power spectrum before and after 20 minutes of 8-CPT application. 8-CPT increased power in the gamma band. **C.** Autocorrelogram from the same data as the power spectrum. 8-CPT increased the second peak amplitude. **D.** Normalised development of KA-induced gamma band power in aCSF (black lines, n=10) and in the presence of 8-CPT (blue lines, n=6). 8-CPT significantly increased normalised gamma power after 20 minutes (p=0.013) compared to controls.

specific A_{2A}-receptor agonist CGS21680 (20 nM) was added to the aCSF. CGS21680 slightly increased the amplitude of recorded network events (Figure 2.9.A). The power spectrum (Figure 2.9.B) shows a minor increase in power within the gamma range mainly around the dominant frequency. Also both lower frequency bands show a small increase in power in this example. The second peak amplitude in the autocorrelogram (Figure 2.9.C) increased

slightly. After 20 minutes the power within the gamma band was significantly increased to 1.99±0.16 (n=8) times starting values while controls only increased to 1.27±0.05 (n=8) times starting values (Student's *t*-test, U_{14}=-4.2, *p*=0.001). The adenosine A_{2A}-receptor antagonist ZM241385 slightly reduced KA induced gamma oscillations (Pietersen et al., 2009a).
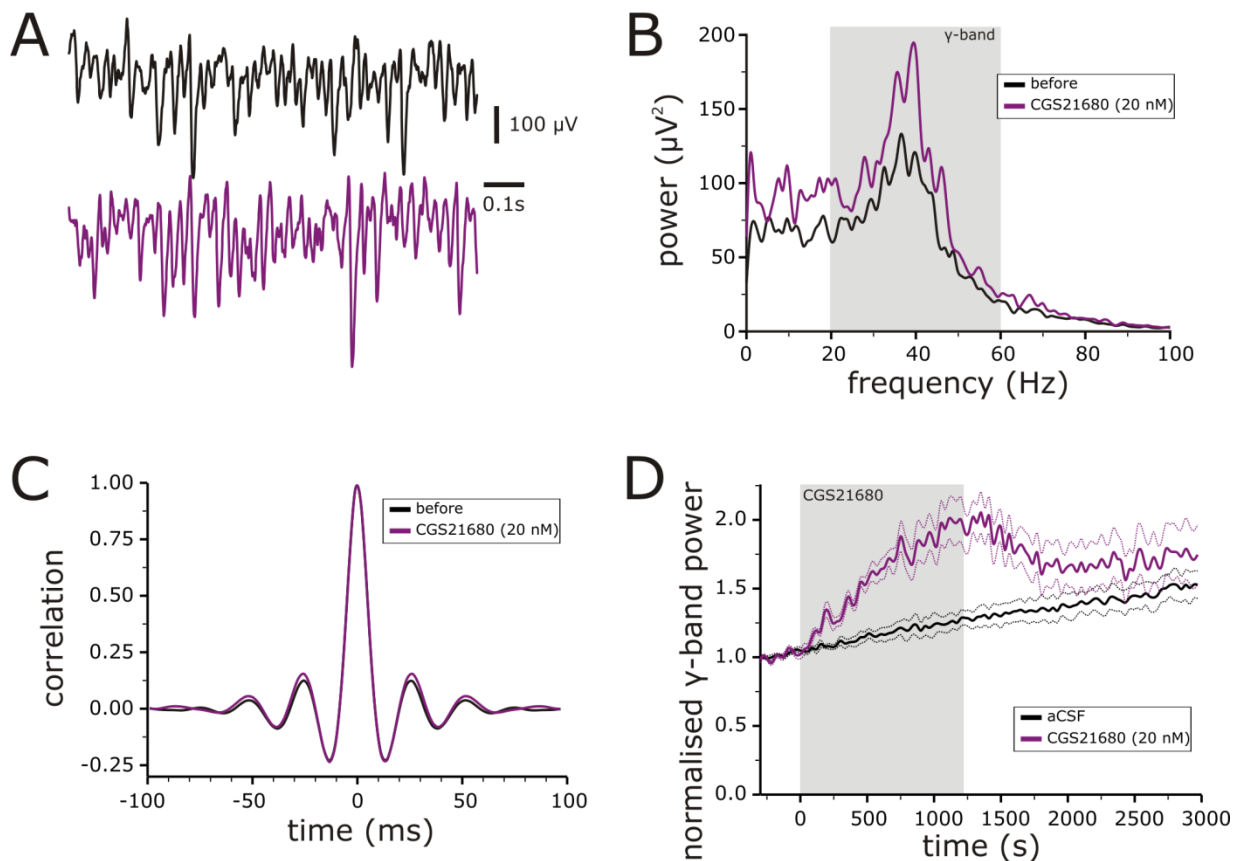
Figure 2.9. Effect of CGS21680 (20 nM) on KA-induced gamma oscillations. The data for this experiment were acquired by Dominic Lancaster. **A.** Example traces before (black) and during CGS21680 (purple, 20 nM) application (20 minutes). CGS21680 slightly increased synchronous network activity. **B.** Power spectrum before and after 20 minutes of CGS21680 application. CGS21680 increased power in the gamma band. **C.** Autocorrelogram from the same data as the power spectrum. CGS21680 marginally increased the second peak amplitude. **D.** Normalised development of KA-induced gamma band power in aCSF (black lines, n=8) and in the presence of CGS21680 (purple lines, n=8). CGS21680 significantly increased normalised gamma power after 20 minutes (p=0.001) compared to controls.

Both adenosine A_1-receptor and A_{2A}-receptor modulation alter KA induced hippocampal gamma oscillations. Where A_1-receptor activation reduces gamma oscillations A_{2A}-receptor activation slightly increases gamma oscillations. With the effects of A_1-receptor modulation being much stronger, the effects of a mixed agonist or antagonist will be mainly due to the A_1-receptor modulation.

2.3.4. The effect of adenosine receptor modulation on spontaneous gamma oscillations.

Adenosine levels in hippocampal slices in normal aCSF fall within the physiological range *in vivo* (Ballarin et al., 1991;Dunwiddie and Diao, 1994). To test if adenosine receptor modulation can also affect gamma oscillations under physiological conditions the effects of adenosine and 8-CPT were tested on spontaneous gamma oscillations.

Similarly to the other models, adenosine (50 µM) decreased the oscillation amplitude (Figure 2.10.A) and reduced the power within the gamma band mainly around the dominant frequency (Figure 2.10.B). The autocorrelogram (Figure 2.10.C) shows a slowing down of the oscillation and a reduction in regularity as a decrease in second peak amplitude. The average dominant frequency in spontaneous gamma oscillations was 32.2±1.0 Hz (n=15). In contrast to the KA and CCH induced models the power over time decreases in spontaneous oscillations. With the decrease in power the dominant frequency also slows down. As a consequence the change in dominant frequency caused by exogenous adenosine was not different from controls (see Table 2.3). The average second peak amplitude was 0.35±0.04 (n=15). Due to the naturally slowing down of the oscillation the second peak amplitude was reduced to almost half the starting value in both adenosine and controls (see Table 2.3). Adenosine significantly decreased the power in all frequency bands (see Table 2.3). Adenosine significantly decreased the power in the gamma band to 0.47±0.04 (n=6)

times starting values (Student's t-test, U_{13}=3.1, p=0.008). The beta band was decreased to 0.74±0.07 (n=6) times starting values, significantly different from controls (1.19±0.14, n=9) (Student's t-test, U_{13}=2.5, p=0.026). The slow band significantly decreased to 0.76±0.07 (n=6) times starting (Student's t-test, U_{13}=2.4, p=0.015).
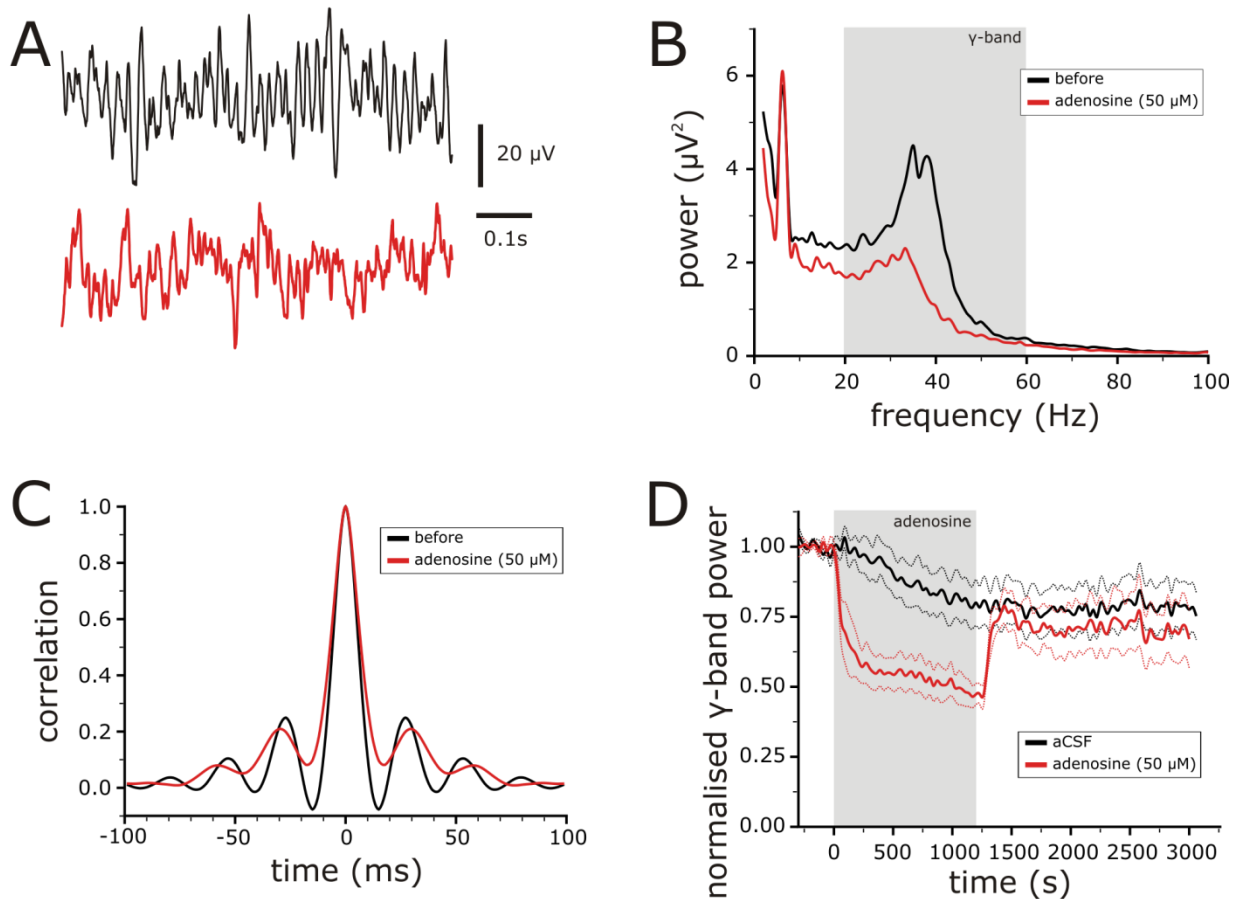
Figure 2.10. Effect of adenosine (50 µM) on spontaneous gamma oscillations. **A.** Example traces before (black) and during adenosine (red, 50 µM) application (20 minutes). **B.** Power spectrum before and after 20 minutes of adenosine application. Adenosine decreased power in the gamma range. **C.** Autocorrelogram from the same data as the power spectrum. Adenosine decreases the second peak amplitude but the change was not significantly different from the change in controls. **D.** Normalised development of spontaneous gamma band power in aCSF (black lines, n=9) and in the presence of adenosine (red lines, n=6). Adenosine significantly decreased normalised gamma power after 20 minutes (p=0.008) compared to controls.

The power in the fast band significantly reduced to 0.78±0.06 (n=6) times starting values (Mann Whitney U-test, U=9.0, p=0.034). The average gamma/beta ratio was 0.82±0.06 (n=15). There was no difference between the change in gamma/beta ratio between controls and adenosine (see Table 2.3).

Just as with KA-induced gamma oscillations 8-CPT increased the spontaneous oscillation power specifically in the gamma range. The raw traces show an increase in signal amplitude (Figure 2.11.A) after 20 minutes of 8-CPT (5 μM) application. The power spectrum shows an increase in power in all frequency bands but most noticeably around the dominant frequency (Figure 2.11.B), which falls within the gamma range. Also visible is the appearance of a small harmonic in the fast frequency band. With the specific increase in power around the dominant frequency the oscillations becomes more specific. This is visible in the autocorrelogram through increased second peak amplitude (Figure 2.11.C). The power in the gamma band rises rather quickly but contrary to the KA-induced model, in spontaneous oscillations the power does not keep increasing but goes down a bit and then levels off during 8-CPT application (Figure 2.11.D). After 20 minutes of 8-CPT application the power in the gamma band increased to 4.42±0.59 (n=7) times the starting values. This is a significant increase compared to controls as in aCSF controls the power decreases to 0.80±0.04 (n=7) times the starting values (Student's t-test, $U_{6.1}$=-6.1, p=0.001).

Adenosine receptors can modulate gamma oscillations under condition where adenosine levels fall within the physiological range.
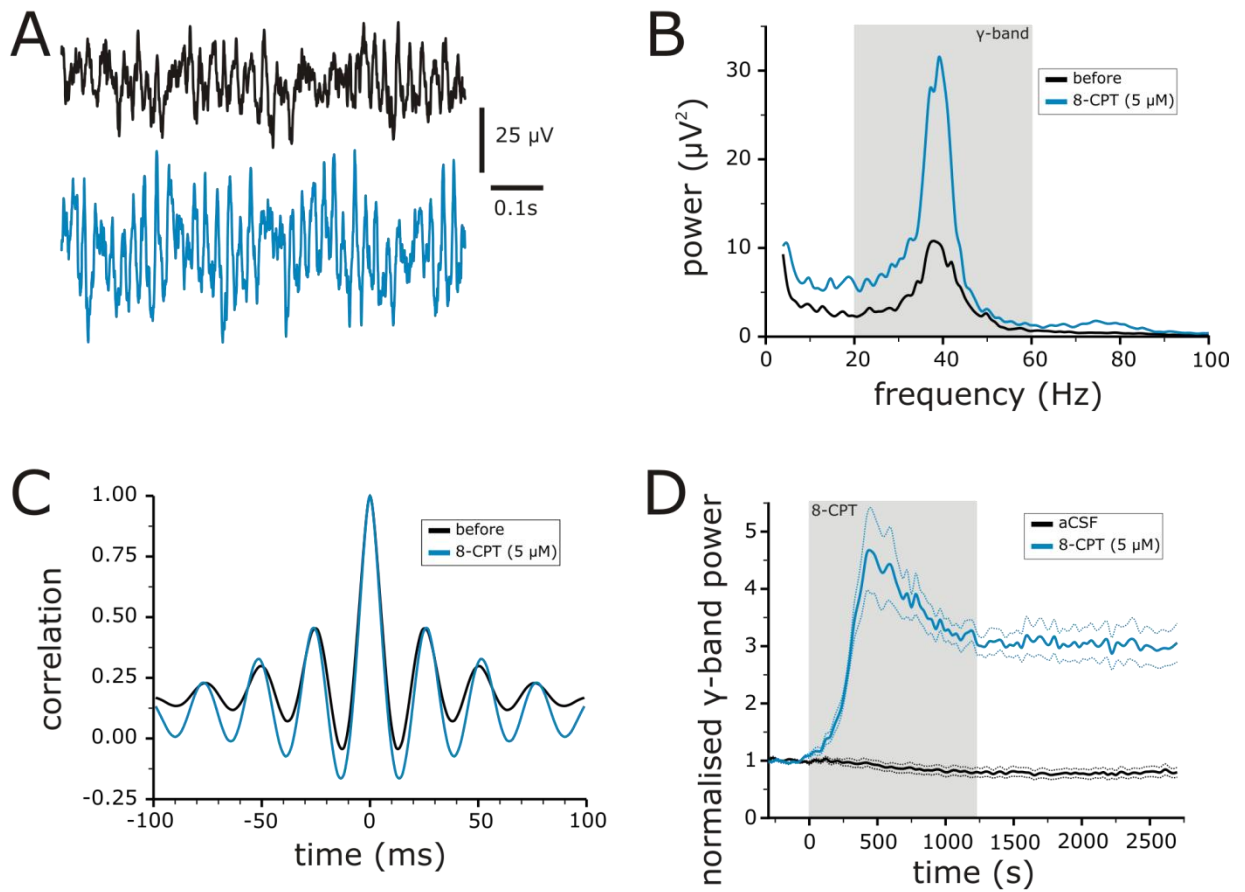
Figure 2.11. Effect of 8-CPT (5 μM) on spontaneous gamma oscillations. The data for this experiment were acquired by Nisha Patel. **A.** Example traces before (black) and during 8-CPT (blue, 5 μM) application (20 minutes). 8-CPT increased synchronous network activity. **B.** Power spectrum before and after 20 minutes of 8-CPT application. 8-CPT increased power in the gamma band. **C.** Autocorrelogram from the same data as the power spectrum. 8-CPT increased the second peak amplitude. **D.** Normalised development of spontaneous gamma band power in aCSF (black lines) and in the presence of 8-CPT (blue lines). 8-CPT significantly increased normalised gamma power after 20 minutes (p=0.001) compared to controls.

2.4. Discussion.

Adenosine receptor modulation alters hippocampal network oscillations especially in the gamma range in three different types of models. Adenosine A_1-receptor activation reduces gamma oscillations. It has been reported that the adenosine A_{2A}-recepter antagonist ZM241385 slightly reduces gamma oscillation power (Pietersen et al., 2009a). Conversely, the adenosine A_1-receptor antagonist PIA (Pietersen et al., 2009a) and A_{2A}-receptor agonist CGS21680 increase gamma oscillation power. CGS21680 has a 180-fold greater affinity for A_{2A}-receptors than A_1-receptors (K_D-value, 16 nM), (Jarvis et al., 1989) making a strong case that A_{2A}-receptor agonists on their own can also increase hippocampal gamma oscillations. In the hippocampus non-selective adenosine agonists and antagonists seem to work mainly through the A_1-receptor. Care has to be taken to extrapolate these results to other brain areas as adenosine receptor distribution might be different than in the hippocampus making it well possible that a non-selective agonist or antagonist can have the opposite effect as described in this chapter.

The modulation of gamma oscillations by adenosine receptors is not model specific as in all three models investigated similar results were obtained. Even though there are differences between different models in physiological properties (Pietersen et al., 2009b), adenosine receptors can alter gamma oscillations in all models. This points to a general mechanism of action of adenosine receptor induced modulation of gamma oscillations.

Adenosine activates both A_1- and A_{2A}-receptors, but A_1-receptors are more abundant in the hippocampus (see introduction Table 1.1, (Fredholm et al., 2005) and adenosine has a higher affinity for the A_1-receptor ((Dunwiddie and Masino, 2001), introduction Table 1.1). Even though A_{2A}-receptors have the opposite effect of A_1-receptors partly, through direct inhibition of A_1-receptors (Lopes et al., 1999), the predominant effect of adenosine is a

decrease in gamma oscillation power through A_1-receptor activation. Similarly the non-selective antagonist caffeine will exert its effects mainly through the A_1-receptor and increase gamma oscillation power at the concentration used in the described experiments. The strong increase of gamma oscillations caused by caffeine or the selective A_1-receptor antagonist 8-CPT (8-CPT has a 1000-fold higher potency in the rat over A_{2A}-receptors, K_D-value, 4 nM (Klotz, 2000)) indicates that ambient extracellular adenosine levels suppress gamma oscillations. Adenosine levels in the slice are estimated between 30 and 300 nM (Dunwiddie and Diao, 1994;Fredholm et al., 2001). With the high affinity of adenosine for the adenosine A_1-receptor (K_d 10-70 nM, (Dunwiddie and Masino, 2001;Huber et al., 2001); introduction Table 1.1), ambient adenosine levels will be able to activate adenosine receptors and suppress of brain oscillations.

Adenosine also acts as a neuroprotector (Cunha, 2001). Adenosine is released in high quantities during energy challenging circumstances like hypoxia (Frenguelli et al., 2003;Winn et al., 1981). Like the high concentration of adenosine (200 µM), hypoxia quickly and dramatically reduces gamma oscillations (Fano et al., 2007;Huchzermeyer et al., 2008), most likely through increased adenosine levels (Pietersen et al., 2009a). With such a big influence on neuronal activity it is no surprise that adenosine levels are tightly regulated in the brain. Adenosine levels are kept in check by the intracellularly located adenosine kinase, which has a high affinity for adenosine (Dunwiddie and Masino, 2001;Lloyd and Fredholm, 1995); see introduction. When adenosine levels rise substantially and adenosine kinase can not clear the excess adenosine, adenosine deaminase (ADA), which has a lower affinity for adenosine, helps to bring adenosine levels down to normal (Dunwiddie and Masino, 2001;Lloyd and Fredholm, 1995). Because of this tight control of adenosine levels, rather high concentrations of exogenous applied adenosine need to be given to suppress gamma oscillations *in vitro*. The lower adenosine concentrations (10 and 50 µM) suppressed the

gamma band without significantly affecting the lower frequency bands. The change in fast frequency band power is linked to the gamma band power in almost all experiments. We take the gamma band from 20 to 60 Hz but very often the tail of the power in the gamma range is slightly beyond 60 Hz (see Figure 2.1.B). If we indeed are looking at the same event a reduction of power in the gamma range will then also reduce power within the fast band.

At concentrations achieved by normal coffee consumption (1-10 µM) (Fredholm et al., 1999) caffeine increases hippocampal gamma oscillations *in vitro* via A_1-receptor antagonism. Gamma oscillations have been linked to cognitive performance and thus could be one of the ways caffeine increases alertness and cognitive function (Fredholm et al., 1999;Lorist and Tops, 2003). Differences in adenosine receptor distribution between A_1- and A_{2A}-receptors can give mixed effects as A_{2A}-receptor antagonists increase gamma oscillations (Pietersen et al., 2009a). Also numerous side effects can be a result of adenosine A_{2A}-receptor activation (Fredholm et al., 1999).

Adenosine levels fluctuate with neuronal activity (Dunwiddie and Masino, 2001) and circadian rhythm (Huston et al., 1996) which could have an effect on the amount of gamma oscillations possible at a given moment during the day. Thus during periods where adenosine levels are low cognitive function would be more efficient compared to periods where adenosine levels are high. The rise in adenosine levels during waking may not occur in all brain areas as some regional differences have been proposed (Haas and Selbach, 2000). Adenosine levels increase with age through increased 5'-nucleotidase activity (Mackiewicz et al., 2006;Sperlagh et al., 1997), which could have an effect on gamma oscillations strength within an aged brain. Increased adenosine levels could be partly responsible for the mild memory impairment associated with normal ageing. This is further

substantiated by an age-related decrease in gamma oscillations in the mouse hippocampus *in vitro* (Driver et al., 2007;Vreugdenhil and Toescu, 2005).

Even a central nervous system specific A_1-receptor antagonist is very likely to have many side effects due to the abundance of adenosine receptors throughout the brain (Fredholm et al., 1999). The best strategy for increasing gamma oscillations would be to find a compound that is an A_1-receptor antagonist and an A_{2A}-receptor agonist. Understanding more about the underlying mechanisms could possibly provide other targets to prevent cognitive decline with age or enhance cognitive performance. An alternate strategy for age associated memory impairment would be to reduce basal adenosine levels.

2.5. Future research.

If controlling adenosine levels could be a potential therapeutic target it is important to investigate if changes in endogenous adenosine levels can modulate gamma oscillations. This will be done in the chapter 3.

Adenosine A_1-receptor activation has been shown to inhibit vesicle release which could be one of the ways gamma oscillations are suppressed. In chapter 4 and 5 the cellular and synaptic changes underlying the observed network changes through A_1-receptor modulation will be investigated.

In chapter 6 all the *in vitro* findings will be assessed in anaesthetised animals.

Parameter		Parameter value	Control	Adenosine (50 µM)	Caffeine (50 µM)
Model		CCH	CCH	CCH	CCH
Normalised power		*n=18*	*n=6*	*n=7*	*n=5*
Gamma (20-60 Hz)	Mean	76.2	1.20	**0.61**	**3.08**
	SEM	16.8	0.09	0.12	0.28
Beta (8-20 Hz)	Mean	41.5	1.09	0.85	**2.31**
	SEM	8.9	0.05	0.10	0.28
Slow (3-8 Hz)	Mean	44.4	1.04	0.93	**1.56**
	SEM	8.9	0.03	0.12	0.12
Fast (60-100 Hz)	Mean	6.0	1.15	**0.60**	**3.06**
	SEM	1.1	0.11	0.11	0.20
ΔGamma/beta ratio	Mean	1.84	0.19	**-0.59**	0.68
	SEM	0.18	0.10	0.29	0.36
Δdominant frequency (Hz)	Mean	34.8	-1.11	-2.19	-1.38
	SEM	0.5	0.31	0.81	0.66
Normalised autocorrelation					
2nd peak amplitude	Mean	0.80	1.08	**0.69**	1.24
	SEM	0.05	0.03	0.07	0.09

Table 2.1. Effect of adenosine receptors on CCH-induced hippocampal gamma oscillations. Bold numbers indicate significant differences ($p<0.05$) compared to controls. Power parameter value is in μV^2. All other columns are normalized data.

Parameter		Parameter value	Control	Adenosine (10 µM)	Adenosine (50 µM)	Adenosine (200 µM)	Control	8-CPT (5 µM)	Control	CGS21680 (20 nM)
Model		KA	KA	KA	KA	KA	KA	KA	KA	KA
Normalised power		*n=30*	*n=10*	*n=8*	*n=9*	*n=3*	*n=10*	*n=6*	*n=8*	*n=8*
Gamma (20-60 Hz)	Mean	43.7	1.42	**1.00**	**0.90**	**0.13**	1.21	**3.96**	1.27	**1.99**
	SEM	7.1	0.03	0.04	0.08	0.07	0.05	0.91	0.05	0.16
Beta (8-20 Hz)	Mean	42.5	1.33	1.27	1.17	**0.56**				
	SEM	5.9	0.04	0.08	0.09	0.04				
Slow (3-8 Hz)	Mean	34.7	1.22	1.30	1.16	1.07				
	SEM	5.4	0.03	0.09	0.08	0.64				
Fast (60-100 Hz)	Mean	3.9	1.45	**1.02**	**0.92**	**0.28**				
	SEM	0.6	0.04	0.05	0.06	0.12				
ΔGamma/beta ratio	Mean	0.98	0.03	**-0.22**	**-0.28**	**-0.54**				
	SEM	0.05	0.03	0.04	0.06	0.11				
Δdominant frequency (Hz)	Mean	36.0	0.5	-4.2	**-6.0**	-13.5				
	SEM	0.8	0.9	1.6	1.2	2.4				
Normalised autocorrelation										
2nd peak amplitude	Mean	0.34	1.06	**0.56**	**0.45**	**0.02**				
	SEM	0.02	0.11	0.05	0.04	0.02				

Table 2.2. Effect of adenosine receptors on KA-induced hippocampal gamma oscillations. Bold numbers indicate significant differences (p<0.05) compared to controls. Power parameter value is in μV^2. All other columns are normalized data.

Parameter		Parameter value	Control	Adenosine (50 µM)	Control	8-CPT (5 µM)
Model		spontaneous	Spontaneous	Spontaneous	Spontaneous	spontaneous
Normalised power		*n=15*	*n=9*	*n=6*	*n=7*	*n=7*
Gamma (20-60 Hz	Mean	4.0	0.80	**0.47**	0.80	**4.42**
	SEM	0.6	0.08	0.04	0.04	0.59
Beta (8-20 Hz)	Mean	5.0	1.19	**0.74**		
	SEM	0.7	0.14	0.07		
Slow (3-8 Hz)	Mean	6.1	1.19	**0.76**		
	SEM	0.7	0.14	0.07		
Fast (60-100 Hz)	Mean	0.3	1.10	**0.78**		
	SEM	0.1	0.15	0.06		
ΔGamma/beta ratio	Mean	0.82	-0.25	-0.33		
	SEM	0.06	0.04	0.08		
Δdominant frequency (Hz)	Mean	32.2	-6.5	-5.3		
	SEM	1.0	1.0	1.0		
Normalised autocorrelation						
2nd peak amplitude	Mean	0.35	0.54	0.55		
	SEM	0.04	0.04	0.12		

Table 2.3. Effect of adenosine receptors on spontaneous hippocampal gamma oscillations. Bold numbers indicate significant differences (p<0.05) compared to controls. Power parameter value is in μV^2. All other columns are normalized data.

CHAPTER 3: ENDOGENOUS ADENOSINE LEVELS MODULATE GAMMA OSCILLATIONS.

3.1. Introduction.

In the previous chapter the effects of exogenous adenosine and blockage of specific adenosine receptors on gamma oscillations showed that adenosine receptors are potent modulators of *in vitro* brain oscillations specifically in the gamma band. In this chapter the effect of endogenous adenosine levels on KA induced gamma oscillations are investigated. Ambient adenosine levels are estimated to be between 30 and 300 nM in hippocampal slices *in vitro* (Dunwiddie and Diao, 1994;Fredholm et al., 2001) which falls well within the physiological range measured *in vivo*. The adenosine concentration measured through microdialysis in awake rats in the extracellular space is 40 nM with elevation up to 460 nM (Ballarin et al., 1991). With the high affinity of adenosine for the adenosine A_1-receptor (K_d 10-70 nM, (Dunwiddie and Masino, 2001), introduction table 1.1), ambient adenosine levels will be able to activate adenosine receptors and give a constant suppression of brain oscillations. Adenosine levels fluctuate and follow a circadian rhythm (Fredholm et al., 1999), which means that the amount of suppression can vary endogenous adenosine levels. Adenosine levels in the extracellular space in the brain are determined by the formation of adenosine from AMP through 5' ecto-nucleotidases, the breakdown of adenosine by ecto-adenosine deaminase and transport of adenosine to the cytoplasm, usually through equilibrium nucleoside transporters, of neurons and glial cells (for review see (Dunwiddie and Masino, 2001)). Intracellular adenosine concentration is determined by influx from the extracellular space, production by 5' nucleotidases and removal by predominantly adenosine kinase. The intracellularly located adenosine kinase largely determines the adenosine concentration under normal physiological circumstances (Dunwiddie and Masino, 2001;Lloyd and Fredholm, 1995). Adenosine deaminase (ADA) has a low affinity for adenosine

(Fredholm et al., 1999;Latini and Pedata, 2001). When adenosine levels rise under energy demanding situations, like hypoxia or an epilepsy seizure, ADA will help break down the excess adenosine to bring adenosine concentrations back down to normal values. In this chapter production and breakdown of adenosine are modulated to alter ambient adenosine concentrations in order to see whether this affects gamma oscillations. First adenosine kinase is blocked using 5-iodotubericidin (5-IT, K_i-value 30 nM, see Figure 1.1), which will increase the intracellular adenosine concentration and subsequently the extracellular adenosine concentration will rise due to transport from the cytosol to the extracellular space through equilibrium transporters. The rise in extracellular adenosine is expected to suppress brain oscillations, specifically in the gamma band. To lower adenosine concentration we first need to make sure extracellular adenosine will not be replenished from the cytosol which means the equilibrium transporters need to be blocked. In the hippocampus the equilibrative nucleotide transporter 1 (ENT-1) is abundantly present and the major equilibrium transporter involved in regulating adenosine concentrations (Dunwiddie and Masino, 2001). After blocking ENT-1, ADA is added to decrease extracellular adenosine concentrations, which is predicted to increase brain oscillations, specifically in the gamma band.

3.2. Materials and methods.

3.2.1. Tissue preparation.

Slices were prepared via the same methods as chapter 2.

3.2.2. Electrophysiological recordings.

Recordings were done the same as in chapter 2.

Drugs were diluted from the following stock solutions: 5-iodotubericidin (5-IT, 1 mM stock in DMSO), S-(4-nitrobenzyl)-6-thioinosine (NBTI, 100 mM in DMSO) and adenosine deaminase type 5 (ADA, 160 U/ml in 50% glycerol, 50 mM K_2PO_4). In experiments where ADA was used aCSF was made without K^+ and a solution of 50% glycerol and 20 mM K_2PO_4 was added to the aCSF in the same volume as was needed to dilute to the used ADA concentration. In the ADA experiments NBTI was added 10 minutes before the point drugs were added in all experiments (i.e. 50 minutes after KA application). Washout was done in the presence of NBTI.

3.2.3. Analysis and statistics.

Statistical analysis was done via the same methods described in chapter 2.

3.3. Results.

3.3.1. Increasing endogenous adenosine levels.

All experiments are done using the KA-induced model of gamma oscillations. To increase endogenous adenosine levels adenosine kinase was inhibited by 5-IT. At high concentrations (1 µM) 5-IT almost completely blocked all oscillatory activity (see Table 3.1). At a low concentration of 0.1 µM, 5-IT showed a delayed effect. 5-IT was applied for 20 minutes, but its biggest effect was seen 10 minutes into washout (Figure 3.1.D). The raw trace shows a small reduction in signal size (Figure 3.1.A) after 20 minutes of 5-IT application. The accompanying power spectrum (Figure 3.1.B) shows a loss of the peak in the gamma band while there is a small increase in the beta band after 20 minutes. The power in the gamma band after 20 minutes of 5-IT application hardly changed from the start of drug application (1.02±0.09, n=6) while controls showed a steady growth to 1.28±0.03 (n=10) times the starting value. This was a significant difference between groups (Student's *t*-test, $t_{5.7}$ =2.7, *p*=0.039). The normalised development over time shows that it takes a while for 5-IT to have its effect (Figure 3.1.D). For the first five minutes the 5-IT treated slices have the same development as controls. By the end of the 20 minute drug application the normalised power is reduced to starting values. The same downward trend continues while 5-IT is washed out and the biggest difference is around 30 minutes after drug application (which is 10 minutes into washout). At 30 minutes the power in the gamma band is reduced to 0.93±0.11 (n=6) times the starting value, while controls keep growing steadily to 1.42±0.03 (n=10) the starting value (Student's *t*-test, t_6 =4.4, *p*=0.005). At 30 minutes the normalised power in the slow and beta bands are not significantly different from controls (see Table 4.1), while the fast band power is reduced to 0.89±0.09 (n=6) times the baseline. Significantly different from controls which show an increase to 1.45±0.04 (n=10)
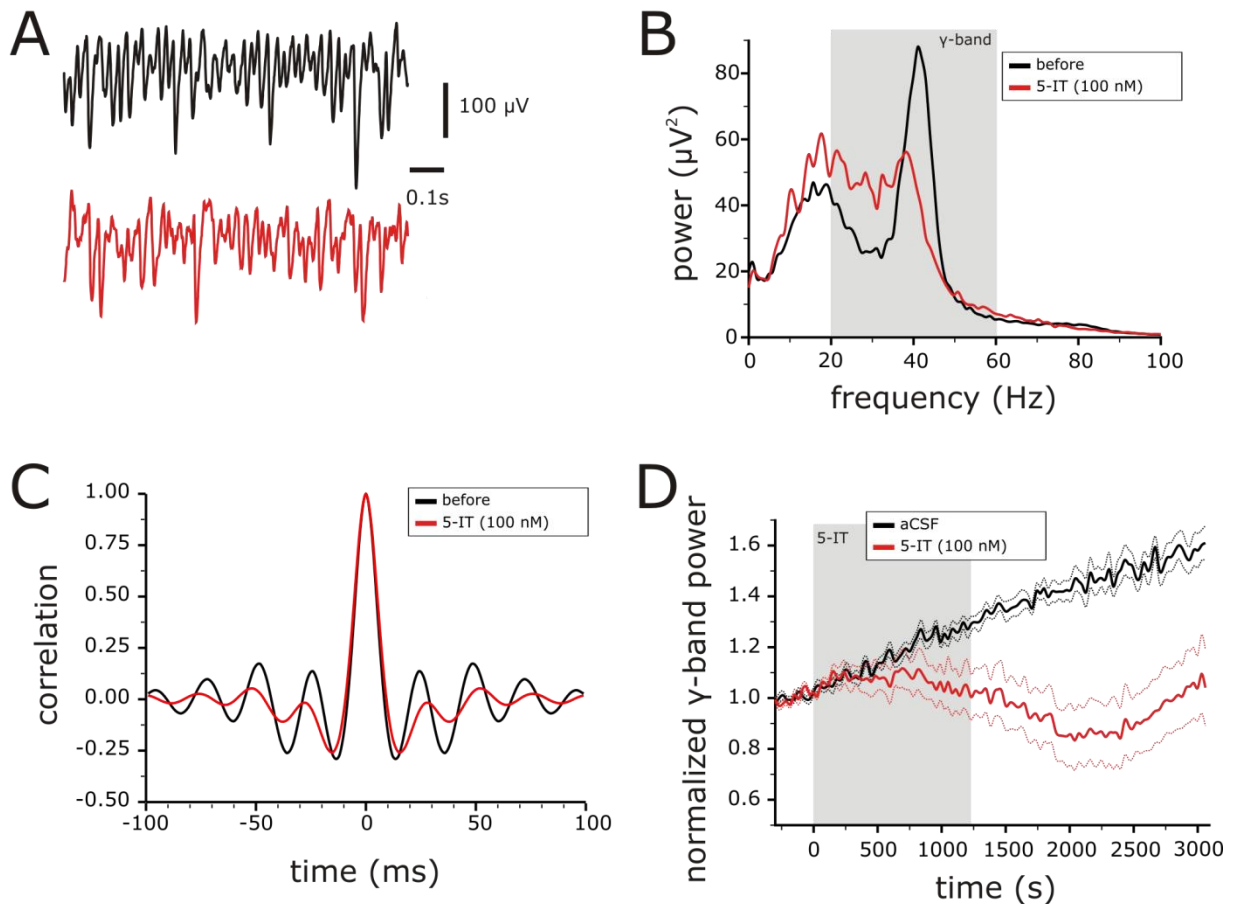
Figure 3.1. Effect of increasing endogenous adenosine levels on KA induced gamma oscillations. **A.** Raw trace of one second before (black line) during 100 nM 5-IT application (red line, 20 minutes). 5-IT causes a small reduction in signal size. **B.** Power spectrum of 300s before (black) and in the presence of 5-IT (red, 20 minutes). The peak in the gamma range reduces in size while the power in the frequencies below the peak increases slightly. The dominant frequency shifts to a slower frequency as well. Grey area indicates the gamma band. **C.** Autocorrelogram from the same data the power spectrum was taken. 5-IT reduces the amplitude of the second peak (red) after 20 minutes compared to before drug application (black). The shift in dominant frequency is also visible in the autocorrelogram through an increase in time to the second peak. **D.** Change of the normalised power in the gamma band. Data was normalised to 5 minutes before 5-IT application. Controls show a steady growth (black, n=10) while 5-IT (red, n=6) initially follows the control development it reduces the power in the gamma band. The downward trend continues even when washout has already started which causes the biggest effect to be around 30 minutes after drug application (10 minutes into washout).

times starting values (Student's t-test, t_{14} =6.3, p=0.00002). In controls the power in all

frequency bands grows at the same rate which creates a steady value for the gamma/beta

ratio. The average gamma/beta ratio was 0.98±0.08 (n=21). During 5-IT application the gamma band is affected much more than the beta band causing the change in gamma/beta ratio to become negative 30 minutes after application, -0.44±0.12 (n=6), which is a significant reduction in gamma/beta ratio compared to controls, 0.06±0.03 (n=10) (Student's t-test, $t_{5.6}$ = 4.1, p=0.008). The average dominant frequency was 35.4±1.1 Hz (n=21). The loss of the peak in the gamma band shifts the dominant frequency by -10.4±3.2 Hz (n=6) in 5-IT exposed slices. This is significantly different from controls as the change in dominant frequency in controls is 0.28±1.49 Hz (n=10), (Mann-Whitney U-test, U=5.0, p=0.007). The change in dominant frequency can also be seen in the autocorrelogram as the time of the second peak is later in the presence of 5-IT compared to before 5-IT was added. The autocorrelation also says something about the regularity of the oscillation. There is a clear reduction in the amplitude of the second peak in the presence of 5-IT after 20 minutes (data from the same period as the power spectrum, Figure 3.1.C) indicating that the oscillation becomes less regular. The second peak reduces to 0.46±0.03 (n=6) times the starting value 30 minutes after 5-IT application while in controls there is a small increase to 1.16±0.15 (n=10) times the starting value (Mann-Whitney U-test, U=0.0, p=0.001).

The adenosine kinase blocker 5-IT decreased brain oscillations in the gamma band and the fast band, slowed down the oscillation and decreased regularity.

3.3.2. Decreasing endogenous adenosine levels.

To reduce endogenous adenosine levels ADA was added to the aCSF. ADA on its own gave varying results. In some slices ADA increased gamma oscillations, while in other slices ADA

decreased gamma oscillations. This average effect was non-significant increase with a large

error bar (see Table 3.1). To prevent replenishment of adenosine from the cytosol, the
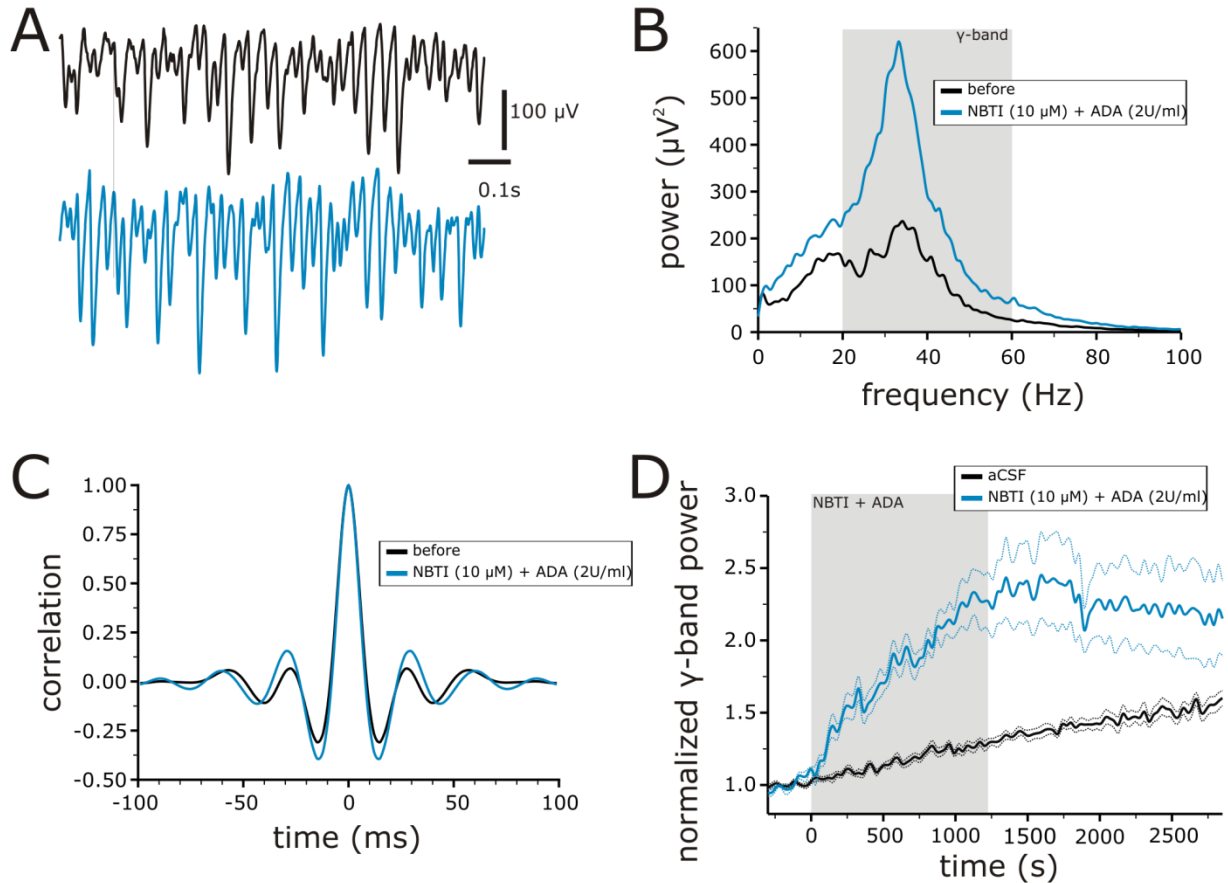
Figure 3.2. Effect of decreased endogenous adenosine concentration on KA induced gamma oscillations. **A.** Raw trace before (black) and after 20 minutes NBTI (10 µM) + ADA (2 U/ml) (blue). NBTI+ADA increases signal size. **B.** Typical power spectrum of 300s before (black) and after 20 minutes NBTI + ADA (blue). Power increases in all frequency bands but mostly in the gamma range (grey area). The dominant frequency shifts slightly to slower frequencies. **C.** Autocorrelogram of the same data the power spectrum was taken. The oscillation becomes more regular visible in the increased amplitude of the second peak. **D.** Normalised gamma band power over time. Data was normalised to 300 seconds before drug application (grey area). NBTI + ADA increases the normalised gamma power to 2.25 times the starting value after 20 minutes of drug application (blue line, n=5) while controls increase to 1.29 times the starting value (black line, n=10).

equilibrium transporter ENT-1 was blocked by NBTI 10 minutes before ADA was applied. NBTI (10 µM) on its own did not change oscillatory activity in the hippocampal network (see Table 3.1). An increase in synchronous activity was observed in the raw data (Figure 3.2.A) in the presence of NBTI (10 µM) and ADA (2 U/ml) after 20 minutes. This is also visible in the power spectrum (Figure 3.2.B) through the increase of the peak in the gamma band. In the presence of NBTI and ADA the power in the gamma band increased to 2.25±0.19 (n=5) times the starting value after 20 minutes of drug application, which is a significantly bigger increase compared to controls, 1.29±0.03 (n=10) (Student's t-test, $t_{4.1}$ = -4.9, p=0.007). The power in both the slow and beta bands did not significantly increase from controls (see Table 3.1). The power in the fast band did increase significantly more than controls to 2.35±0.22 (n=5) the starting values (Student's t-test, $t_{4.2}$ = -4.7, p=0.008), see Table 3.1. The power in the gamma band increased more than the power in the beta range visible through the increase in gamma/beta ratio. The gamma/beta ratio changed by 0.47±0.07 (n=5) after 20 minutes of NBTI and ADA application, while in controls there is hardly any change, 0.03±0.03, (Student's t-test, t_{13} = -7.2, p=0.000007). The peak in the gamma band became sharper (Figure 3.2.B) making the oscillation more regular. This is reflected in the increased amplitude of the second peak in the autocorrelogram (Figure 3.2.C). The amplitude of the second peak increased to 1.48±0.1 (n=5) times its starting value while in significantly different from controls, 1.06±0.11 (n=10) times the starting value (Mann-Whitney U-test, U=5.0, p=0.014). In the example power spectrum (Figure 3.2.B) a small shift in dominant frequency was observed. On average the dominant frequency shifts by -2.14±1.42 Hz (n=5) after 20 minutes of NBTI and ADA application though this is not significantly different from the change in controls (see Table 3.1).

ADA increased brain oscillations in the gamma band and fast band and increased the regularity of the oscillation.

3.4. Discussion.

Modulation of endogenous adenosine levels powerfully affects *in vitro* gamma oscillations. Increasing extracellular adenosine levels by blocking adenosine kinase with 5-IT suppresses gamma oscillation power, distorts rhythmic activity by making the brain oscillation less regular and shifts the dominant frequency to a slower frequency. Decreasing adenosine levels by blocking ENT-1 and adding ADA to the aCSF increases gamma oscillations and increases rhythmic activity.

3.4.1. Increasing adenosine levels.

Applying a saturating dose of 5-IT (5 μM) to hippocampal slices increases basal adenosine concentrations by about 1 μM (Etherington et al., 2009). Applying a concentration of 1 μM 5-IT already blocked almost all oscillatory activity within the hippocampal network. The low dose of 100 nM 5-IT slowly starts to reduce hippocampal brain oscillations, and prolonged application significantly decreased the power in the gamma band. As a high dose of 5-IT is able to increase the amount of extracellular adenosine by 1 μM it is expected that 100 nM 5-IT will gradually increase adenosine concentration within the hundreds of nanomolar range. An increase of hundreds of nanomolar falls within the physiological variation *in vivo* (Ballarin et al., 1991). This means that natural variations in adenosine concentration can have a big impact on the amount of gamma oscillations. The effects of blocking adenosine kinase are strikingly similar to adding exogenous adenosine to the aCSF. When the increase in adenosine is small gamma oscillations are suppressed specifically. A big increase in adenosine levels, with 200 μM adenosine (Figure 2.6) or 1 μM 5-IT, blocks oscillations in all frequency bands ((Pietersen et al., 2009a), see table 3.1). The time course when using low concentrations of 5-IT is rather slow, probably because it takes some time for adenosine

concentrations to rise sufficiently high intracellularly and be transported to the extracellular space. When 5-IT is washed out it takes a long time for the system to recover and suppression of gamma oscillations continues well in to the washout with the peak effect about 10 minutes into the washout which was about 30 minutes after drug application. Given enough time slices can recover from low doses of 5-IT. The cytosolic location of adenosine kinase is most likely the reason for the slow build up and recovery. When adenosine levels rise very quickly during abnormal physiological conditions like hypoxia (Frenguelli et al., 2003;Winn et al., 1981) a reduction in gamma oscillations in observed as well (Fano et al., 2007;Huchzermeyer et al., 2008). This reduction in gamma oscillations during hypoxia can be prevented by adding 8-CPT to the aCSF (Pietersen et al., 2009a). Adenosine can also be released in an activity-dependent manner (Wall and Dale, 2008). Though the precise mechanism is not yet clear it does mean that adenosine can reduce network activity through feed-back loops. When adenosine levels rise because the network is active, the release of adenosine can suppress the effectiveness of any subsequent neurotransmission until adenosine levels are brought back to normal.

3.4.2. Decreasing adenosine levels.

Both ADA (1-2U/ml) and the ENT-1 blocker NBTI (10 µM) on their own did not have a consistent effect on gamma oscillations. Blocking ENT-1 has been shown to have no influence on adenosine levels (Wall et al., 2007). In the presence of NBTI extracellular adenosine levels cannot be replenished from the cytosol, thus ADA can lower extracellular adenosine concentrations. Reducing adenosine levels by adding ADA to the aCSF very potently increased brain oscillations specifically in the gamma band. Due to the low affinity of ADA for adenosine (Dunwiddie and Masino, 2001) increasing gamma oscillations by

reducing adenosine levels with ADA is only feasible under circumstances where adenosine levels are relatively high. When adenosine levels are low ADA has a much smaller effect on gamma oscillations (Pietersen et al., 2009a).

These results indicate that small fluctuations in adenosine levels can alter gamma oscillations and possibly also the cognitive functions related to gamma oscillations. With the increase in adenosine levels during ageing (Mackiewicz et al., 2006;Sperlagh et al., 1997) cognitive processes that decline during ageing could be boosted by lowering adenosine levels in the brain.

3.5. Future research.

To be able to say something about using adenosine levels as possible cognitive enhancers the exact adenosine concentrations that influence gamma oscillations need to be known. It would be really interesting to see how the adenosine levels correlate with the reduction in gamma oscillations. Adenosine levels can be measured accurately in hippocampal slices using an adenosine probe (Etherington et al., 2009). A possible experiment would be to use the low dose of 5-IT used in this chapter (100 nM) while recording the adenosine concentration. Then a correlation between the extracellular adenosine concentration and the degree gamma oscillations are affected can be made. Because of the slow time course seen when applying low doses of 5-IT it is possible to accurately measure adenosine concentration and gamma oscillations power. If adenosine levels rise too quickly it will be hard to determine at which concentration adenosine will start to significantly change gamma oscillations *in vitro*. A similar experiment can be done using an ENT-1 blocker and ADA. If adenosine levels drop too quickly ADA concentrations can be increased incrementally to decrease adenosine levels more slowly. These findings will have to be confirmed *in vivo* before anything can be said about adenosine levels and adenosine receptors as cognitive enhancing agents.

parameter		parameter value	control	5-IT (100 nM)	control	NBTI (10 µM) + ADA (2 U/ml)	NBTI (10 µM)	ADA (1-2U/ml)	5-IT (1 µM)
			30 min	30 min	20 min	20 min	20 min	20 min	20 min
normalised power		*n=21*	*n=10*	*n=6*	*n=10*	*n=5*	*n=10*	*n=5*	*n=9*
gamma (20-60 Hz)	Mean	44.6	1.42	**0.93**	1.29	**2.25**	1.52	1.81	**0.08**
	SEM	6.4	0.03	0.11	0.03	0.19	0.16	0.53	0.02
beta (8-20 Hz)	Mean	47.0	1.33	1.41	1.26	1.55	1.32	1.18	**0.17**
	SEM	7.8	0.04	0.11	0.04	0.14	0.12	0.34	0.03
slow (3-8 Hz)	Mean	34.4	1.22	1.29	1.20	1.76	1.27	1.44	**0.33**
	SEM	3.7	0.03	0.07	0.04	0.21	0.10	0.28	0.05
fast (60-100)	Mean	4.0	1.45	**0.89**	1.32	**2.35**	1.42	1.64	**0.15**
	SEM	0.6	0.04	0.09	0.03	0.22	0.15	0.53	0.03
Δgamma/beta ratio	Mean	0.98	0.06	**-0.44**	0.03	**0.47**			
	SEM	0.08	0.03	0.12	0.03	0.07			
Δdominant frequency	Mean	35.4	0.28	**-10.4**	0.5	-2.1			
	Sem	1.1	1.49	3.2	0.9	1.4			
normalised autocorrelation									
2nd peak amplitude	Mean	0.32	1.16	**0.46**	1.06	**1.48**			
	SEM	0.03	0.15	0.03	0.11	0.10			

Table 3.1. Effect of changes in endogenous adenosine levels on gamma oscillations. Bold numbers indicate significant differences (p<0.05) compared to controls. NBTI was given 10 minutes prior to ADA application in the experiments using both drugs.

CHAPTER 4: ADENOSINE RECEPTOR MODULATION OF CELLULAR AND SYNAPTIC PROPERTIES.

4.1. Introduction.

The effects of adenosine receptor modulation on gamma oscillations recorded through field potentials *in vitro* have been investigated in the past two chapters. Adenosine A_1-receptor agonists and A_{2A}-receptor antagonists reduce gamma oscillation strength, while adenosine A_1-receptor antagonists and A_{2A}-receptor agonists increase gamma oscillation strength. The effect of a non-specific adenosine receptor agonist (adenosine) or antagonist (caffeine) will depend on receptor distribution and receptor density in the investigated brain area. Also modulation of endogenous adenosine levels has an impact on the recorded oscillation. Increasing adenosine levels decreases oscillation strength specifically within the gamma range, while decreasing adenosine levels has the opposite effect.

In this chapter the cellular and synaptic changes that underlie the effects caused by adenosine receptor acting drug on gamma oscillations are investigated. Figure 4.1 is a simplified schematic drawing of the hippocampal network (an extension of the figure shown in the introduction, see Figure 1.3). One of the key features is the convergent input of pyramidal cells onto interneurons and the divergent output from interneurons to pyramidal cells. Adenosine receptors are widespread throughout the brain and present on both the pre- and postsynaptic membrane of pyramidal cells and interneurons (see figure 1.2). This means that adenosine receptors could possibly affect both inhibition and excitation within the hippocampal network. The numbers in Figure 4.1 show possible sites where adenosine receptors could modulate gamma oscillations. Several synaptic and cellular effects of adenosine A_1-receptor activation
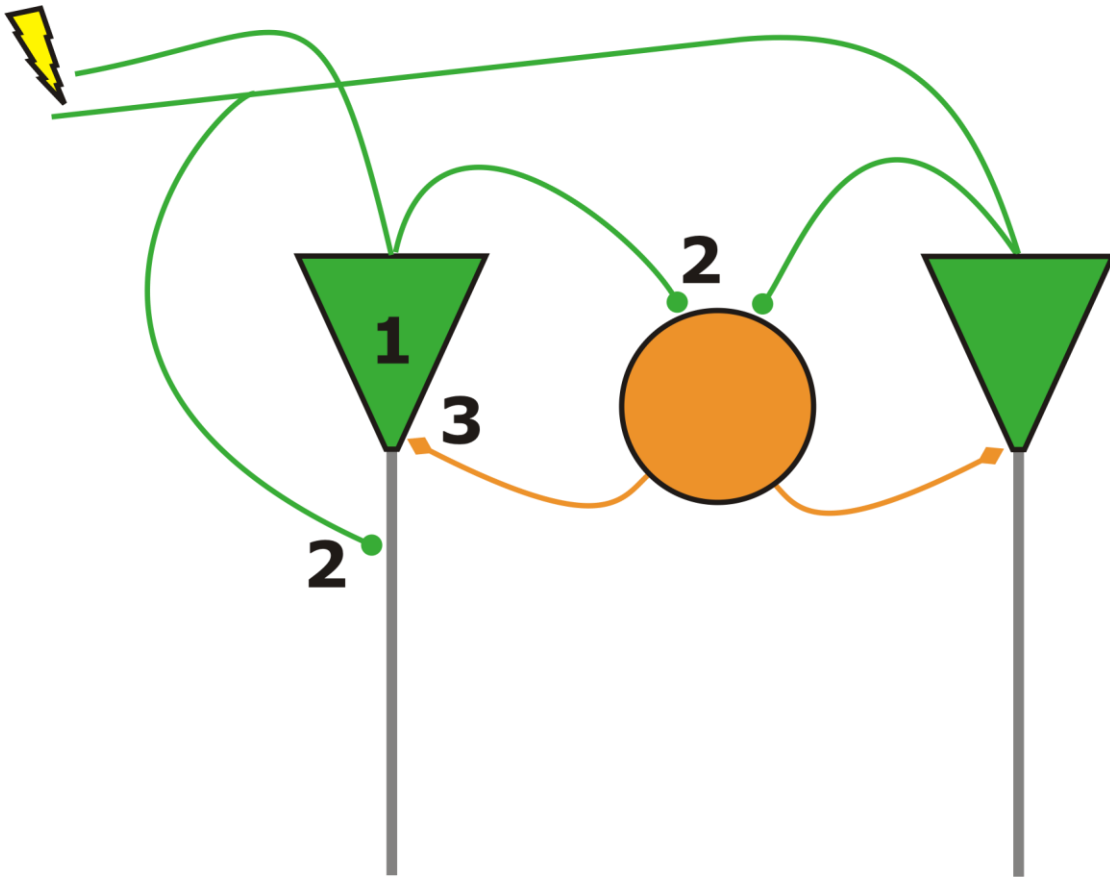
Figure 4.1. Simplified schematic drawing of a CA3c hippocampal network. The green triangular cells are pyramidal cells and the orange round cell represents an interneuron. The numbers indicate possible sites where adenosine receptor modulation can change cellular or synaptic properties that can underlie the changes observed in the field recordings. 1. cellular properties. 2. excitatory inputs. 3. inhibitory inputs. The lightning symbol represents antidromic stimulation of the Schaffer-collaterals.

have already been described in literature. Adenosine has been shown to reduce excitatory synaptic activity in various brain areas including the hippocampus (Fredholm et al., 1999;Haas and Selbach, 2000). There is evidence that adenosine A_1-receptor activation inhibits primarily N-type Ca^{2+} currents (Mogul et al., 1993) and thereby vesicle release. A hyperpolarization of the post-synaptic membrane will also reduce the effect of the released neurotransmitters. Adenosine A_1-receptors have been found to hyperpolarise the membrane potential of pyramidal cells (Haas and Selbach, 2000;Luscher et al., 1997) and interneurons

in the hippocampus (Li and Henry, 2000) through activating inward rectifying K^+ currents (Haas and Selbach, 2000). In contrast to the reduction in excitation, adenosine does not seem to affect monosynaptic inhibition, while the polysynaptic IPSP was almost totally blocked (Thompson et al., 1992).

In this chapter the effects adenosine and 8-CPT have on pyramidal cells in the hippocampus will be investigated. Adenosine and 8-CPT were chosen to be able to relate the findings in this chapter with the findings from the field recordings. The effects described in literature will be reproduced and subsequently a deeper look will be taken at other parameters that could underlie the changes observed in the previously described field recordings. Firstly, intrinsic properties will be studied. It is expected that adenosine will activate G-protein Inward Rectifying K^+-channels (GIRK channels) and thereby increase the flow of K^+ ions across the membrane causing a hyperpolarization of the membrane potential. Secondly, both excitatory and inhibitory synaptic properties will be looked at. It is expected adenosine will reduce excitatory synaptic transmission, though the underlying cellular mechanisms will not be studied. With inhibition being a very important feature of gamma oscillations a closer look will be taken at IPSPs, though literature predicts that adenosine receptor modulation does not affect inhibitory synapses.

4.2. Materials and methods.

4.2.1. Tissue preparation.

Male Sprague-Dawley rats (200 – 400 grams, from Charles-River, Margate, UK) were anaesthetised with a mixture of ketamine (75 mg/Kg) + medetomidine (1 mg/Kg) by i.p. injection. Rats were used instead of mice because the goal is to eventually do *in vivo* and behavioural experiments which are easier done in rats. Using a new technique seems a natural point to change the kind of animal used though the assumption is made there are not major differences in the hippocampal networks between rats and mice. The rat's blood was replaced via cardiac perfusion through the left ventricle with an oxygenated and chilled sucrose based solution containing (in mM): sucrose, 205; KCl, 2.5; $NaHCO_3$, 26; NaH_2PO_4, 1.25; D-glucose 10; $MgCl_2$, 5; $CaCl_2$, 0.1. Subsequently the rat was killed by cervical dislocation after which the brain was removed and kept cold in oxygenated sucrose solution. Using an Integraslicer (Campden Instruments, Loughborough, UK) 400 μm thick horizontal slices were made from the ventral hippocampus (coordinates from bregma: -7.5 till -5.0 mm) and put either in a Haas-type recording chamber at the interface between moist carbogen (95%, O_2, 5% CO_2) and aCSF (containing (in mM): D-glucose, 10; $NaHCO_3$, 26; NaCl, 125; KCl, 3; NaH_2PO_4, 1.25; $CaCl_2$, 2; $MgCl_2$, 1) at 32°C, or stored in a static interface type chamber containing aCSF at 21°C for later use. Fluid levels in the recording chamber were kept high using a perfusion rate of 8±1 ml/min minimizing gravitational pull onto the mesh, but making sure the slices were not submerged or started floating. All procedures were in accordance with the UK 'Animals (Scientific Procedures) Act 1986', and the studies were approved by the Biomedical Ethics Review Sub-Committee.

4.2.2. Electrophysiological recordings.

Intracellular recordings from CA3c pyramidal cells were made using sharp glass pipette recording electrodes filled with 3M potassium methylsulfonate (KCH$_3$SO$_4$, resistance >50 MΩ). Electrodes were placed in stratum pyramidale of the CA3c area. Individual cells were not visualised. The membrane potential was amplified using an Axoclamp-2A amplifier (Axon Instruments, Burlingham, CA, USA) and a Neurolog NL106 DC amplifier (Digitimer, Welwyn Garden City, UK), low-pass filtered at 2 kHz and sampled at 10 kHz. The signal was then digitised and sampled by using a CED-1401 (Cambridge Electronical Design, Cambridge, UK) and analyzed using Signal 3 and Spike 2 software (Cambridge Electronical Design, Cambridge, UK). All cells were recorded in current clamp.

Cells were bridge balanced and used for experiments when the resting membrane potential was stable and the cell needed less than 0.5 nA current to stay at -65 mV resting membrane potential, and had overshooting action potentials. Schaffer collaterals were stimulated by a 0.1 ms square pulse using a bipolar twisted 50 μm diameter nickel/chromium wire (Advent Research Materials Ltd, Halesworth, UK) and a DS2A isolated stimulator (Digitimer). The stimulus electrode was placed on the border of CA3a and CA1.

Drugs were diluted from the following stock solutions: adenosine (10 mM stock in aCSF), 8-cyclopentyl-1,3-dimethyxanthine (8-CPT; 10 mM stock in 0.1 M NaOH). All drugs and aCSF salts were purchased from Sigma (Poole, UK).

After running all protocols for the first time in normal aCSF (before phase) drugs were washed in for 10 minutes by adding them to the aCSF flowing in the system. If the cell was still healthy and the membrane potential was stable after the drugs were washed in, the same protocols were done in the presence of the added drug (drug phase). Once all protocols were run once again the drugs were washed out by changing to a fresh aCSF

solution. After 10 minutes of wash out the cell was checked to assess if it was still healthy, and if it was the protocols were done a third time (after phase).

4.2.3. Analysis and statistics.

Statistical comparisons were made between the change (drug phase – before phase) in aCSF controls and the change in cells treated with either adenosine or 8-CPT. The unpaired comparison was chosen over the paired comparison to make sure that any change occurring over time will not be mistaken for a change caused by adenosine or 8-CPT. Every variable was first analyzed for normality and any difference in starting value between groups. If data was normally distributed a Student's *t*-test was used for comparison while if data was not normally distributed a non-parametric equivalent was used. Unless stated otherwise, there was no difference in the starting values between the different treatment groups. Because the effects of adenosine on field potential were totally reversible (see chapter 2), the adenosine group was analyzed by calculating the "drug effect". The drug effect was obtained by averageing the parameter values from the before and after phase and using that average in subsequent comparison and calculations. The change of the parameter was then calculated by subtracting the calculated average from the value obtained in the drug phase. Because the effects of 8-CPT on the field recording were not reversible, comparisons were made between the drug and before phase and the change was calculated by subtracting the before phase from the drug phase. All parameters were checked for normality using the Kolmogorov-Smirnov test in SPSS 15.0, and if data was normally distributed statistical comparison was made using a Student's *t*-test. If data was not normally distributed the non-parametric Mann-Whitney U test was used. Data are expressed as means±standard error of the mean (s.e.m.). If the significance level was below 0.05, data were considered significantly different from controls.

4.3. Results.

4.3.1. Intrinsic properties.

Changes in passive cell properties can complicate interpreting results therefore it is important to check the stability of the cells parameters recorded.

4.3.2. Cell resistance and capacitance.

Negative current steps and positive current steps that did not elicit an action potential were used to calculate the slope resistance. Cells were kept at a membrane potential of -65 mV and the response to a 0.2 second current step was recorded. A typical response to a -0.5 nA current step is shown in Figure 4.2.A. To get the most accurate resistance measurement the response was fitted with single exponential fit using Signal software version 3.10 (CED). Using the equation: value = amplitude * e(-x/tau_m) + offset, three values are obtained from the fit: amplitude, membrane time constant (tau_m) and offset. The fit was measured between cursors 2 and 3 with cursor 1 (Figure 4.2.A) as a reference. Cursor 1 was placed at the start of the current step. To compensate for any bridge imbalance and to avoid inclusion of incompletely-compensated capacitance transient in the fit, cursor 2 was placed slightly after the start of the stimulus on the clearly exponential part of the response. Cursor 3 was placed at the end of the stimulus except in cases where the hyperpolarisation-activated cat-ion current (I_h) caused an increase in membrane potential during the current step. In these cases cursor 3 was placed at the point just before the visible depolarization in membrane potential caused by I_h was observed. The amplitude is the deviation from baseline (in mV) induced by the current injected, the offset is the voltage to where the cell is polarised to (in

mV) and the tau_m is the time constant of the exponential decay to the offset. Cursor 3 was repositioned if unrealistic values were obtained. The tau_m should theoretically not change with different current injections in the same condition
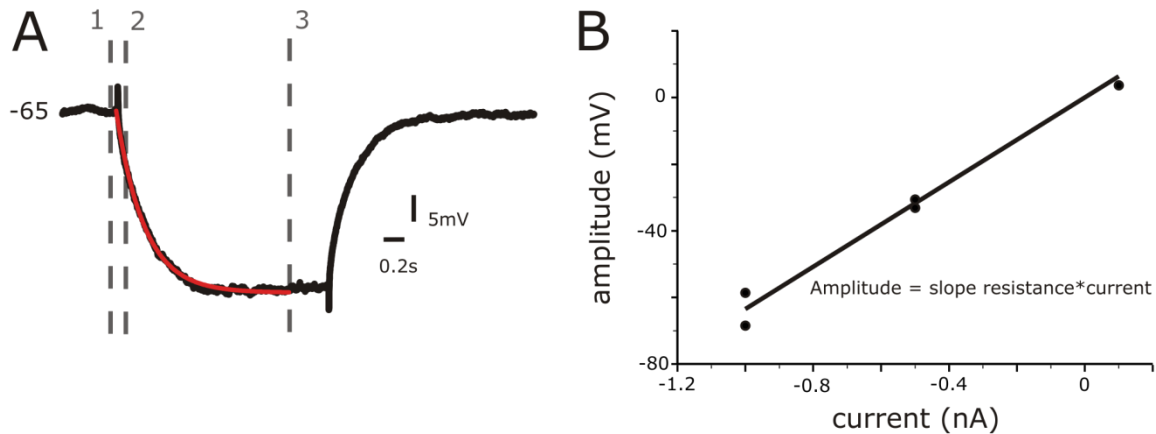
Figure 4.2. Slope resistance. **A.** Example of a response to a -0.5 nA current step. The response is fitted with a single exponential fit between cursors 2 and 3, after which membrane resistance (R_m) can be calculated (R_m=amplitude (mV) / current (nA)). **B.** Slope resistance is calculated from two -0.5 nA, two -1 nA and one 0.1 nA current steps via a linear fit (amplitude=slope resistance*current).

because it is dependent on the cell resistance and cell capacitance which remain the same under the same experimental conditions. Therefore the tau is calculated by taking the average from all responses used in Figure 4.2.B. The average tau_m from all cells before any drugs was added was 41.5±2.4 ms (n=22). No significant difference was found in the change in tau_m (Δtau_m) between aCSF controls (2.1±3.0 ms, n=6) and adenosine (50 µM, -5.7±3.0 ms, n=8) or aCSF controls (5.7±4.2 ms, n=6) and 8-CPT (5 µM, 2.2±3.6 ms, n=8 see Table 4.1). The Δoffset was also not significantly different from controls in both adenosine and 8-CPT (not shown). As a measure of resistance the slope resistance was calculated using four negative current injections (two times -0.5 and two times -1.0 nA) and one positive current injection (0.1 nA). The amplitude was plotted against the size of the

current injection, see Figure 4.2.B. When the positive current injection caused the cell to fire an action potential, the response could not reliably be fitted with an exponential fit and was therefore not used. To calculate the slope resistance the amplitude of the response from the fit was set out against the current injected and subsequently fitted with a linear fit using with the formula: amplitude = slope resistance * current. The fit was forced through zero because a zero nA injection does theoretically not produce a deviation from baseline. The slope resistance had an average of 50.0±3.3 MΩ/nA (n=22) before any drugs were tested. The change in slope resistance (Δslope resistance) in cells treated with adenosine (-2.8±4.2 MΩ, n=8) or 8-CPT (3.7±4.0 MΩ, n=8) was not different from the Δslope resistance in aCSF controls (1.1±2.7 MΩ, n=6) (see Table 4.1).

The capacitance of a cell can be calculated by dividing the membrane time constant by the cells resistance. The capacitance is proportional to the surface area of the cell and is thus an indirect measure of cell size. As you would not expect a cell to change its size during an experiment it is an important measure to check the condition of the recorded cell. The average membrane capacitance (C_m) of all cells recorded before drugs were tested was 0.91±0.08 pF (n=22). The change in capacitance (ΔC_m) with adenosine (-0.13±0.07 pF, n=8) and 8-CPT (-0.02±0.04 pF, n=8) did not differ significantly from the change in aCSF controls (0.08±0.12 pF, n=6, see Table 4.1).

4.3.3. Action potential properties.

From positive current steps that caused action potential firing, the action potential properties were measured. To make sure similar action potentials were compared the first action potential of the first current step that caused an action potential within 10 ms of the start of the current step was used to determine firing threshold (AP_{thres}), action potential upward

slope ($AP_{slope\ up}$) and action potential downward slope ($AP_{slope\ down}$). Figure 4.3.A.I shows a typical response of a cell that fires action potentials after a depolarizing current step (0.7 nA). Very typical for CA3c neurons is that the action potential are grouped in the early part of the depolarizing current. From the first derivative of the original response, the maximum $AP_{slope\ up}$ and the maximum $AP_{slope\ down}$ (see Figure 4.3.A.II) were measured. Figure 4.3.B is an enlargement of the first action potential and its derivative (grey area in Figure 4.3.A). $AP_{slope\ up}$ and $AP_{slope\ down}$ are
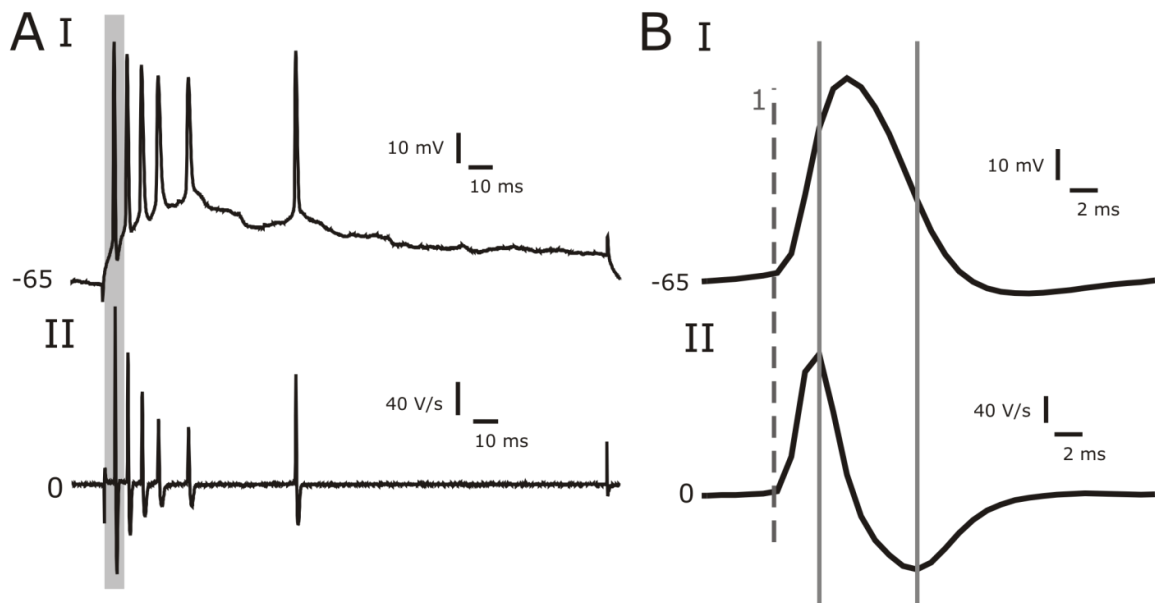
Figure 4.3. Action potentials. **A.I.** Example of a response to a 0.7 nA current step. Typical for Ca3c neurons is that the evoked action potentials are grouped in the early part of the depolarizing pulse. **II.** First derivative of the response in A.I. used to determine action potential slope up and slope down and where the action potential threshold was measured. **B.** Enlargement of the grey area in A. **I.** The first action potential cause by the 0.7 nA current step used in A. **II.** First derivative of the action potential in B.I used for measuring the up and downward slopes indicated by the vertical grey bars. The grey dotted line indicates the point where the first big change in membrane potential occurred. This is the start of the action potential and a measure for action potential threshold. Action potential threshold was taken from the same position from the original trace (A.I).

measured by taking the peak values, which correspond to the slopes of the action potential in the original recording. The average $AP_{slope\ up}$ was 174 ± 13 V/s (n=21). The change in $AP_{slope\ up}$ ($\Delta APslope_{up}$) with adenosine (6.1 ± 5.0 V/s, n=8) or 8-CPT (-4.9 ± 3.8 V/s, n=8) did not significantly differ from aCSF controls (2.9 ± 2.2 V/s, n=6, see Table 4.1). $AP_{slope\ down}$ had an average of -71 ± 6 V/s (n=21) before drugs were tested and showed no significant difference in $\Delta AP_{slope\ down}$ between treatments. The first big positive inflection of the first derivative corresponds to the start of the action potential, and was taken as AP_{thres} (see Figure 4.3.B). The average AP_{thres} was -53.9 ± 1.0 mV (n=21) but no significant difference was observed in ΔAP_{thres} between adenosine (-1.63 ± 1.5 mV, n=8) or 8-CPT (-0.51 ± 0.9 mV, n=8) compared to aCSF controls (-0.47 ± 1.7 mV, n=6).

4.3.4. Resting membrane potential.

A possible way for adenosine receptors to affect gamma oscillations is by changing a cell's resting membrane potential (V_m). Figure 4.4.A shows a typical example of the effect of 50 µM adenosine has on the membrane potential during wash in. The cell was held at a membrane potential of -65 mV before drugs were added. Adenosine hyperpolarised the CA3 pyramidal cell resting membrane potential very quickly after application. Within a few minutes a new stable equilibrium was reached. The average V_m before drug application without injecting any current was -58.6 ± 0.77 (n=22). Adenosine caused a significant hyperpolarisation compared to aCSF controls (Figure 4.4.B), $\Delta V_m = -4.34\pm1.16$ mV in adenosine (n=8), $\Delta V_m = -0.49\pm0.88$ mV in controls (n=6), Student's t-test, $t_{12} = 2.5$, $p=0.029$ (see Table 4.1). There was no difference in ΔV_m between 8-CPT (-1.08 ± 0.72 mV, n=8) and aCSF controls.
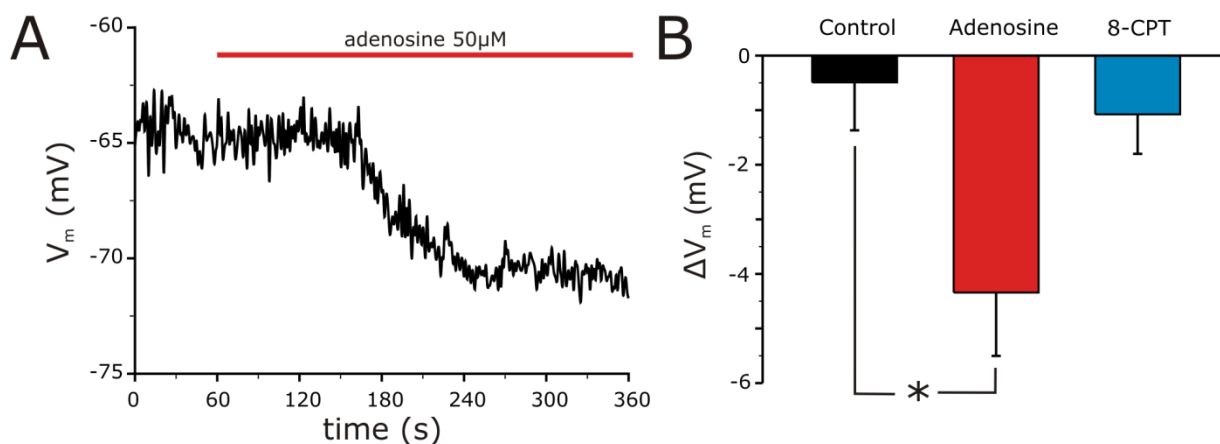
Figure 4.4. Resting membrane potential. **A.** Example of the effect of adenosine (50 µM) on membrane potential of a CA3 pyramidal cell during wash in. A quick hyperpolarisation is observed after adenosine application. The red horizontal bar indicates the time when adenosine (50 µM) was applied. **B.** Adenosine (50 µM, n=8) caused a significant hyperpolarisation to the resting membrane of CA3 pyramidal cells compared to controls (n=6), (p=0.029) while 8-CPT (5 µM, n=8) had no effect.

4.3.5. Slow afterhyperpolarization.

One of the mechanisms by which A_1-receptor acting drugs could influence gamma oscillations is by changing the slow afterhyperpolarisation (AHP_{slow}) seen after action potential firing. A typical example is shown in Figure 4.5.A where a CA3c pyramidal cell, kept at -65 mV, was given a 0.7 nA current injection causing the cell to fire a number of action potentials. The AHP_{slow} was fitted with a single exponential fit: value = AHP_{max} * e(-x/AHP_{tau}) + offset. From the fit three values were taken: amplitude (AHP_{max}), time constant (AHP_{tau}) and offset. The fit was taken between cursors 2 and 3 with cursor 1 as a reference. Cursor 1 was placed at the end of the current step, cursor 2 was placed approximately 50 ms after the trough and cursor 3 was placed at a time where it was clear the membrane potential had recovered back to baseline (see Figure 4.5.A). A response was refitted when the offset was

not within 1 mV of baseline values (the average of the 300 ms before the current injection) or if the AHP_{tau} gave unrealistic values. The amplitude obtained from the fit is an overestimation of the real amplitude as signal software extrapolates the amplitude to the reference cursor (cursor 1 in Figure 4.5.A). A more realistic afterhyperpolarisation amplitude (AHP_{amp}) was calculated from the values obtained from the fit using the equation above. To determine the time at which to calculate a realistic AHP_{amp} all responses from all analysed cells were compared and 800 ms after the end of the current injection was chosen because all cells were definitely past the trough of the response at that time. As not every cell responds to current injections the same way it is hard to choose a response that is comparable from cell to cell. To obtain a more reliable measurement of the AHP_{slow} the AHP_{amp} was set out against the number of action potentials (Figure 4.5.B) and then fitted with a linear equation ($AHP_{slow} = y0 + AHP_{angle} *$ number of AP). The fit angle (AHP_{angle}) then captures all the responses from one cell in a single value. The value obtained from y0 was so small in every cell analyzed, that it was considered to be equal to 0. The average AHP_{angle} was 1.7±0.3 mV/action potential (n=22) before drugs were added. The change in AHP_{angle} (ΔAHP_{angle}) did not differ significantly between groups (see Figure 4.5.C and Table 4.1).

The AHP_{tau} was calculated for every cell by averaging all the time constants from every response used in Figure 4.5.B that had action potentials. The AHP_{tau} had an average value of 1.3±01 s, n=22, but no significant differences were found in ΔAHP_{tau} (see Table 4.1). The AHP in CA3c pyramidal cells in response to an action potential is large compared to CA1 pyramidal cells (Greene and Haas, 1985).
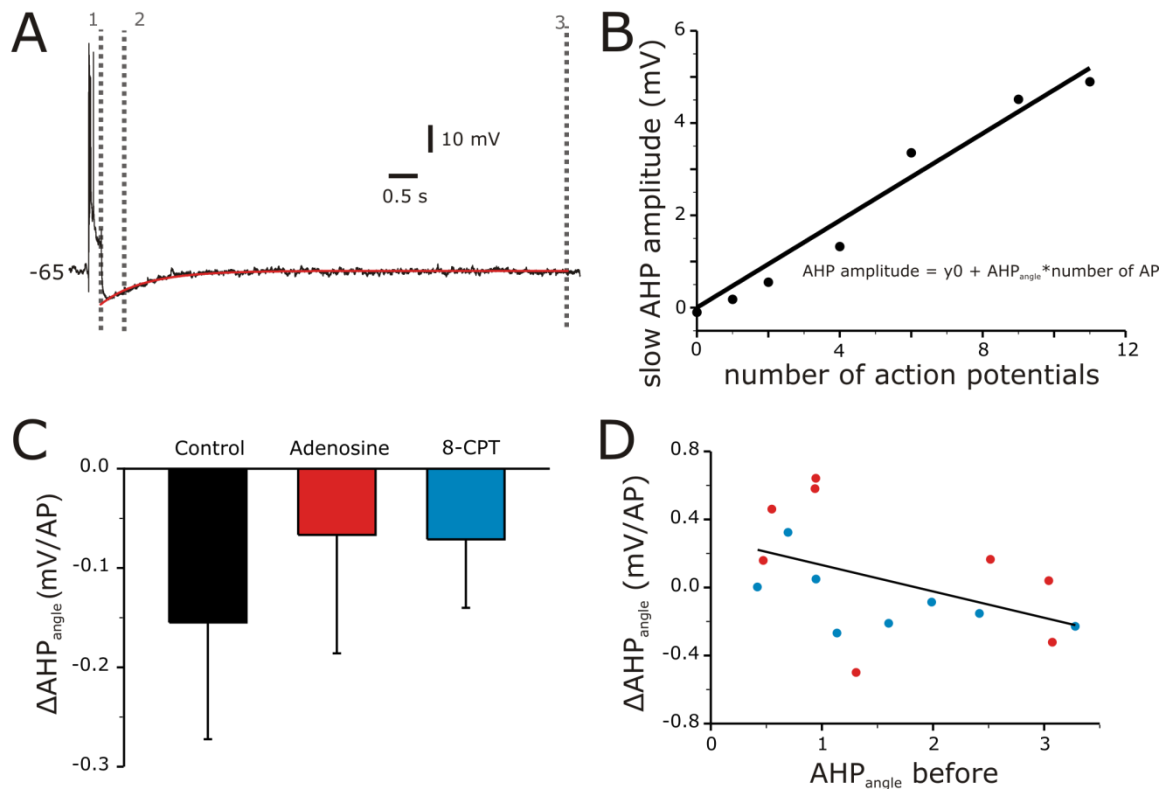
Figure 4.5. Slow afterhyperpolarization (AHP). **A.** Typical response to action potential firing showing the slow AHP in a CA3c pyramidal neuron (0.7 nA current injection). The slow AHP was fitted with a single exponential fit to measure the amplitude and time constant. **B.** Response effect relationship between AHP amplitude and number of action potentials. The data was fitted with a linear fit. The fit is not forced through zero because a depolarization without an action potential could also open a small amount of K+-channels and thereby create a small AHP. **C.** Change in AHP_{angle} between drug and before phase. There is no significant difference between adenosine (n=8) or 8-CPT (n=8) groups and the control group (n=6). **D.** Relationship between the change in AHP_{angle} and AHP_{angle} before. There is a significant regression (p=0.031) between cells exposed to adenosine receptor activation or blockage showing that the starting value can influence whether or not an effect can occur. Red dots are cells exposed to adenosine and blue dots are cells exposed to 8-CPT.

There were cells that already reached the maximum AHP amplitude after only two action potentials. It was expected from literature (see introduction) that adenosine increases AHP amplitude. Due to the big AHP before any drugs were added, the starting value can influence the change we can observe. If the AHP amplitude is already at its maximum there is little

room for adenosine to increase the response even further. To find out if the starting value had any influence on the observed change the ΔAHP_{angle} was set out against the AHP_{angle} in the before phase (see Figure 4.4.D) for all adenosine (red) and 8-CPT (blue) treated cells. There was a significant negative regression between the starting value and the change in AHP_{angle}, Spearman's rho -0.538, p=0.031. This indicates that part of the variation seen can be explained by the variation in starting value.

4.3.6. Signal variance.

One of the noticeable things besides the obvious hyperpolarisation in Figure 4.5.A is the reduction in the size of the signal before and during adenosine application. To quantify the effect of adenosine receptor acting drugs on signal size, signal variance was calculated as the signal variance is proportional to signal power. The power in an electrical signal is defined as voltage * current (Power = V * I). The current is unknown but Ohm's law dictates that I = V / R (with R being the resistance). Inserting that into the previous formula gives: Power = V^2 / R. As the cells resistance did not significantly change over time (see Figure 4.6.B and Table 4.1) R can be seen as a constant which leaves us with: Power = V^2. Signal software (CED) can calculate the signal standard deviation which once squared will give the Variance. At V_m the average signal variance was 1.04±0.17 mV^2 (n=22). Figure 4.6.A shows typical examples of all treatment groups. Just from looking at the raw data it becomes apparent that in aCSF controls (Figure 4.6.A.I) signal variation does not change while in cells exposed to 50 µM adenosine a reduction is signal variation (about 30%) is observed (Figure 4.6.II). In cells exposed to 8-CPT there is an increase in signal variation which seems to be mostly an increase in big upward deflections (Figure 4.6.A.III). Adenosine significantly reduced the variance at resting membrane potential compared to aCSF controls,

Δvariance$_{Vm}$, adenosine (-0.34±0.10 mV^2, n=8), control (-0.07±0.01 mV^2, n=6), (Mann-Whitney U-test, U=6.0 and p=0.02 (see Table 4.1)), see Figure 4.6.B. The change in 8-CPT (5 µM, 0.24±0.14 mV^2, n=8) did not differ significantly from the change in controls (-0.05±0.11 mV^2, n=6, see Table 4.1 and Figure 4.6.B). Because adenosine hyperpolarised resting membrane potential (see Figure 4.4.B), the significant change in Δvariance$_{Vm}$ could be a result of a difference in resting membrane potential. At a more hyperpolarised V$_m$ the same incoming current will be recorded as a smaller potential and thus reduce the variance. To have a more comparable value of the change in variance, the variance was calculated while the cell was held at -65 mV. Figure 4.6.C shows the raw traces (details as in Figure 4.6.A) before and during drug application. While there is little difference between before and during drug traces in controls (Figure 4.6.C.I) and adenosine (Figure 4.6.C.II), the traces recorded in the presence of 8- CPT Figure 4.6.C.III) shows a clear increase in raw signal (about 3 times). The variance calculated at -65 mV had an average value of 0.57±0.1 mV^2 (n=22). The change in variance at -65 mV significantly increased in 8-CPT (0.67±0.31 mV^2, n=8) treated cells compared to aCSF controls (0.07±0.10 mV^2, n=6) (Mann-Whitney U-test, U=6.0, p=0.02, see Table 4.1) while the change in adenosine (-0.04±0.07 mV^2, n=8) did not differ from the change in controls (0.04±0.11 mV^2, n=6, see Table 4.1).
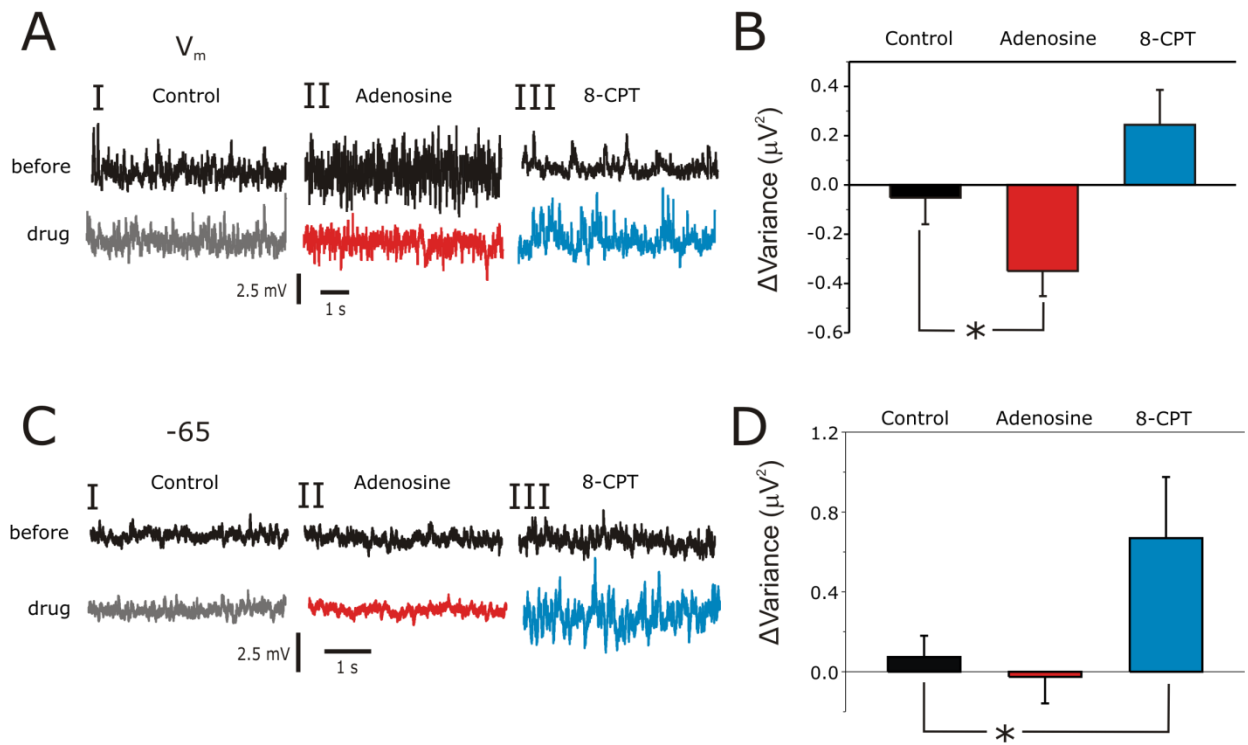
Figure 4.6. Signal Variance. **A.** Raw traces of the effect adenosine receptor acting drugs has on signal size at V_m. Black lines represent traces before any drugs were added. **I.** Typical example of control data where aCSF was applied continuously. The grey line was taken at the time that corresponds to 20 minutes of drug exposure. **II.** Typical example of the effect 50 µM adenosine on signal size. The red trace was taken 20 minutes after adenosine application. **III.** Typical example of the effect 5 µM 8-CPT has on signal size. The blue trace was taken 20 minutes after 8-CPT application. **B.** Difference between signal variance 20 minutes after drug application and before drug application at Vm. Adenosine (50 µM, n=8) showed a significant decrease in signal variance (p=0.02) while 8-CPT (5 µM, n=8) was not significantly different from control data (n=6). **C.** Raw traces of the effect adenosine receptor acting drugs have on signal size while the membrane potential was kept at -65 mV. **I, II, and III.** Details same as in A. **D.** Difference between signal variance 20 minutes after drug application and before drug application at -65 mV. 8-CPT (5 µM, n=8) caused a significant increase in signal variance (p=0.02) while adenosine (50 µM, n=8) had no effect compared to the change in controls (n=6).

4.3.7. Firing rate.

Firing rate was assessed at resting membrane potential. The average firing rate before drug application was 0.35±0.16 Hz, n=18. Figure 4.7.A shows every individual cell before and during drug application. In aCSF controls one cell increased its firing rate while the rest of the cells did not change its firing rate. All cells treated with 50 µM adenosine that had a firing rate above zero before drug application decreased their firing rate while the cells that had no firing rate before drug application in the same group did not change their firing rate.
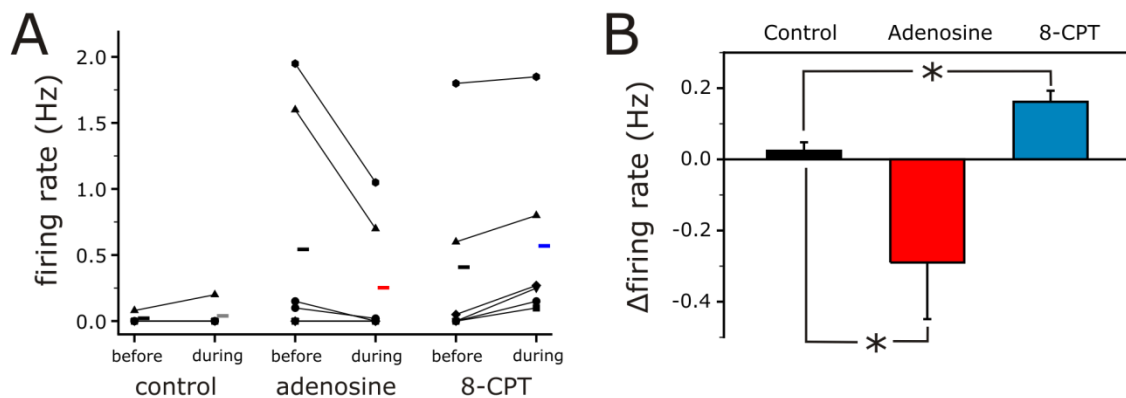
Figure 4.7. Firing rate. **A.** Firing rate before and during drug application. Individual cells are depicted and connected by lines. Horizontal bars indicate the group average. **B.** Difference in firing rate during and before drug application. Adenosine (50 µM, n=7) decreased firing rate significantly (p=0.037) while 8-CPT (5 µM, n=6) increased firing rate significantly (p=0.009) compared to controls (n=6).

In the 8-CPT (5 µM) exposed group all cells increased their firing rate. The firing rate changed (Δfiring rate, see Figure 4.7.B) significantly after adenosine (50 µM) application (-0.29±0.16 Hz, n=7), compared to controls (0.02±0.02 Hz, n=6), Mann-Whitney U-test, *U*=6.0 and *p*=0.037, (see Table 4.1). 8-CPT (5 µM) had the opposite effect and significantly

increased firing rate (0.16±0.03 Hz, n=6), Mann-Whitney U-test, U=5.0 and p=0.009 (see Table 4.1).

4.3.8. Intrinsic properties conclusion.

Of all the cellular parameters investigated adenosine significantly hyperpolarised the resting membrane potential, reduced signal variance at resting membrane potential and reduced firing rate. The changes in all these parameters fit well with the observed field effects and are likely to contribute to the reduction in oscillations specifically in the gamma range. On the other hand, 8-CPT significantly increased signal variance when cells were kept at -65 mV and increased firing rate. These effects are likely to contribute to the increase in hippocampal gamma oscillations described in the previous chapters (chapter 2 and 3).

4.3.9. Synaptic properties.

Adenosine receptors are also present on the pre- and post-synaptic membrane in the synaptic cleft (see Figure 1.2) and could therefore influence synaptic transmission directly. Both the inhibitory post-synaptic potential (IPSP) and excitatory post-synaptic potential (EPSP) were investigated.

4.3.10. Excitatory post-synaptic potentials (EPSPs).

To investigate EPSPs cells were hyperpolarised to a membrane potential of -90 mV at the soma. This is close to the IPSC reversal potential (see Table 4.1) to minimise the influence of the IPSP on the change in potential after the stimulus, giving an as pure as possible EPSP. Figure 4.8.A shows a typical example of the response of a cell to an increasing Schaffer collateral stimulus. With increasing stimulus intensity the EPSP response increases in amplitude until eventually an action potential is evoked. As a measure of the EPSP size the upward slope is taken. To measure the EPSP slope the original trace is taken (Figure 4.8.B.I) and subsequently the first derivative was calculated (Figure 4.8.B.II). From the first derivative trace the first peak is taken as the maximum upward slope. Because the first derivative from the signal does not have a distinct single peak a horizontal cursor (grey dotted line) is used to measure the average peak. That value depicts the maximum change during the rising part of the EPSP which is a measure of the EPSP slope. If a stimulus evoked an action potential (see Figure 4.8.A) the EPSP slope was measured before the start of the action potential (Figure 4.8.B.III). The action potential is clearly visible in the very steep increase in the first derivative. The EPSP slope was plotted against the stimulus strength to obtain a stimulus-response curve (Figure 4.8.C). The data points were fitted with the sigmoidal function: amplitude=$EPSP_{max}$/1+(exp(-(S-ES_{50})/$EPSP_{slope}$)), where $EPSP_{max}$ is the fitted maximum EPSP amplitude, ES_{50} is the stimulus strength (S) required to reach half maximum effect and the $EPSP_{slope}$ is an inverse measure of the steepness of the curve. In control conditions, continuous aCSF, the response changed very little (see Figure 4.9.A). On the other hand 50 μM adenosine reduced the response (see Figure 4.9.B) while 5 μM 8-CPT increased the response (see Figure 4.9.C) to a Schaffer collateral stimulus of fixed stimulus strength. For cells treated with 8-CPT the after phase is not shown because 8-CPT does not wash out. The three values obtained from every fitted cell were averaged and used to

construct an average stimulus response curve, which gives an indication of the effects drugs have on the EPSP slope (Figure 4.9.B, D and F, for values see Table 4.1). In control there were no differences during the three recording phases (before, drug and after).
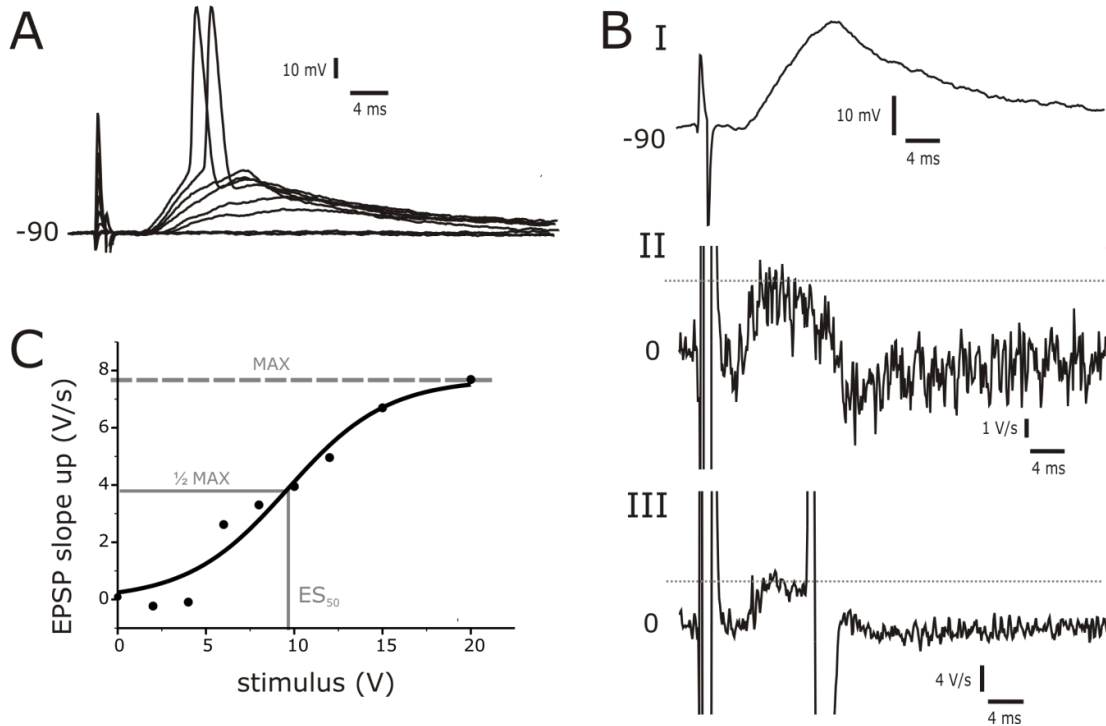
Figure 4.8. Excitatory post-synaptic potential (EPSP) measured at -90 mV. **A.** Example of the responses to increasing Schaffer collateral stimulus (0, 2, 4, 6, 8, 10, 12, 15 and 20 V) at a membrane potential of -90 mV. With increasing stimulus strength the EPSP becomes bigger and the strongest two stimuli evoked an action potential. **B.** The upward EPSP slope is calculated for every individual response by taking the first derivative. **I.** The response to the 10 V stimulus in panel A. **II.** The first derivative of the response in panel B.I. The peak of the first derivative shows the maximum change and therefore the maximum EPSP slope. Because the response is noisy a horizontal cursor (grey dotted line) is used to determine the average peak. **III.** In responses where the stimulus evoked an action potential the slope was determined before the start of the action potential. The start of the action potential is clearly visible in the very steep change in membrane potential derivative. Again a horizontal cursor is used to determine the peak. **C.** A stimulus response curve is made from the stimulus intensity and upward EPSP slope and subsequently fitted with a sigmoidal function.
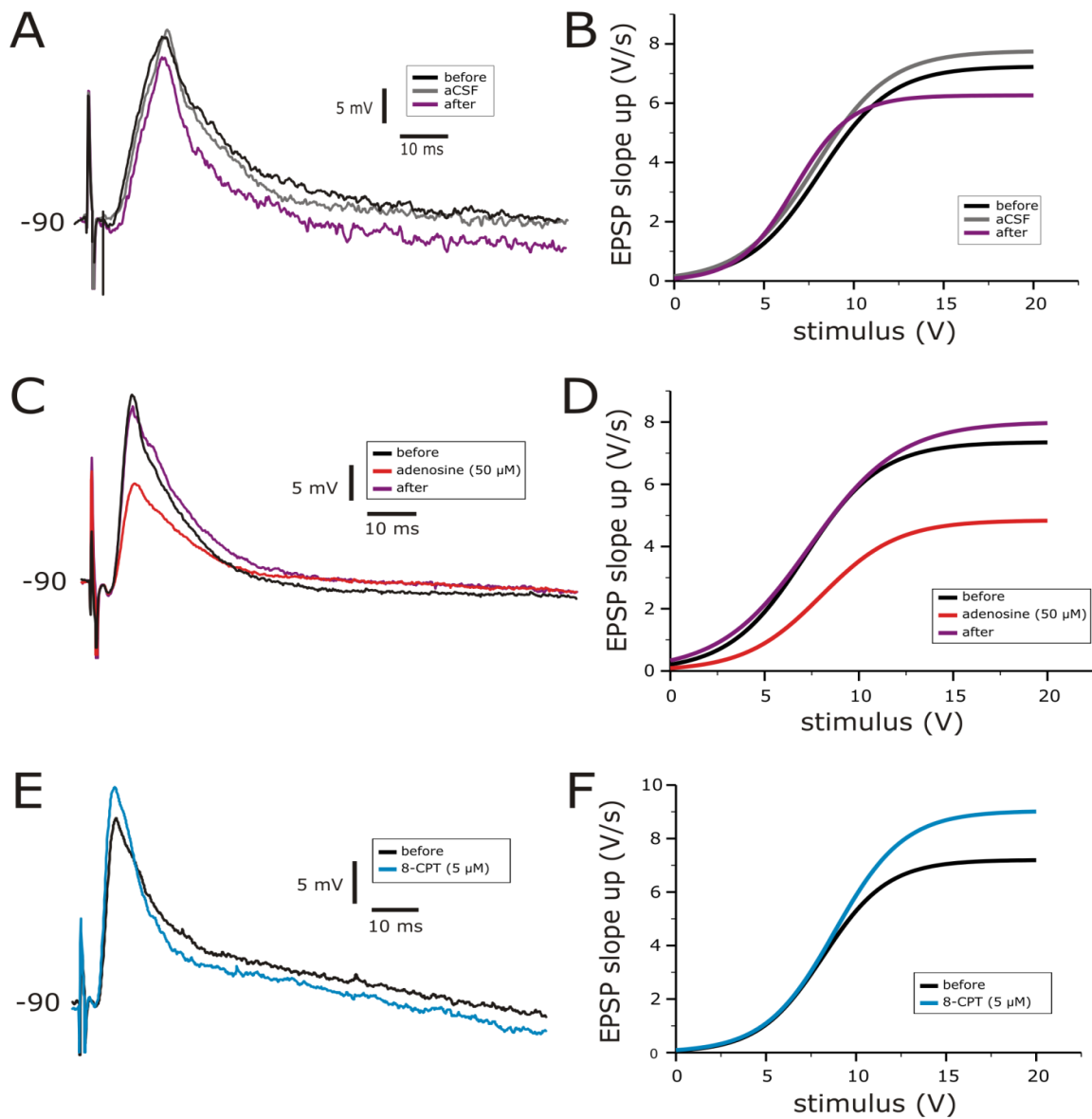
Figure 4.9. Excitatory post-synaptic potential (EPSP) measured at -90 mV. **A. C. E.** Typical examples of the response to a Schaffer collateral stimulation before, during and after drug application (aCSF control, adenosine (50 µM) and 8CPT (5 µM) respectively) of a single cell. Adenosine reduces the recorded response while 8-CPT increases the recorded response. Stimulus intensity 10, 15 and 8 V respectively. **B. D. F.** For every cell a stimulus response curve was made from which three values were derived (see Figure 4.8). From these values an average was calculated (n=6-8) and the curves shown in this figure are reconstructed sigmoidal curves from these average values. Adenosine reduced the fitted maximum and shifted the stimulus response curve to higher values while 8-CPT increased the fitted maximum.

The average fitted maximum EPSP slope was 7.27 ± 0.76 V/s (n=22). Adenosine reversibly reduced the maximum EPSP slope ($\Delta EPSP_{max} = 2.64\pm0.53$ V/s, n=8, Student's t-test, $t_{10} = 4.1$, $p=0.002$) while 8-CPT increased the maximum EPSP slope ($\Delta EPSP_{max} = 1.84\pm0.49$ V/s, n=8, Two sample Kolmogorov-Smirnov Test, $Z=1.4$, $p=0.048$), compared to controls (0.58 ± 0.57 V/s, n=6), see Figure 4.10. The average EPSP ES_{50} was 7.8 ± 0.4 V (n=22). For the unpaired comparison with controls, the adenosine induced shift in ES_{50} was not significant (Student's t-test, p=0.097). However a paired comparison between the before phase and the drug phase did reveal a shift to higher values during adenosine application (paired Student's t-test, $t=3.7$ $p=0.011$, n=8). The average slope was 1.92 ± 0.22 (n=22) but showed no significant changes between groups.
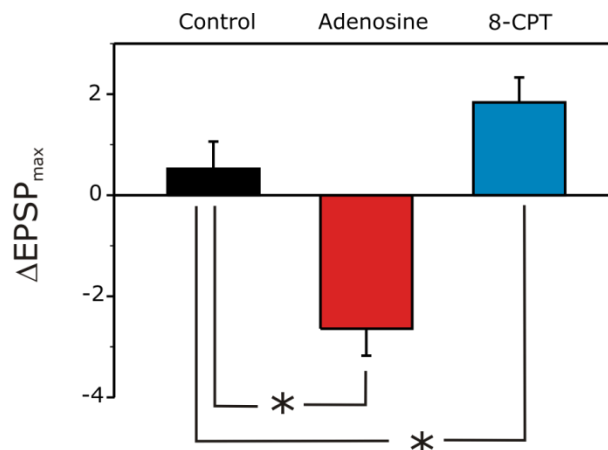
Figure 4.10. Change in EPSP fitted maximum in aCSF controls, adenosine (50 µM, n=8) and 8-CPT (5 µM, n=8). Adenosine significantly reduced the fitted maximum (p=.002) while 8-CPT significantly increased the fitted maximum (p=0.048) compared to the change in controls (n=6). Functionally this means that the EPSP is reduced in adenosine and increased in 8-CPT treated cells.
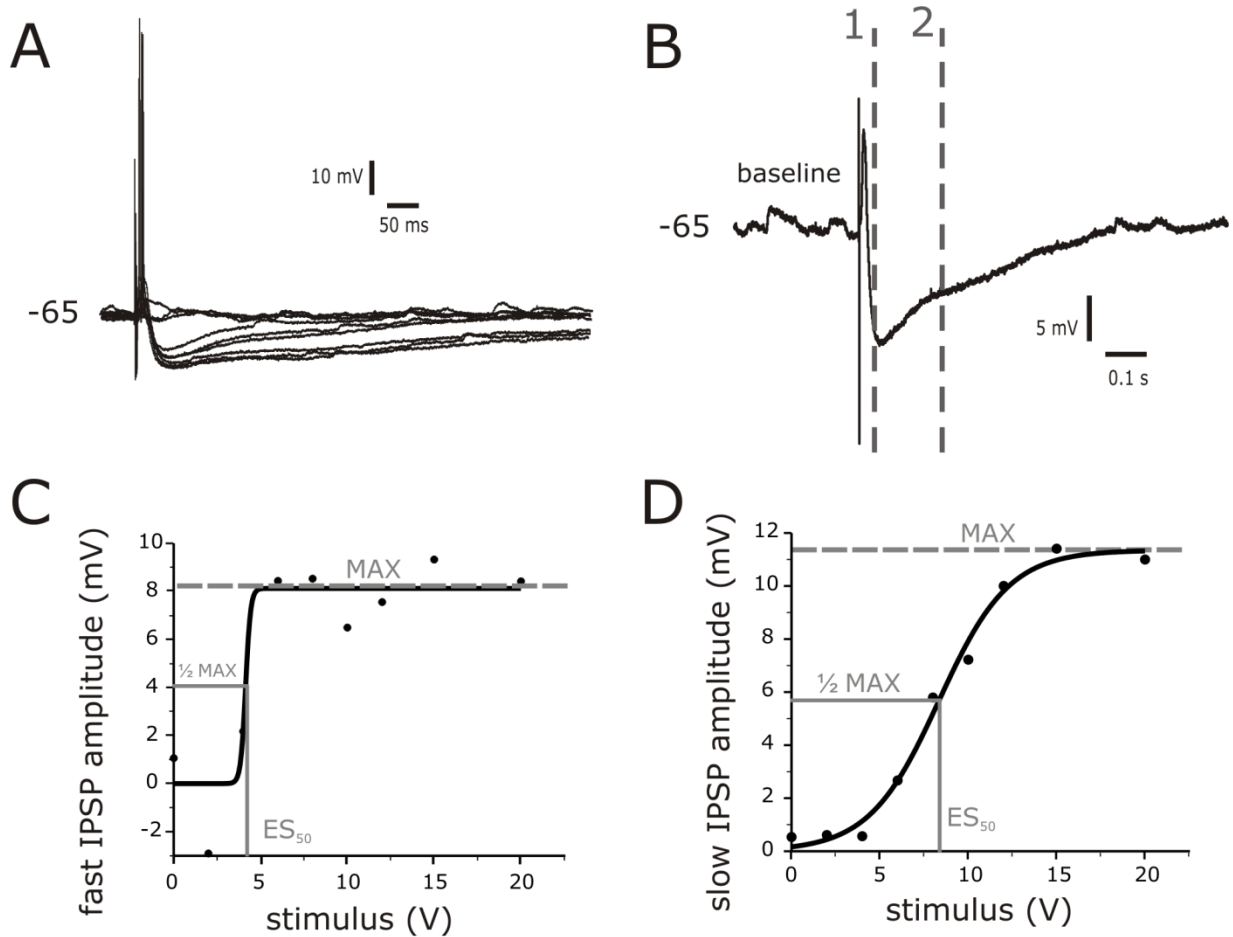
Figure 4.11. Inhibitory post-synaptic potentials (IPSP) measured at -65 mV. **A.** Example of the response to increasing Schaffer collateral stimulation (0, 2, 4, 6, 8, 10, 12, 15, and 20V) at a membrane potential of -65 mV. The fast IPSP reaches its maximum quickly while the slow IPSP needs a stronger stimulus to reach its maximum. **B.** The response to the 10V stimulus from panel A. Fast and slow IPSP amplitude was measured by taking the average Vm before the start of the stimulus (baseline with a length of 0.3 s) and subtracting Vm at the cursors. To measure the fast IPSP the cursor (dotted grey line 1) was placed just before the trough which was usually 33 ms after the start of the stimulus. To measure the slow IPSP a cursor (dotted grey line 2) was placed 200 ms after the start of the stimulus. **C+D.** Stimulus response curve from the same data shown in panel A. Data was fitted with the same sigmoidal function as in Figure 4.8.C. The fast IPSP amplitude had a very small slope resulting in a sharp rising sigmoidal curve. The slow IPSP showed a more gradual profile. From the fits three values are taken: the fitted maximum, the half maximum value (ES_{50}) and the slope.

4.3.11. Inhibitory post-synaptic potentials (IPSPs).

To assess the effect of adenosine receptor acting drugs on IPSPs, a Schaffer collateral stimulus was given while the cells were kept at -65 mV. The individual responses to stimuli of increasing intensity are shown in Figure 4.11.A. Both the fast and slow IPSP were measured from the same responses (see Figure 4.11.B).

4.3.12. Fast inhibitory post-synaptic potentials (fast IPSPs).

The fast IPSP amplitude was measured just before the trough. To measure an as pure as possible fast IPSP amplitude, the potential just before the trough (approximately 33 ms after the stimulus) was subtracted from the baseline potential (the average of 300 ms before the stimulus). The fast IPSP amplitude was plotted against the stimulus intensity (Figure 4.11.C). A sigmoidal function was used to fit the data: amplitude=fast $IPSP_{max}$/1+(exp(-(S-fast IPSP ES_{50})/fast $IPSP_{slope}$)). The fast IPSP amplitude as a function of stimulus intensity was fitted with a sigmoidal function with a very small slope. In aCSF controls the fast IPSP kinetics changed little over time (Figure 4.12.A). Adenosine (50 µM) reversibly increased the maximum fast IPSP amplitude (Figure 4.12.C) and reversibly reduced the EPSP amplitude just before the start of the IPSP. On the other hand 8-CPT (5 µM) did not change the IPSP amplitude but did increase the amplitude of the preceding EPSP (Figure 4.12.E). The average stimulus-effect relationships were constructed from the averaged three variables (Figure 4.12.B, D, and F). Adenosine reversibly increased the IPSP amplitude and shifted the whole stimulus response curve to higher values. The average fast $IPSP_{max}$ was 9.91±0.60 mV (n=22). The increase in fast $IPSP_{max}$ during adenosine was greater than (about 5 times) the increase in controls (Figure 4.13.A), Δfast $IPSP_{max}$, adenosine = 2.73±0.53 mV, n=8, control = 0.51±0.37 mV, n=6, Student's t-test, t_{12} = -3.4, *p*=0.006,
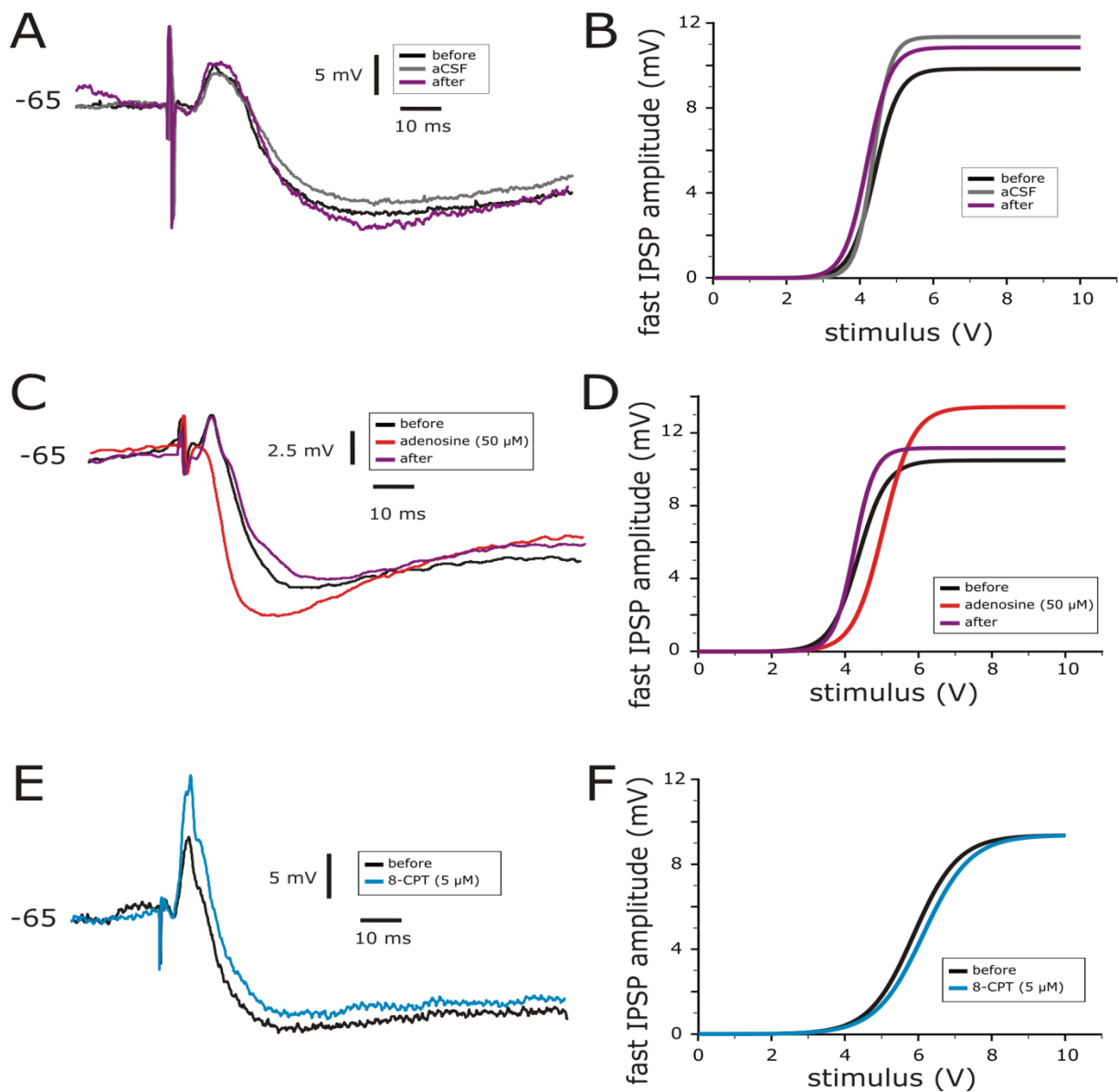
**Figure 4.12.** Fast inhibitory post-synaptic potential (IPSP) measured at -65 mV. **A. C. E.** Typical examples of the response to a Schaffer collateral stimulus before during and after drug application (aCSF control, adenosine (50 µM) and 8CPT (5 µM) respectively) of a single cell. Adenosine reduced the EPSP visible right before the fast IPSP and increased the fast IPSP amplitude, while 8-CPT slightly increased the EPSP but does not affect the fast IPSP amplitude. Stimulus strength 10, 8 and 6 V respectively. **B. D. F.** For every cell a stimulus response curve was made from which three values were derived (see Figure 4.11). From these values an average (n=6-8) was calculated and the curves shown in this figure are reconstructed sigmoidal curves from the average values. Adenosine increased the fitted maximum and shifted the stimulus response curve to higher intensities while 8-CPT had no effect.
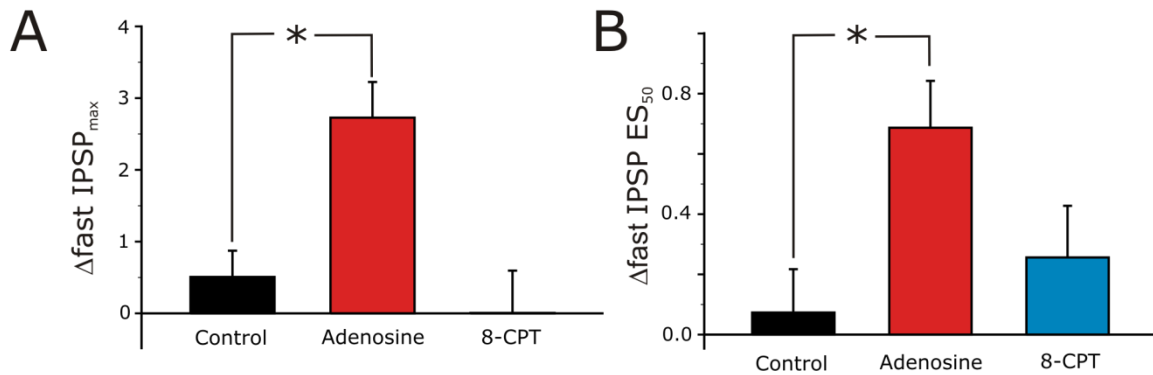
**Figure 4.13.** Significant changes in fast IPSP fitted curve values **A.** Change in fast IPSP fitted maximum in aSCF control (n=6), adenosine (50 µM, n=8) and 8-CPT (5 µM, n=8). Adenosine significantly increased the maximum IPSP amplitude (p=0.006) compared to the change in controls. 8-CPT had no effect on the IPSP maximum amplitude. **B.** Adenosine increased the ES_{50} significantly (p=0.016) while 8-CPT showed no significant difference from the change in aCSF controls.

while the Δfast $IPSP_{max}$ during 8-CPT (0.01±0.59 mV, n=8) did not significantly differ from controls (see Table 4.1). The average ES_{50} was 4.9±0.3 V (n=22). Adenosine shifted the ES_{50} by 0.69±0.16 V (n=8) while there was hardly any shift in control (0.07±0.14 V, n=6, see Figure 4.13.B, and Table 4.1), Student's t-test, t_{12} = -2.8, p=0.016. 8-CPT did not significantly shift the fast IPSP ES_{50} (0.26±0.17, n=8, see Figure 4.13.B and Table 4.1). The fast IPSP stimulus response curve had a steep slope, 0.45±0.8 (n=22). There was no difference in Δfast $IPSP_{slope}$ between adenosine or 8-CPT and controls.

The fast IPSP reversal potential was analyzed. To calculate the fast IPSP reversal potential a stimulus that gave a clear IPSP response at -65 mV but did not cause an action potential to be generated was selected. This intensity was used to evoke synaptic potentials at varying V_m (-50 to -95 mV). Figure 4.14.A shows a typical example of the synaptic potentials evoked at different membrane potentials using the same stimulus intensity. The traces are zeroed to the start of stimulus for display purposes. The IPSP amplitude was calculated in the same

was as previously described (see Figure 4.11). The fast IPSP amplitude was plotted against the membrane potential (Figure 4.14.B) and fitted with a linear function. The reversal potential was calculated by solving the linear equation for y=0. The average fast IPSP reversal potential was -82.1±1.6 mV (n=22).
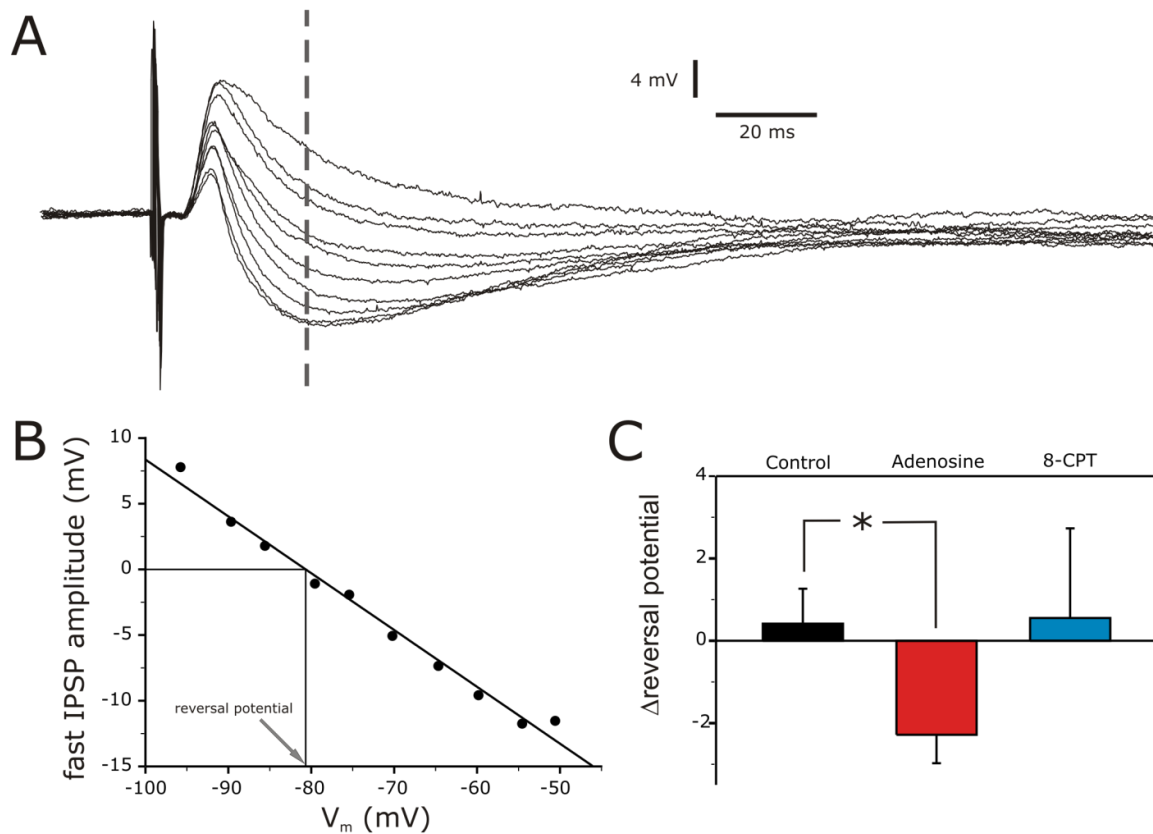
Figure 4.14. IPSP reversal potential. **A.** Response to a Schaffer collateral stimulus at varying V_m. A voltage from the fast IPSP stimulus response curve (see figure 4.11) that did gave a clear IPSP at -65 mV but did not evoke an action potential was used. Cells were kept at a V_m between -95 and -50. The cursor (grey dotted line) shows where the IPSP amplitude was measured. **B.** The measured IPSP amplitude was plotted against V_m and fitted with a linear curve, the reversal potential was calculated by solving the linear equation for y=0. **C.** Change in reversal potential in aCSF controls (n=6), adenosine (50 µM, n=8) and 8-CPT (5 µM, n=8). Adenosine makes the reversal potential significantly more negative compared to controls which show a small change towards zero (p=0.028). There was no significant change in IPSP reversal potential in cells exposed to 8-CPT.

Adenosine shifted the reversal potential by -2.28±0.69 mV, n=8, which was significantly different from the shift in controls, 0.42±0.85, n=6, Student's *t*-test, t_{11} = 2.5, *p*=0.032 (see Table 4.1). There was no significant change in IPSP reversal potential in cells exposed to 8-CPT.

4.3.13. Slow inhibitory post-synaptic potentials (slow IPSPs).

The slow IPSP amplitude was measured 200 ms after the start of the stimulus (cursor 2 in Figure 4.11.B). To measure slow IPSP amplitude, the potential at 200 ms after the stimulus was subtracted from the baseline potential (the average of 300 ms before the stimulus). The slow IPSP amplitude was set out against the stimulus intensity (Figure 4.11.D)**.** A sigmoidal function was used to fit the data: amplitude=slow $IPSP_{max}$/1+(exp(-(S-slow IPSP ES_{50})/slow $IPSP_{slope}$)). The slow IPSP amplitude increased more gradually with stimulus intensity compared to the fast IPSP amplitude. Average stimulus-effect relationships were constructed for all treatment groups (Figure 4.15). The average slow $IPSP_{max}$ was 9.94±0.76 mV and the slow $IPSP_{slope}$ was 1.33±0.26 (n=22). There was no significant difference in Δslow $IPSP_{max}$ or Δslow $IPSP_{slope}$ between adenosine (n=7) or 8-CPT (n=6) and controls (n=6). The average slow IPSP ES_{50} was 7.23±0.56 V (n=22). Adenosine shifted the slow IPSP ES_{50} by 1.8±0.81 V (n=7) which was significantly different from the change in controls, (0.185±0.38 V, n=6), Mann-Whitney U-test, *U*=7.0, *p*=0.028. There was no significant difference in Δslow ES_{50} between 8-CPT (0.93±0.95 V, n=6) and control (0.16±0.42 V, n=6, see Figure 4.16 and Table 4.1).

There was no reliable measure of the slow IPSP reversal potential in the data recorded, thus the slow IPSP reversal potential was not analyzed.
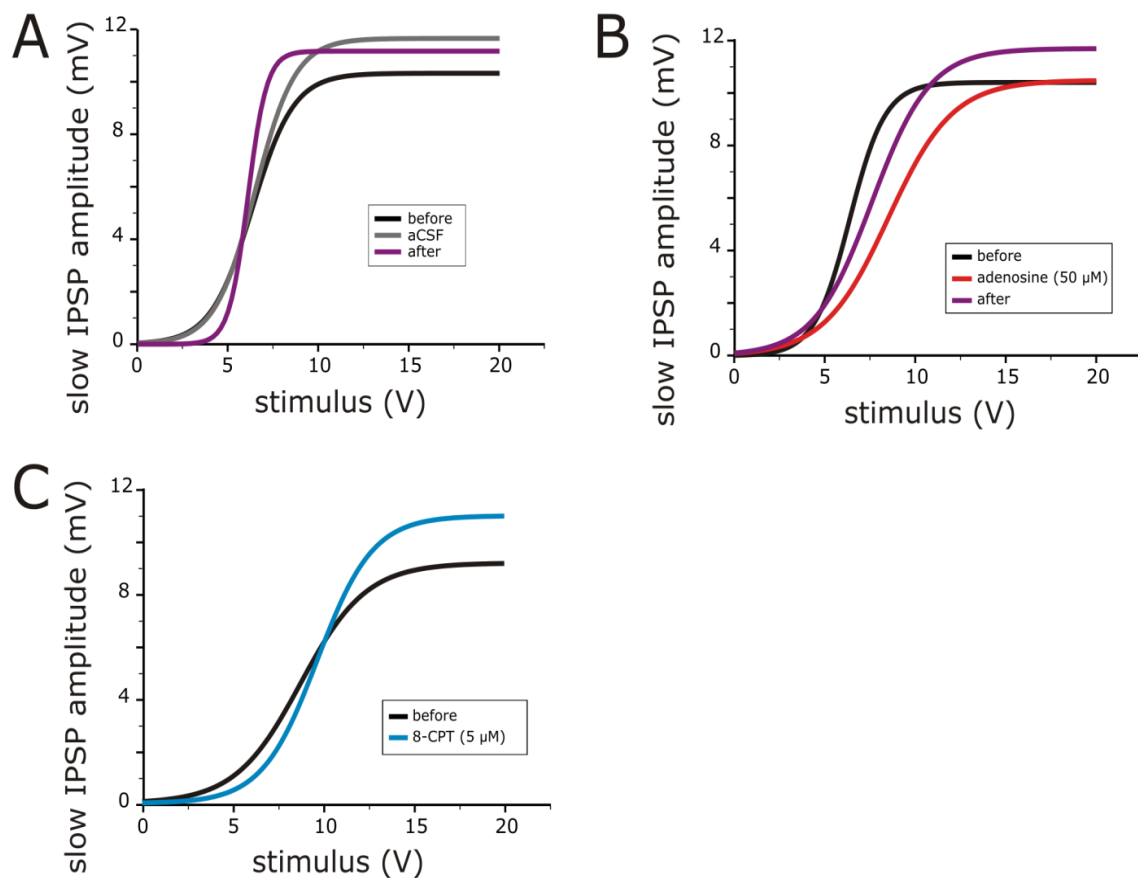
Figure 4.15. Slow inhibitory post-synaptic potential (IPSP) measured at -65 mV. **A. B. C.** For every cell a stimulus response curve was made from which three values were derived (see Figure 4.11). From these values an average (n=6-7) was calculated and the curves shown in this figure are reconstructed sigmoidal curves from the average values. Adenosine shifted the stimulus response curve to higher intensities while 8-CPT slightly increases the maximum.
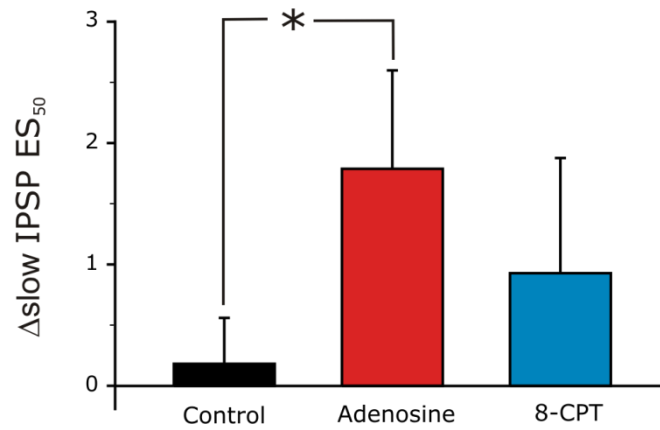
Figure 4.16. Change in slow IPSP ES_{50} in aSCF control (n=6), adenosine (50 µM, n=7) and 8-CPT (5 µM, n=6). Adenosine significantly increased the ES_{50} (p=0.028) compared to the change in controls thereby shifting the stimulus response curve to higher intensities. 8-CPT showed no significant difference from the change in aCSF controls.

4.4. Discussion.

Cellular and synaptic responses to the adenosine receptor agonist adenosine and the specific adenosine A_1-receptor antagonist were investigated. Adenosine (50 µM) hyperpolarised the resting membrane potential, decreased the signal variance at resting membrane potential, decreased the firing rate at resting membrane potential, decreased the EPSP amplitude, shifted the EPSP stimulus response curve to higher stimulus intensities, increased the fast IPSP amplitude, shifted the fast IPSP and slow IPSP stimulus response curve to higher stimulus intensities and made the fast IPSP reversal potential more negative. 8-CPT (5 µM) increased the signal variance when cells were kept at -65 mV, increased the firing rate at resting membrane potential and increased the EPSP amplitude.

4.4.1. Intrinsic properties.

It has been previously described in literature that adenosine increases the slow AHP duration in CA1 pyramidal cells (Greene and Haas, 1985). We found no difference in slow AHP duration in CA3c pyramidal cells. Very noticeable was the very large slow AHP, even after a single action potential in CA3c pyramidal cells, which was different from that in CA1 pyramidal cells. There was a significant relationship between the value in the before phase and the drug induced change in AHP amplitude per action potential. In cells where only two action potentials already evoked maximum slow AHP amplitude there was little room for adenosine to increase the amplitude. We also found no difference in the slow AHP relaxation time constant, which is contradictory to what has been previously reported in literature (Greene and Haas, 1985;Haas and Selbach, 2000). One possible explanation could be that we compared the change in adenosine with the change in aCSF controls instead of paired comparisons from previous reports. However, also a paired comparison did not show

significant differences. Another difference with previous reports is that we compared the slow AHP per action potential, and not just one response. When considering the relevance of the slow AHP in CA3c pyramidal neurons for gamma oscillations, it is actually the slow AHP observed after one or two action potentials that can be of great influence on the oscillating network. That we found no significant prolongation of the slow AHP could also be down to a regional difference between CA3c and CA1 pyramidal cells within the hippocampus. This is unlikely as no difference in intracellular signalling mechanisms has been described between the two hippocampal regions.

The lack of slow AHP prolongation characterised in CA3 pyramidal neurons can therefore not explain the adenosine-induced change in gamma oscillations observed. A more likely candidate is the resting membrane hyperpolarization caused by adenosine. Adenosine activates GIRK channels through the A_1-receptor thereby increasing the K^+ conductance across the membrane, which leads to a hyperpolarization of the resting membrane potential (Alzheimer and ten Bruggencate G., 1991;Luscher et al., 1997;Takigawa and Alzheimer, 2002). Adenosine levels in the slice are high enough for A_1-receptor antagonists to increase brain oscillations specifically in the gamma range *in vitro* (see chapter 2 and 3), and fall within the physiological range (Ballarin et al., 1991;Dunwiddie and Diao, 1994;Fredholm et al., 2001). The lack of effect of 8-CPT on resting membrane potential is therefore unexpected. A possible explanation is that the open probability of GIRK channels under resting conditions at the soma is very small, while further away from the soma in the dendrites, in the apical dendrites, the open probability is higher (Chen and Johnston, 2005). It is therefore possible that blocking adenosine A_1-receptors might depolarise the dendrites without a noticeable effect on the soma. Activating the adenosine A_1-receptor will increase the GIRK channel open probability, including the channels at the soma, and thus enhance the K^+ current, which leads to the observed hyperpolarization. The hyperpolarization of

pyramidal cells and also interneurons (Li and Henry, 2000) will reduce their firing rate. The activity within the network is thereby disrupted and the oscillation desynchronised. It will be harder for pyramidal cells to activate interneurons as the interneuron needs more depolarization which means fewer interneurons will be activated per cycle. The opposite is true for the increase in firing rate in the presence of 8-CPT. With an increased firing probability of pyramidal cells, more interneurons will be activated in the same cycle. This leads to increased synchronicity between cells which will be visible through larger field potentials.

The decrease in signal variance measured at resting membrane potential was significantly reduced in the presence of adenosine. The hyperpolarization was mainly responsible for this change, as there was no significant difference compared to controls when the membrane potential was fixed at -65 mV. The reduction signal variance fits well with the decrease in gamma oscillations. 8-CPT increases signal variance while measured at a fixed membrane potential, but not at resting membrane potential. An increase in signal variance does fit nicely with increased network activity.

4.4.2. Synaptic properties.

Adenosine also decreased EPSP size significantly. This will be partly due to the hyperpolarization of the membrane, but adenosine also inhibits neurotransmitter release from the pre-synaptic terminal (Haas and Selbach, 2000;Yoon and Rothman, 1991) possibly through a PKC mediated process (Thompson et al., 1992). A reduction in neurotransmitter release from excitatory synapses will reduce the oscillation even more. Not only does adenosine reduce the amount of action potentials, adenosine also makes the vesicle release caused by action potential less effective. The shift of the stimulus response curve to higher

intensities caused by adenosine will have a noticeable effect on gamma oscillations. This can be explained by the hyperpolarization of the membrane potential and reduction of vesicle release. The increase in EPSP amplitude during 8-CPT will have a positive effect on network oscillations because cells are activated more easily by a stronger EPSP. This leads to increased synchronised interneuron activation causing a larger field potential.

The most surprising finding in our data was the increased fast IPSP amplitude. The shift in the fast IPSP stimulus response curve to higher intensities is most likely due to the decreased efficacy of incoming EPSPs. In the presence of adenosine it will take more glutamatergic synapses to be active to cause a strong enough depolarization to activate the same amount of interneurons. The steepness of the fast IPSP stimulus response curve shows that it takes only the activation of a small portion of pyramidal cells to evoke an IPSP of maximum amplitude. This means that a shift in the stimulus response curve to higher intensities will have a dramatic effect on the amount of inhibition. If cells operate on the steep part of the curve in a normal functioning network than the presence of adenosine would cause a stimulus that would have been on the high end of the curve will now be on the bottom part of the curve. This will diminish the amount of synchronous inhibition in the network thereby reducing gamma oscillations. The adenosine induced shift in the slow IPSP stimulus response curve will be caused by a similar process. It is interesting to look at why the maximum fast IPSP is increased. Literature tells us that adenosine blocks the polysynaptic IPSP but that the monosynaptic IPSP is not affected (Thompson et al., 1992). There is a small but significant change in fast IPSP reversal potential to a more negative value. This change in fast IPSP reversal potential increases the driving force of the fast IPSP and can partly account for the increase in fast IPSP amplitude. If there is only an increase in inhibition it would be expected that gamma oscillations are increased as they are inhibition based (Fisahn et al., 1998;Fries et al., 2007). The fact that a decrease in gamma oscillations

is observed in the presence of adenosine indicates that the hyperpolarization of the resting membrane potential, and reduced effectiveness of excitatory inputs outweigh the increase in maximum fast IPSP amplitude.

4.4.3. Modelling the significant findings.

To find out whether the significant changes observed are sufficient to explain the increase in maximum fast IPSP amplitude, we modelled these changes in a computer model of a simplified model neuron using Neuron software (Michael Hines, John W. Moore, and Ted Carnevale, http://www.neuron.yale.edu/neuron/). The modelling is based on the "Interactions of synaptic potentials" tutorial from "Neurons In Action", which models three independent synaptic inputs, one for the EPSP, one for the fast IPSP and one for the slow IPSP. The simulation models a single compartment cell with a resting membrane potential of -65 mV, at 32 °C, for which the leakage conductance is set at 0.001 S/cm^2. First a control response is constructed to mimic the average response to Schaffer collateral stimulation in the before phase (black line in Figure 5.16.A.). The average response in the before phase and in the presence of adenosine (red line in Figure 4.17.A) were constructed from responses to a Schaffer collateral stimulus that evoked a maximal fast IPSP but not an action potential. The parameters used to mimic the response in the before phase are as followed:

EPSP parameters: onset = 5 ms, Tpeak = 5 ms, gmax = 0.4 µS, e = 0 mV.

Fast IPSP parameters: onset = 6 ms, Tpeak = 18 ms, gmax = 4 µS, e = -82 mV.

Slow IPSP parameters: onset = 16 ms, Tpeak = 130 ms, gmax = 1.3 µS, e = -90 mV.
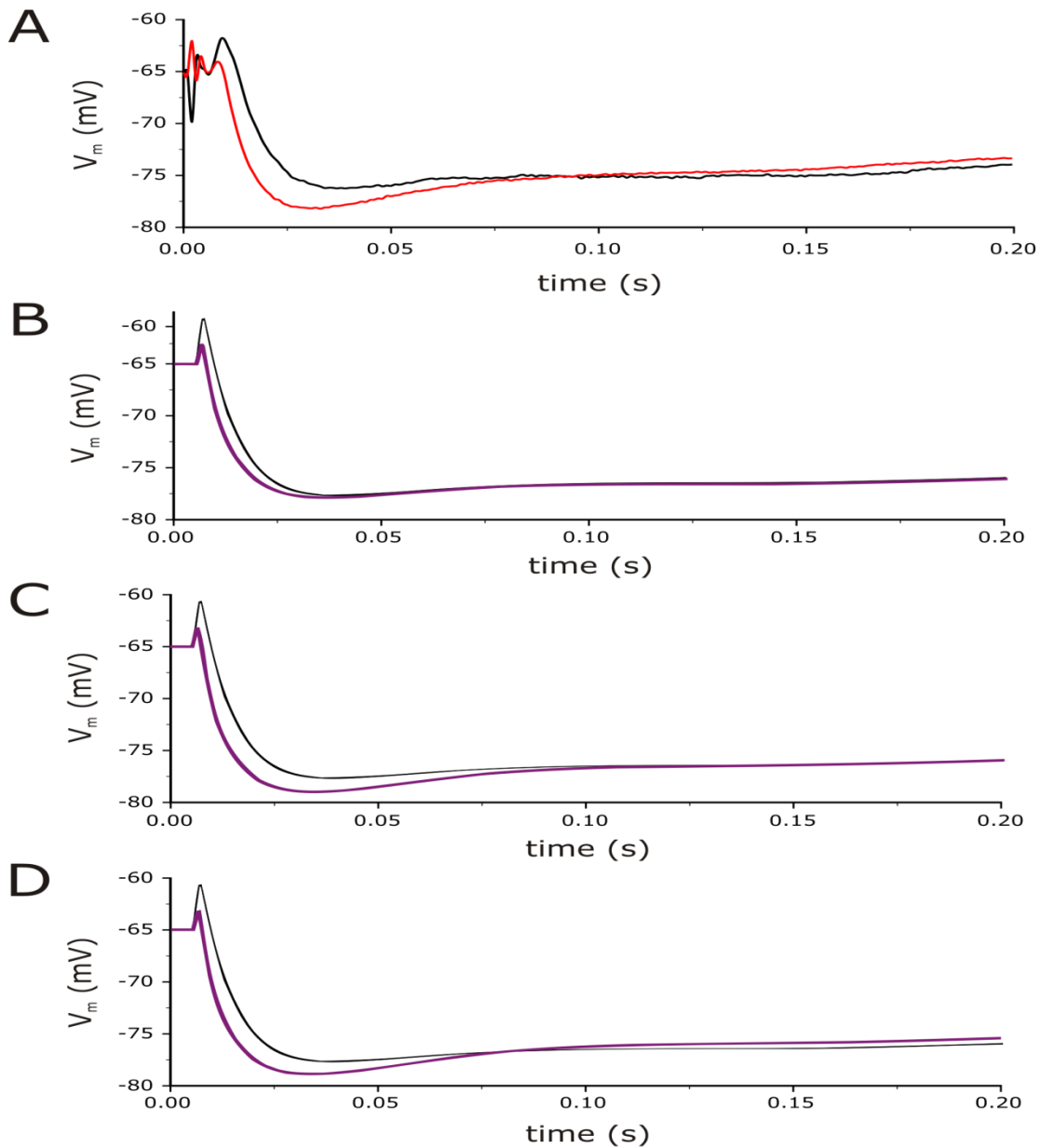
Figure 4.17. Modelling of the response to a Shaffer collateral stimulus at -65 mV. **A.** Average response of 7 cells before (black line) and during 50 µM adenosine (red line) to a Schaffer collateral stimulus that did not evoke an action potential. **B. C. D.** Black represents response in the before phase, yellow line represents response with changed parameters. **B.** First the EPSP conductance was reduced by half causing a reduction in the preceding EPSP and a shift of the response to the left but no change in amplitude. **C.** Then the fast IPSP reversal potential was set more negative by 2 mV causing a small increase in fast IPSP amplitude. **D.** The last change modelled was the shift in slow IPSP stimulus response curve by slightly decreasing the slow IPSP current. This made the response almost completely look like the recorded response indicating the observed changes are sufficient to explain the change in shape while adenosine is present.

Subsequently only the significant changes described in the result section are modelled. First the EPSP conductance was halved to model the change in EPSP amplitude. The EPSP preceding the IPSP was reduced and the hyperpolarizing line towards the fast IPSP maximum was shifted to the left (figure 4.17.B.). As this did nothing to the fast IPSP amplitude the change in fast IPSP reversal potential is added by changing the reversal potential to -84 mV (Figure 4.17.C). This increases the fast IPSP amplitude, which made the response almost look like the measured average in Figure 4.17.A. The only difference is that the modelled response stayed more hyperpolarised than the before response. The final change modelled was the shift in slow IPSP stimulus response curve by slightly reducing the conductance to 1.2 µS. With the changes in EPSP conductance, fast IPSP reversal potential and slow IPSP conductance the modelled synaptic response looks very similar to the recorded response in the presence of adenosine. This indicates that the observed changes described in this chapter are enough to explain the change in synaptic response induced by adenosine.

4.4.4. Conclusion.

The changes observed in cellular and synaptic properties upon adenosine receptor modulation support the data from the field recordings in previous chapters. The reduction in gamma oscillations by adenosine are most likely mediated by a hyperpolarization of the resting membrane potential of pyramidal cells and interneurons (Li and Henry, 2000), a reduction in the effectiveness of EPSPs through prevention of vesicle release and a hyperpolarised membrane potential, and a reduced activation of interneurons with the same excitatory input. The maximum fast IPSP amplitude is increased through a shift of the fast IPSP reversal potential to a more negative potential, which should increase synchronicity and thereby increase gamma oscillations. A decrease in gamma oscillations is observed because the hyperpolarization of the resting membrane potential and the decrease in the effectiveness in EPSPs outweigh the increase in fast IPSP amplitude. The adenosine A_1-receptor antagonist 8-CPT probably increases gamma oscillations through increased pyramidal cell firing, and increased excitatory inputs to interneurons, resulting in more synchronous activity within the network as more interneurons will be activated at the same time leading to an increased gamma oscillation.

4.5. Future research.

The experiments described in this chapter show that adenosine receptors can modulate gamma oscillations through cellular and synaptic processes. It would be interesting to find out what the contribution of each observed change is. Is it as simple as just hyperpolarizing the resting membrane potential, or do all observed effects have equal value? To find out we could assess the effect adenosine has on gamma oscillations *in vitro* in the presence of a GIRK-channel blocker. This would prevent the neurons from hyperpolarizing and thus we can see how much the cellular changes contribute to the observed modulation of gamma oscillations.

It is also interesting to find out more about the lack of depolarization in the presence of 8-CPT. Ambient adenosine levels are high enough to activate GIRK channels at our experimental conditions but under normal conditions somatic GIRK channels have a low open probability while this increases along the dendritic tree (Chen and Johnston, 2005). To find out more we could patch dendrites of CA3c hippocampal neurons and measure resting membrane potential and GIRK channel activity before and in the presence of 8-CPT. Another option would be to increase somatic GIRK channel activity by other means than activation adenosine A_1-receptors and then apply 8-CPT.

As membrane potential control over the whole cell is not great while using sharp electrodes some findings will be more credible if repeated under patch clamp conditions. The change in fast IPSP reversal potential is very small yet has quite a big effect. The prediction would be that in an isolated cell while using patch clamp recording we could get a better estimation of the shift in fast IPSP reversal potential. This will be looked at in the next chapter. We will also assess resting membrane potential and monosynaptic IPSC to confirm previous findings.

Parameter		Parameter value	ΔaCSF	Δadenosine (50 µM)	ΔaCSF	Δ8-CPT (5 µM)
Intrinsic properties		*n=22*	*n=6*	*n=7-8*	*n=6*	*n=6-8*
Tau_m (ms)	Mean	41.5	2.1	-5.7	5.7	2.2
	SEM	2.4	3.0	3.0	4.2	3.6
Slope resistance (MΩ)	Mean	50.0	1.1	-2.8	2.2	3.7
	SEM	3.3	2.7	4.2	3.5	4.0
C_m (pF)	Mean	0.91	0.08	-0.13	0.13	-0.02
	SEM	0.08	0.12	0.07	0.11	0.04
$AP_{slope\ up}$ (V/s)	Mean	174	5.3	6.1	2.9	-4.9
	SEM	13	2.2	2.0	2.2	3.8
$AP_{slope\ down}$ (V/s)	Mean	-71	-0.5	-1.3	-0.5	2.8
	SEM	6.0	0.9	0.9	1.2	1.1
AP_{thres} (mV)	Mean	-53.9	-0.47	-1.63	-0.72	-0.51
	SEM	1.0	1.7	1.5	2.7	0.9
AHP_{tau} (s)	Mean	1.3	0.10	-0.09	0.18	0.04
	SEM	0.1	0.07	0.09	0.11	0.19
AHP_{angle} (mV/action potential)	Mean	1.7	-0.15	-0.07	0.09	-0.07
	SEM	0.3	0.12	0.12	0.31	0.07
V_m (mV)	Mean	-58.6	-0.49	**-4.34**	-0.49	-1.08
	SEM	0.77	0.88	1.16	0.88	0.72
$Variance_{Vm}$ (mV^2)	Mean	1.04	-0.07	**-0.34**	-0.05	0.24
	SEM	0.17	0.10	0.10	0.11	0.14
$Variance_{-65}$ (mV^2)	Mean	0.57	0.04	-0.04	0.07	**0.67**
	SEM	0.10	0.11	0.07	0.1	0.31
Firing rate (Hz)	Mean	0.35	0.02	**-0.29**	0.02	**0.16**
	SEM	0.16	0.02	0.16	0.02	0.03

Table 4.1. Sharps parameters. Change in intrinsic properties in the presence of aCSF, adenosine (50 µM) and 8-CPT (5 µM). Bold numbers indicate significant differences (p<0.05) compared to the change in controls.

Parameter		Parameter value	ΔaCSF	Δadenosine (50 μM)	ΔaCSF	Δ8-CPT (5 μM)
Synaptic properties		*n=22*	*n=6*	*n=7-8*	*n=6*	*n=6-8*
EPSP fit values						
$EPSP_{max}$ (V/s)	Mean	7.27	0.58	**-2.64**	0.52	**1.84**
	SEM	0.76	0.57	0.53	0.54	0.49
$EPSP_{slope}$	Mean	1.92	0.08	-0.13	0.05	0.16
	SEM	0.22	0.28	0.23	0.26	0.50
EPSP ES_{50} (V)	Mean	7.8	0.02	**0.74**	-0.22	0.64
	SEM	0.4	0.4	0.2	0.3	0.4
Fast IPSP fit values						
Fast $IPSP_{max}$ (mV)	Mean	9.91	0.51	**2.73**	1.50	0.01
	SEM	0.60	0.37	0.50	0.80	0.59
Fast $IPSP_{slope}$	Mean	0.45	-0.09	0.06	-0.09	0.04
	SEM	0.08	0.04	0.04	0.04	0.16
Fast IPSP ES_{50} (V)	Mean	4.9	0.07	**0.69**	-0.04	0.26
	SEM	0.3	0.14	0.16	0.24	0.17
Reversal potential (mV)	Mean	-82.1	0.42	**-2.28**	-0.83	0.55
	SEM	1.6	0.85	0.69	1.17	2.18
Slow IPSP fit values						
Slow $IPSP_{max}$ (mV)	Mean	9.94	0.44	-0.41	1.33	1.80
	SEM	0.76	0.47	0.78	0.92	0.83
Slow $IPSP_{slope}$	Mean	1.33	0.10	0.63	-0.04	-0.28
	SEM	0.26	0.16	0.38	0.20	0.43
Slow IPSP ES_{50} (V)	Mean	7.2	0.18	**1.8**	0.16	0.93
	SEM	0.6	0.38	0.81	0.42	0.95

Table 4.1 (continued). Sharps parameters. Change in synaptic properties in the presence of adenosine (50 μM) and 8-CPT (5 μM). Bold numbers indicate significant differences (p<0.05).

CHAPTER 5: ADENOSINE RECEPTOR MODULATION OF MONO-SYNAPTIC IPSCS.

5.1. Introduction.

The previous chapter showed that adenosine application unexpectedly increased the fast IPSP amplitude possibly through causing the fast IPSP reversal potential to become more negative. The unexpected finding that adenosine application increased IPSP amplitude, (see chapter 4) casted doubt on the previous reported finding that adenosine receptors do not affect inhibitory synapses (Thompson et al., 1992;Yoon and Rothman, 1991). Experiments in the previous chapter were done in slices without any additional pharmacological modification to suppress activity to mimic the same conditions used in field recordings. To get more insight into the mechanism underlying the increased IPSP amplitude, isolated mono-synaptic inhibitory postsynaptic current (IPSC) and the IPSC reversal potential will be investigated using patch clamp recordings. Using patch clamp allows for better voltage control of the neurons which together with pharmacological isolation of IPSCs will allow for proper assessment of the effect A_1-receptor modulation has on IPSCs and IPSC reversal potential.

Recordings were made in the CA1 area of the hippocampus because attempts to patch CA3c neurons failed. CA3c neurons are notoriously hard to patch and to be able to obtain useful data we moved to CA1. Thus we make the assumption that the location and actions of A_1-receptors are not different between the two areas. No differences have been described in literature in A_1-receptor density or cellular location between CA3c and CA1 neurons (for receptor distribution see introduction Figure 1.2).

It is predicted that the IPSC will not be altered by adenosine receptor modulation as it has been shown that mono-synaptic IPSPs are not affected (Thompson et al., 1992;Yoon and Rothman, 1991). It is predicted that the selective adenosine A_1-receptor agonist CPA will

hyperpolarise the resting membrane potential. The A_1-receptor antagonist 8-CPT is expected to not change the resting membrane potential because GIRK channels at the soma are have a low probability of being open at the membrane potential recorded (Chen and Johnston, 2005). It is hard to predict what will happen to the IPSC reversal potential but if the results from the previous chapter are confirmed CPA will make the IPSC reversal potential more negative. If 8-CPT will have any effect on the IPSC reversal potential it is expected to make it more positive.

5.2. Materials and methods.

5.2.1. Tissue preparation.

Sprague-Dawley rats (17-32 days old, 40-170 grams, from Charles-River, Margate, UK) were anaesthetised with a mixture of ketamine (75 mg/kg) + medetomidine (1 mg/kg) by i.p. injection. The rat's blood was replaced via cardiac perfusion through the left ventricle with an oxygenated and chilled sucrose based solution containing (in mM): sucrose, 205; KCl, 2.5; $NaHCO_3$, 26; NaH_2PO_4, 1.25; D-glucose 10; $MgCl_2$, 5; $CaCl_2$, 0.1. Subsequently the rat was killed by cervical dislocation after which the brain was removed and kept cold in oxygenated sucrose solution. Using an Integraslicer (Campden Instruments, Loughborough, UK) 250 µM thick horizontal slices were made from the ventral hippocampus (coordinates from bregma: -7.5 to -5.0 mm) and put either in a submerged recording chamber containing oxygenated aCSF (containing (in mM): D-glucose, 10; $NaHCO_3$, 26; NaCl, 125; KCl, 3; NaH_2PO_4, 1.25; $CaCl_2$, 2; $MgCl_2$, 1) at 30°C, or stored in a static interface type chamber containing aCSF at 23°C for later use. All procedures were in accordance with the UK 'Animals (Scientific Procedures) Act 1986', and the studies were approved by the Biomedical Ethics Review Sub-Committee.

5.2.2. Electrophysiological recordings.

Patch clamp recordings from CA1 pyramidal cells were made using glass pipette recording electrodes filled with internal solution (containing (in mM): KCH_3SO_4, 140; NaCl, 8; 4-(2-Hydroxyethyl)-1-piperazineethanesulfonic acid (HEPES), 10; Mg-ATP, 2; Na-GTP, 0.3) with a pH of 7.4±0.1. The membrane potential was amplified using an Axoclamp-2A amplifier

(Axon Instruments, Burlingham, CA, USA) and a Neurolog NL106 DC amplifier (Digitimer, Welwyn Garden City, UK), low-pass filtered at 2 kHz and sampled at 10 kHz. The signal was then digitised and sampled by using a CED-1401 (Cambridge Electronical Design, Cambridge, UK) and analyzed using Signal 3 and Spike 2 software (Cambridge Electronical Design, Cambridge, UK).

Cells were visualised using an infrared microscope. Before breaking through the cell membrane a seal resistance of at least 1 GΩ was made. CA1 hippocampal cells were used for experiments when the resting membrane potential was stable and the cell needed less than 0.01 nA current to stay at -60 mV resting membrane potential, and had overshooting action potentials. Cells were bridge balanced in current clamp and access resistance was not allowed to vary more than 10% over the course of the experiment. When switching to voltage clamp recordings the cell was balanced again, to compensate for any action potentials as good as possible without running the risk of losing the cell, using gain, phase lag and anti-alias filter. Mono-synaptic IPSPs, recorded in voltage clamp, were evoked by stimulating the stratum pyramidale layer using a 0.1 ms square pulse via a concentric stimulating electrode (Harvard Apparatus Ltd, Kent, UK). The stimulus electrode was placed in stratum pyramidale less than 100 μm from the recorded cell.

Drugs were diluted from the following stock solutions: DL-2-Amino-5-phosphonovaleric acid (APV, 25 mM), 1,2,3,4,-Tetrahydro-6-nitro-2,3-dioxo-benzo(f)quinoxaline-7-sulfonamide disodium salt hydrate (NBQX, 20 mM), adenosine (10 mM stock in aCSF), 8-cyclopentyl-1,3-dimethyxanthine (8-CPT; 10 mM stock in 0.1 M NaOH), N^6-Cyclopentyladenosine (CPA; 50 μM stock in aCSF), -[2-[[6-Amino-9-(*N*-ethyl-*b*-d-ribofuranuronamidosyl)-9H-purin-2-yl]amino]ethyl]benzenepropanoic acid hydrochloride (CGS21680; 100 mM stock in DMSO). All drugs and aCSF salts were purchased from Sigma (Poole, UK).

All experiments were done in the presence of AP-5 (25 µM) and NBQX (20 µM) to block excitatory synaptic activity. After running all protocols for the first time in normal aCSF (before phase) drugs were washed in for 10 minutes by adding them to the aCSF flowing in the system. If the cell was still healthy and the membrane potential was stable after the drugs were washed in, the same protocols were done in the presence of the added drug (drug phase). Once all protocols were run once again the drugs were washed out by changing to a fresh aCSF solution. After 10 minutes of wash out the cell was checked to assess if it was still healthy, and if it was the protocols were done a third time (after phase).

5.2.3. Analysis and statistics.

Statistical comparisons were made between the change (drug phase – before phase) in aCSF controls and the change in the presence of adenosine receptor acting drugs. The comparison between experiments (unpaired) was chosen over the comparison within experiments (paired) to make sure that any change occurring over time will not be mistaken for a change caused by adenosine or 8-CPT. Every variable was first analyzed for normality using the Kolmogorov-Smirnov test in SPSS 15.0, and any difference in starting value between groups. If data was normally distributed a Student's *t*-test was used for comparison while if data was not normally distributed a Mann-Whitney U-test was used. Unless stated otherwise, there was no difference in the starting values between the different treatment groups.

5.3. Results.

5.3.1. Cellular properties.

Figure 5.1.A gives a response of a CA1 pyramidal cell to a +0.5 nA and -0.5 nA current injection. The action potentials in CA1 pyramidal cells are not as grouped compared to CA3c cells (see Figure 4.4.A). This is most likely because the AHP in CA1 cells is not as strong as in CA3c cells.
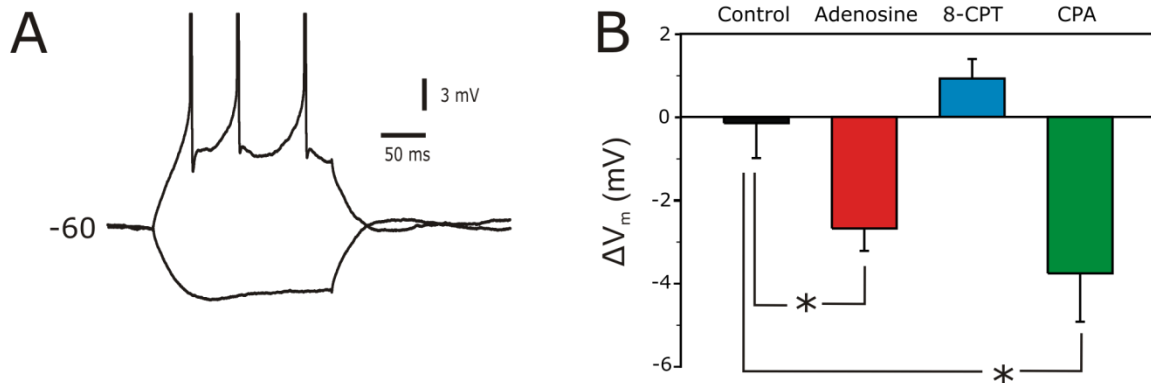
Figure 5.1. Patch-clamp cellular properties. **A.** Response to a -0.5 and +0.5 nA current injection. Contrary to CA3c cells action potentials are not grouped and the slow afterhyperpolarisation is a lot smaller. Action potentials are cropped. **B.** Change in membrane potential during drug wash in. Adenosine (p=0.035, n=6) and CPA (p=0.036, n=6) significantly hyperpolarised the membrane potential. 8-CPT (n=7) slightly increased resting membrane potential though not significantly different from controls (n=5).

The slope resistance was calculated using the same methods described in chapter 4. The average slope resistance was 152±11 MΩ (n=27). In controls the slope resistance changed significantly over time (Student's paired *t*-test, *p*=0.001, n=5), while there was no significant difference between the before phase and drug phase in all the drug groups. As a consequence of the controls changing significantly over time all the changes in the drug groups are significantly different from the change in controls (64.1±7.2 MΩ, n=5, (Student's

t-test; adenosine (50 µM, 11.8±7.9 MΩ n=6), t_9=4.8, *p*=0.001; 8-CPT (5 µM, 19.9±10.6 MΩ, n=7), t_{10}=3.2, *p*=0.01; Mann-Whitney U-test; CPA (50 nM, 10.7±13.8 MΩ, n=6), *U*=4.0, *p*=0.045).

The average resting membrane potential before drug application was -60.9±0.6 mV (n=27). To measure the change in membrane potential cells were held at -60 mV. Then adenosine receptor modulating drugs were added to the aCSF. Three minutes after wash in, the membrane potential was measured again if the membrane potential was stable. The change in membrane potential during 50 µM adenosine application was -2.7±0.5 mV (n=6). This was significantly different from the change in controls (-0.1±0.8 mV, n=5), see Table 5.1 and Figure 5.1.B (Student's *t*-test, t_8=2.5, *p*=0.035). The adenosine A_1-receptor agonist CPA (50 nM) significantly hyperpolarised the membrane potential by -3.8±1.2 mV (n=6) (Student's *t*-test, t_8=2.5, *p*=0.036). The A_1-receptor antagonist 8-CPT (5 µM, 0.9±0.5 mV, n=7) and the A_{2A}-receptor agonist CGS21680 (20 nM, 0.7±0.2 mV, n=3) did not significantly change the resting membrane potential compared to controls (see Table 5.1).

5.3.2. Inhibitory post-synaptic current (IPSC).

The unexpected finding that adenosine application increased IPSP amplitude, (see Chapter 4) casted doubt on the previous reported finding that adenosine receptors do not affect inhibitory synapses (Thompson et al., 1992;Yoon and Rothman, 1991). Figure 5.2.A shows the responses of a CA1 pyramidal cell to monosynaptic stimulation of increasing stimulus strength. To measure the IPSC amplitude the baseline (dotted line 1 in Figure 5.2.B) was subtracted from the maximum response (dotted line 2 in Figure 5.2.B). As the recordings were quite noisy the maximum was determined by estimating the average peak value with a cursor. The IPSC amplitude was set out against the stimulus strength and fitted with a

sigmoidal function, IPSC amplitude=$IPSC_{max}/1+(exp(-(S-ES_{50})/slope))$. $IPSC_{max}$ is the fitted

maximum IPSC amplitude, ES_{50} is the stimulus strength (S) required to reach half maximum

effect and the slope is an inverse measure of the steepness of the curve (see Figure 5.2.C).

The average $IPSC_{max}$ was 0.2±0.02 nA (n=26) and the average ES_{50} was 21.9±1.5 V

(n=26). There was no significant difference in the change in $IPSC_{max}$ or ES_{50} between aCSF

controls and adenosine
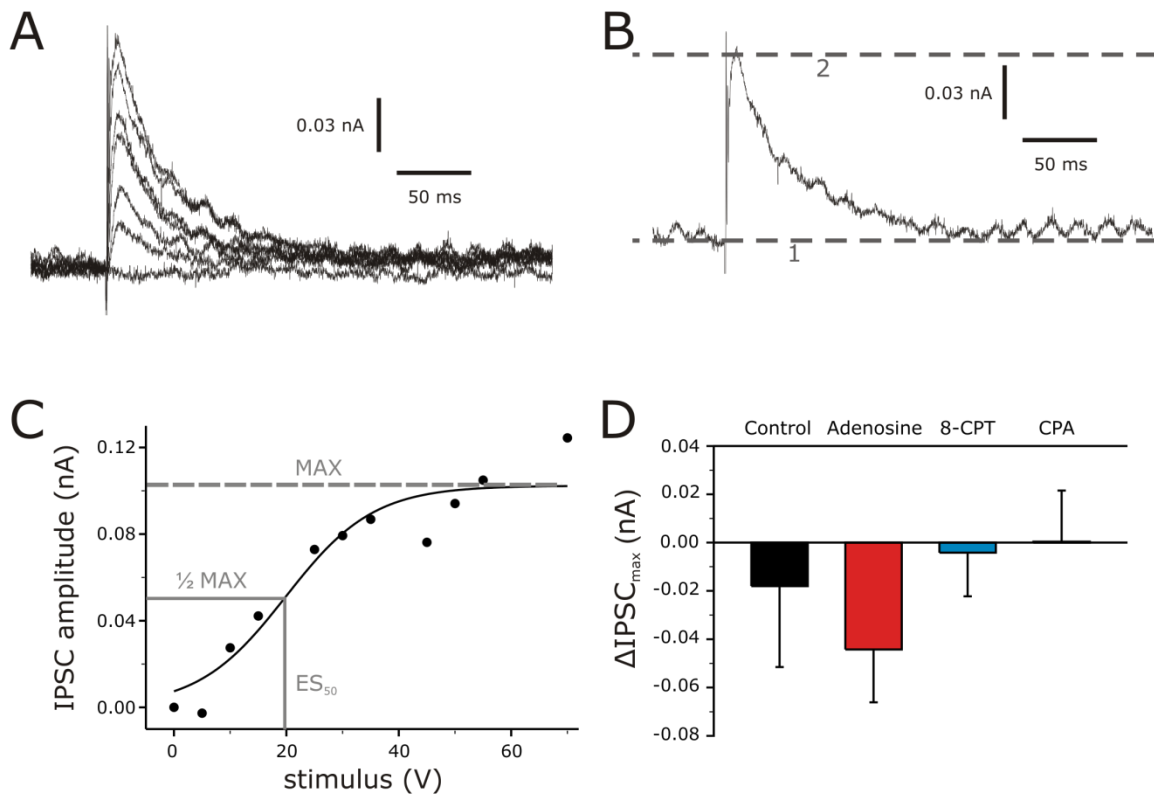
Figure 5.2. Inhibitory post-synaptic currents (IPSCs). **A.** Responses of a CA1 pyramidal cell in the presence of APV (25 µM) and NBQX (10 µM), recorded in voltage clamp, to increasing mono-synaptic stimulation (0, 10, 15, 25, 35 ,55, 70 V). **B.** Response to the 55 V stimulus. IPSC amplitude was measured by subtracting the baseline (dotted line 1) from the peak current (dotted line 2). **C.** The IPSC amplitude was set out against the stimulus intensity and fitted with a sigmoidal curve. From the fits three values are taken: the fitted maximum, the half maximum value (ES_{50}) and the slope. **D.** Change in fitted IPSC maximum in aCSF controls (n=5), adenosine (50 µM, n=6), 8-CPT (5 µM, n=6) and CPA (50 nM, n=6). There was no statistical significant difference between groups.

receptor modulating drugs (see Figure 5.2.D and Table 5.1). The average slope was 7.7±0.7

(n=26). The change in slope was not different between controls and adenosine or CPA (see

Table 5.1). 8-CPT changed the slope by 0.3±1.0 (n=6) which was significantly different from

controls (-2.9±0.8, n=5) (Mann-Whitney U-test, U=4.0, p=0.045). CGS21680 also

increased the IPSC$_{slope}$ slightly but significantly (0.6±0.1, n=3, Mann-Whitney U-test, U=0.0,

p=0.025), though numbers in this group are low (n=3).

5.3.3. IPSC reversal potential.

In the previous chapter a minor but significant change in IPSP reversal potential was

described. Here the reversal potential of the underlying current is investigated under better

controlled conditions. Figure 5.3.A shows the responses to a sub-maximal stimulus at

varying membrane potential. The stimulus chosen had to give a clear response in the

stimulus response curve used to measure IPSC amplitude, but not cause a maximum IPSC.

The IPSC amplitude was measured every 5 mV between -110 and -50 mV. To determine the

IPSC reversal potential the IPSC amplitude was set out against the membrane potential.

Under the assumption that the constant field theory can be applied and ion concentrations

inside and outside are equal the relationship is predicted to be linear. All the cells recorded

under our conditions showed a rectification from this predicted linear relationship. To obtain

the most accurate measure of the IPSC reversal potential the data were fitted with a 3

parameter exponential function (see Figure 5.3.B); IPSC amplitude=y0+a*exp(b*V$_m$). To

calculate the reversal potential the equation was solved for amplitude=0. The average

reversal potential was -70.3±1.0 mV (n=26). Adenosine and CPA made the IPSC reversal

potential slightly more negative, while 8-CPT and aCSF controls made the IPSC reversal

potential more positive (see Table 5.1). But there are no significant differences between

controls and adenosine receptor modulating drugs. There is a significant difference between the change caused by 8-CPT (4.4±1.5 mV, n=6) and change caused by CPA (-1.2±1.5 mV, n=6, Mann-Whitney U-test, U= 5.0, p=0.022). This indicates that adenosine A_1-receptor activity can influence the IPSC reversal potential. A_1-receptor and A_{2A}-receptors often have opposite effects on second messenger pathways and thus cause opposite effects (Fredholm et al., 2001). The A_{2A}-receptor agonist CGS21680 (20 nM) also causes a positive change in IPSC reversal potential (see Table 5.1) indicating a post-synaptic mechanism linked to both A_1- and A_{2A}-receptors could be involved in altering the reversal potential. Figure 5.3.D shows a scatter plot of the change in reversal potential against the change in resting membrane potential. There is a significant correlation through all data points (Pearson correlation coefficient = 0.476, p=0.019, n=26). Using a quick cluster analysis in SPSS 15 two clusters were identified. The open squares in Figure 5.3.D show cluster centres and the two clusters are separated by the dotted line. The left clusters contains mainly cells exposed to CPA and adenosine (A_1-receptor agonist) while the right cluster mainly consists of cells exposed to 8-CPT (A_1-receptor antagonist). Thus, cells that have a large hyperpolarisation of the resting membrane potential are also likely to have a negative shift in the reversal potential.

The current across a membrane is determined by the driving force and the conductance. To rule out that the change in IPSP amplitude is due to a change in membrane conductance the slope conductance was calculated. From the same plot where the IPSC reversal potential was calculated from (Figure 5.3.B) the slope conductance was calculated. The points above the reversal potential were fitted with a linear function (amplitude=y0+slope conductance*V_m). The average slope conductance was 0.51±0.05 µS (n=26). None of the adenosine receptor acting drugs changed the slope conductance significantly from starting values. There were no differences in the change in slope conductance between controls and the different adenosine receptor acting drug groups (see Table 5.1).
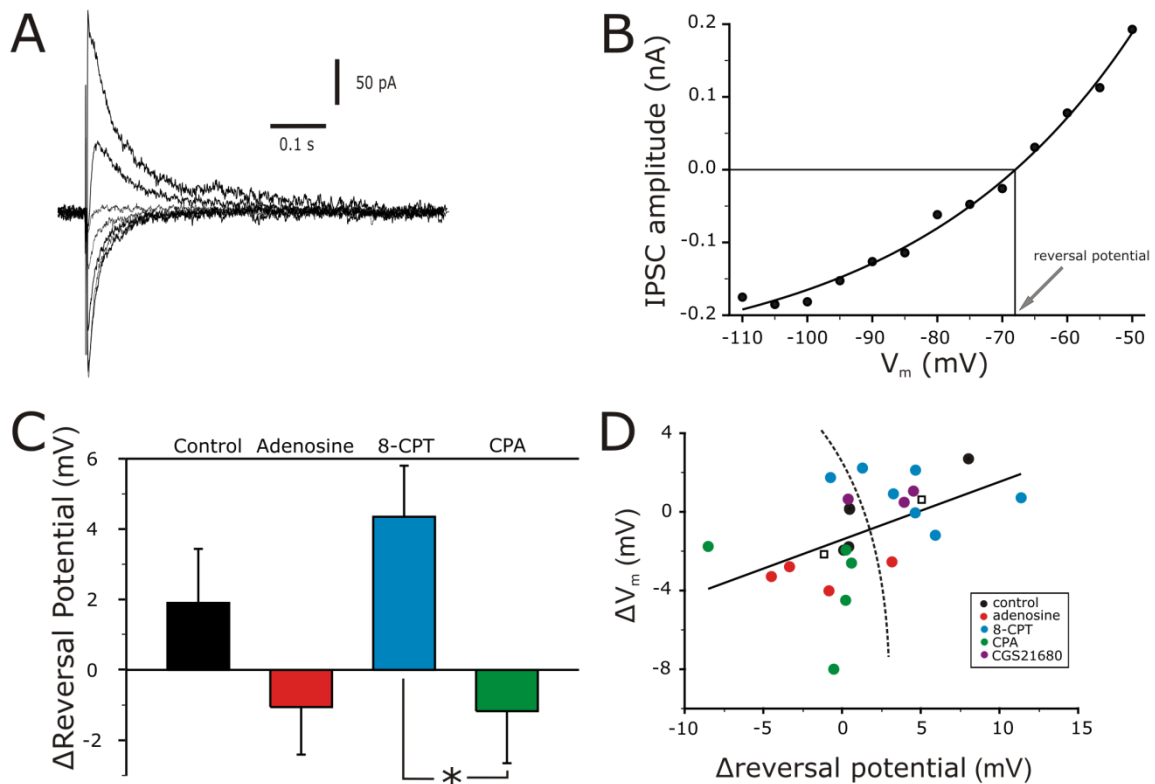
Figure 5.3. IPSC Reversal potential. Experiments were done in the presence of APV (25 µM) and NBQX (10 µM). **A.** Responses to mono-synaptic stimulation (40 V) at varying membrane potential. **B.** IPSC amplitude against membrane potential plot. All data points were fitted with a 3 parameter single exponential fit: IPSC amplitude=$y0+a*exp(b*V_m)$. The reversal potential was calculated by solving the equation for IPSC amplitude =0. **C.** Change in reversal potential during aCSF (n=5), adenosine (50 µM, n=6), 8-CPT (5 µM, n=6) and CPA (50 nM, n=6). There was no significant difference between controls and drug groups. There was a significant difference in the change in reversal potential between 8-CPT and CPA (p=0.022). **D.** Scatter plot of the change in membrane potential and the change in reversal potential. There is a significant correlation through all data points (p=0.019, n=26). There are two clusters of points distinguishable. The open squares indicate cluster centres; the dotted line separates the two clusters.

5.4. Discussion.

Adenosine A_1-receptor activation significantly hyperpolarises the resting membrane potential and shifts the IPSC reversal potential to more negative potentials. Blocking the adenosine A_1-receptor with 8-CPT has no significant effect on the resting membrane potential compared to the change in controls and makes the IPSC reversal potential more positive. The IPSC was not affected by any adenosine receptor modulation.

In line with the results from chapter 4 the resting membrane potential was also hyperpolarised in patch recordings during A_1-receptor activation. The selective A_1-receptor agonist CPA also hyperpolarised the resting membrane potential. In patch recordings 8-CPT did show a change in the opposite direction but it was not significantly different from aCSF controls. This strengthens the idea proposed in the previous chapter that GIRK-channels have a very low open probability at the soma (see chapter 4 discussion) which makes recording a reduction in channel activity difficult.

To shed more light on why the IPSP amplitude was increased the underlying current was investigated. Just as previously reported the conductance underlying the IPSC was not affected by adenosine receptor modulation (Thompson et al., 1992;Yoon and Rothman, 1991). This finding is consistent with the fact that adenosine receptors are most likely not present on inhibitory pre-synaptic terminals (Thompson et al., 1992;Yoon and Rothman, 1991). This leaves the question of how does adenosine increase the IPSP amplitude. In the previous chapter a shift of the IPSP reversal potential to more negative values by adenosine A_1-receptor activation has been shown to be a likely candidate. Because the intracellular chloride concentration was clamped at 8 mM changes were expected to be small as only the extracellular Cl^- concentration can vary. Though no significant differences between controls and adenosine receptor modulating drugs have been found in the change in reversal

potential, there was a significant difference between the specific A_1-receptor modulating drugs CPA and 8-CPT. Together with the specific grouping of cells in the ΔV_m and Δreversal potential plot (Figure 5.3.D) this can indicate that a shift in reversal potential can account for the increase in fast IPSP amplitude. In the model described in the discussion of chapter 4 the shift in reversal potential was enough to account for the increase the fast IPSP amplitude. The fact that the change in membrane potential correlates with the change in reversal potential suggests a common second messenger pathway is involved. One possible mechanism by which A_1-receptor modulation can hyperpolarise the membrane potential and shift the reversal potential is via modifying the AC, cAMP and PKA pathway through $G_{i/o}$ signalling. $G_{i/o}$ signalling modifies GIRK channel activity (Lei et al., 2003) and is also coupled to AC activity which can alter PKA activity through cAMP levels (Sebastiao and Ribeiro, 2000). A reduction in cAMP levels and thereby reduced PKA activity through A_1-receptor activation can lead to a reduced activity of the NKCC transporter (Haas and Forbush, III, 1998;Sebastiao and Ribeiro, 2000). This in turn leads to a reduced Cl^- uptake which increases the driving force for the fast IPSP through an increase in extracellular chloride. Thus A_1-receptor activation can hyperpolarise the resting membrane potential and the shift the IPSP reversal potential via $G_{i/o}$ signalling.

In conclusion the findings in this chapter are in line with literature and the finding in the previous chapters. The increase in fast IPSP amplitude is most likely caused by a shift in reversal potential. An increase in inhibition would in theory be able to increase the power of an inhibition based network oscillation. This increase is unlikely to have an effect on the gamma oscillation as the other cellular and synaptic effects that suppress network activity outweigh the increase in driving force for IPSPs.

5.5 Future research.

The fact that the experiments in this chapter were done in CA1 pyramidal cells instead of CA3c pyramidal cells does mean care has to be taken to make conclusions about the CA3c area. It would be good to repeat the shift in reversal potential in CA3c pyramidal cells in patch clamp recordings.

There is little information on the cellular mechanism by which adenosine A_1-receptor modulation can change the fast IPSP reversal potential. The proposed mechanism in the discussion is hypothetical and needs to be backed up by real data. One possible way would be to alter every step within the chain (cAMP, NKCC activity) and see whether or not this affects the reversal potential.

Another useful tool to further investigate the change in reversal potential is using the perforated patch method. In perforated patch the chloride concentration inside the cell is unaltered by pipette solution and thus changes in chloride concentrations can be picked up easier.

Parameter		Parameter value	ΔaCSF	Δadenosine (50 µM)	Δ8-CPT (5 µM)	CPA (50 nM)	ΔCGS21680 (20 nM)
Intrinsic properties		*n=27*	*n=5*	*n=6*	*n=7*	*n=6*	*n=3*
Slope resistance (MΩ)	Mean	150	64.1	**11.8**	**19.9**	**10.7**	40.2
	SEM	11	7.2	7.9	10.6	13.8	11.4
V_m (mV)	Mean	-60.9	-0.1	**-2.7**	0.9	**-3.8**	0.7
	SEM	0.6	0.8	0.5	0.5	1.2	0.2
IPSC fitted values		n=26	n=5	n=6	n=6	n=6	n=3
$IPSC_{max}$ (mV)	Mean	0.20	-0.02	-0.04	0.00	0.00	0.02
	SEM	0.02	0.03	0.02	0.02	0.02	0.03
slope	Mean	7.7	-2.9	-5.9	**0.3**	0.7	**0.6**
	SEM	0.7	0.8	2.4	1.0	2.0	0.1
ES_{50} (V)	Mean	21.9	-1.9	-7.7	0.0	1.4	1.5
	SEM	1.5	2.3	2.6	1.7	3.9	1.5
Reversal potential (mV)	Mean	-70.3	1.9	-1.1	**<u>4.4</u>**	**<u>-1.2</u>**	3.0
	SEM	1.0	1.5	1.4	1.5	1.5	1.3
Slope conductance (µS)	Mean	0.51	0.02	0.04	0.00	0.01	0.19
	SEM	0.05	0.06	0.08	0.08	0.02	0.11

Table 5.1. Patch parameters. Change in intrinsic and synaptic properties in the presence of aCSF, adenosine (50 µM), 8-CPT (5 µM), CPA (50 nM) and CGS21680 (20 nM). Bold numbers indicate significant differences ($p < 0.05$) compared to the change in controls. Bold and underlined numbers within are significantly different from each other but not from the change in controls.

CHAPTER 6: ADENOSINERGIC MODULATION OF HIPPOCAMPAL GAMMA OSCILLATIONS *IN VIVO*.

6.1. Introduction.

In the previous chapters it has been shown that adenosine modulates brain oscillations most specific for the gamma range *in vitro*. *In vivo* gamma oscillations (30-100 Hz) are associated with a variety of cognitive functions including memory (Fell et al., 2001;Herrmann et al., 2004) and sensory processing (Engel and Singer, 2001;Singer, 1993). In rodents an increase in hippocampal gamma oscillation power is observed during explorative behaviour (Buzsaki et al., 2003;Csicsvari et al., 2003). Adenosine receptor modulation is able to alter cognitive function (Fredholm et al., 1999) including memory (Kopf et al., 1999;Pereira et al., 2002). However there is little direct evidence showing that adenosine receptor modulation alters cognitive function through changing gamma oscillations. There are some clues that adenosine receptors can alter cognitive function through affecting gamma oscillations. With age there is a decrease in hippocampal gamma oscillations in rodents (Vreugdenhil and Toescu, 2005). This could be related to the increase in ambient adenosine levels with age (Sebastiao et al., 2000). This makes it quite possible that changes in adenosine levels or receptor function can underlie the age-related decrease in memory function.

To have an indication whether adenosine receptor modulation is a possible target for preventing cognitive decline or increasing cognitive function, the *in vitro* results have to be verified *in vivo*. In slice experiments many brain regions that project to the hippocampus are cut off during slice preparation. Because adenosine receptors are abundantly expressed throughout the brain (see table 1.1), projections to the hippocampus from other brain areas can have unexpected effects on gamma oscillations *in vivo*. Because the *in vitro* experiments

showed that the A_1-receptor is most effective in modulating hippocampal gamma oscillations (see chapter 2 and 3), the selective A_1-receptor agonist CPA and the selective A_1-receptor antagonist 8-CPT were used in the experiments in this chapter. In this chapter the effect of the A_1-receptor agonist CPA and the A_1-receptor antagonist 8-CPT on *in vivo* hippocampal gamma oscillations will be investigated in an anaesthetised animal. It is predicted that A_1-receptor modulation has similar effects as seen in *in vitro* experiments (see chapter 2 and 3) where activating A_1-receptors will decrease gamma oscillation strength and inhibiting A_1-receptors will increase gamma oscillation strength.

6.2. Materials and methods.

6.2.1. Animal preparation.

Male Sprague-Dawley rats (250-400 grams, from Charles-River, Margate, UK) were anaesthetised by an i.p. urethane (1.25 g/kg) injection. When needed an i.p. injection of a mixture of ketamine (75 mg/kg) + medetomidine (1 mg/kg) was given to keep the animal well anaesthetised. Urethane is not suitable as a top-up anaesthetic because its effects are not immediate. After the urethane injection the rat was left alone for at least 45 minutes to allow the animal to be properly anaesthetised. The animal's skull was shaved and if needed a ketamine-medetomidine mixture was given before the animal was put into a stereotactic frame. Once in the stereotactic frame the eyes were lubricated to prevent them from drying out and the animal was set up with a breathing monitor and a heart rate and blood oxygen monitor. The animal was kept warm with an electrical heating pad and the temperature was monitored via a rectal probe. The animal was covered with bubble wrap to reduce heat loss as much as possible. The animal's temperature was kept at 36.5±0.5 °C and blood oxygen levels, measured at the foot, were kept between 80 and 90 %. If blood oxygen levels dropped below 80% extra oxygen was given via a small tube aimed at the rat's nose. The pedal reflex test, pressure on the rat's hind limb that causes retraction of the paw if not properly anaesthetised, was tested every 10 minutes and if needed a quarter dose of ketamine medetomidine mixture was given to make sure the animal was well anaesthetised. The skull was exposed and a small window perpendicular to the line bregma – interaural was made at the recording site on one side of the brain. For the ventricular injection of drugs a single burr hole was made. All procedures were in accordance with the UK 'Animals

(Scientific Procedures) Act 1986', and the studies were approved by the Biomedical Ethics Review Sub-Committee.

6.2.2. Electrophysiological recordings.

Recordings from the CA3c (coordinates from bregma (Paxinos and Watson, 1998): anterior-posterior (AP); -3.8, medio-lateral (ML); 3.5/-3.5, dorso-ventral (DV); -3.5) and the CA1 (coordinates from bregma (Paxinos and Watson, 1998): AP; -3.8, ML; 2.4/-2.4, DV; -2.2) area of the hippocampus (see Figure 6.1) were made using bipolar twisted Teflon-coated wire electrodes (Nickel (80%)/Chromium (20%), 0.05 mm, Advent Research Materials Ltd, Eynsham, Oxford, England, UK). The electrode was strengthened with a thin coating of nail varnish to prevent them from bending while lowered into the brain. One of the electrodes was cut shorter so the two ends could straddle the stratum pyramidale (distance between the two ends: 0.4 mm). Recordings were amplified using Neurolog NL104 AC-coupled amplifiers (Digitimer Welwyn Garden City, UK) and band-pass filtered at 3-2000 Hz. Noise locked to the powerline frequency 50 Hz was removed with Humbug noise eliminators (Digitimer Welwyn Garden City, UK). Subsequently the signal was digitised and sampled at 5 kHz using a CED-1401 interface (Cambridge Electronic Design, Cambridge, UK) and analyzed using Spike-2 software (Cambridge Electronic Design, Cambridge, UK). Drugs were injected using a 10 µl Hamilton syringe (Hamilton Company, Reno, Nevada, USA) in the third ventricle (coordinates from bregma: AP; -0.8, ML; 1.3, DV; -3.5). The Hamilton syringe was inserted under a slight angle (see Figure 6.1) to prevent possible damage to a major artery running over the injection site.

Drugs were diluted from the following stock solutions: 8-cyclopentyl-1,3-dimethyxanthine (8-CPT; 10 mM stock in 0.1 M NaOH), N^6-Cyclopentyladenosine (CPA; 50 µM stock in sterile

aCSF). Drugs were diluted so that the injection volume was between 1 and 3 μl. The concentration used was aimed to be around 100 times higher than the receptor saturation concentration *in vitro*. All drugs were purchased from Sigma (Poole, UK).
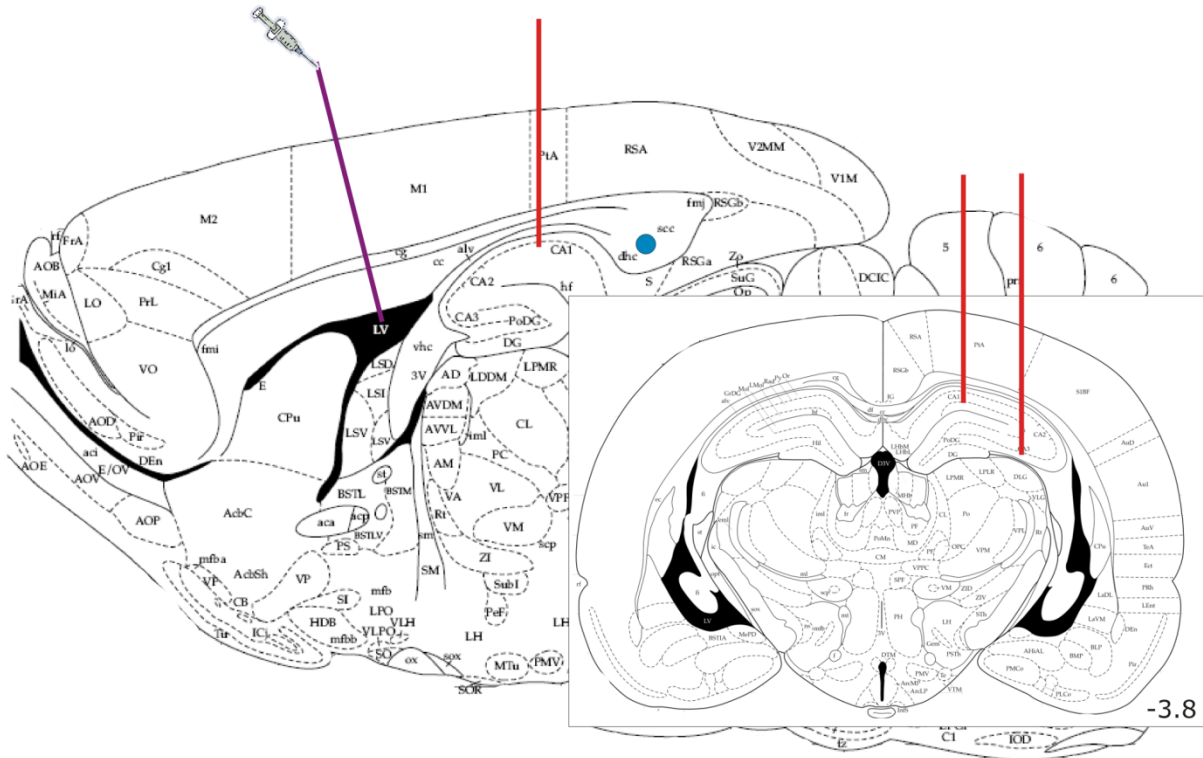
Figure 6.1. Recording and injection site in the hippocampus used in *in vivo* experiments. The two red lines indicate the position of the bipolar recording electrodes targeting the CA3c and CA1 area of the hippocampus. The electrode was aimed so that the ends of the bipolar electrode were straddling the stratum pyramidale. The purple line represents the Hamilton syringe used to inject drugs into the third ventricle. The blue dot indicates a stimulation site used in pilot experiments to find the optimal recording site.

6.2.3. Electrode placement.

The aim of this study was to investigate the influence of adenosinergic modulation of gamma oscillations in the hippocampus. It was less important to record from the exact same spot in the hippocampus than to record a good signal from the CA3c and CA1 area. To test whether

the stereotaxic placement of the recording electrode in CA3c was correct (straddling stratum pyramidale) the dorsal hippocampal commissure (coordinates from bregma (Paxinos and Watson, 1998): AP;-4.5, ML; 0.3/-0.3, DV;-2.4, see Figure 6.1) was stimulated with a bipolar electrode (identical to the recording electrodes). As soon as the longest tip of the electrode passed the stratum pyramidale any stimulus given at the dorsal hippocampal commissure will invert at the recording site. Using this technique for both CA3c and CA1, the coordinates found were very similar from experiment to experiment (n=9). Thus it was chosen to place the electrodes without relying on the stimulus in all subsequent experiments. Electrodes were lowered slowly to the pre-defined coordinates and if there was a good signal that had a measurable power in the gamma range (30-100 Hz) within 0.2 mm of the depth aimed for, that position was taken. For electrodes recording from the CA1 area it meant that when power in the gamma range would increase the hippocampus was reached. For the CA3c area the electrodes must first pass through the CA1 area (see Figure 6.1). Power in the beta and gamma range would increase while passing through the CA1 area, to then disappear while in the molecular layers to emerge again when approaching the CA3c area. Variation in this area was also kept within 0.2 mm of the targeted coordinates. The placement of the Hamilton syringe was tested in one of the pilot experiments via dissection of the brain, making sure the predetermined coordinates were correct.

6.2.4. Analysis and statistics.

Data was analyzed in 5 minute epochs just before and 30 minutes after drug injection. Oscillation power was calculated from the recordings for four frequency bands (slow: 3-13 Hz, beta: 13-30 Hz, gamma: 30-100 Hz, fast: 100-250 Hz) using fast fourier transform (1 Hz bin size). Average power was calculated from the unfiltered power spectrum only correcting for line noise if the Humbug was unable to filter all line noise out.

Data was filtered using the phase-true-FIR filter. Figure 6.2 shows the effect of filtering for different frequency bands has on the recordings and accompanying power spectra. A one second recording of the hippocampal CA3c area before any drugs were injected in the ventricle was used (see Figure 6.2.A and B). A low pass filter (13 Hz cut-off) selected all the slow waves and effectively removed all faster activity (see Figure 6.2.C and D). A band-pass filter (FIR, >30 Hz and <100 Hz) was used to extract the gamma band waveform from the original recording (see Figure 6.2.E). The power spectrum made from the filtered gamma oscillations shows that filtering was successful and selective (see Figure 6.2.F). The fast frequencies were filtered out using a high pass filter (>100 Hz) effectively removing all the low and gamma waveforms (see Figure 6.2.G and H).

Markers were placed on gamma troughs (from the filtered data) that were clear gamma cycles with a size of at least 30% of the maximum amplitude. Single units were determined by filtering the original recording with a high pass filter above 300 Hz. Subsequently, an event was determined to be a single unit if the amplitude of that event was greater than three times the signal standard deviation. Signal standard deviation was calculated for every 5 minute epoch separately. Only the negative deflecting deviations were marked as single units even though in theory a single unit can also be seen as a positive deflection dependent on electrode position. As the recordings were made bipolar the sign of the recorded event depends on the relative location of the cell in comparison to the poles of the recording electrode.

Data was analyzed using non-parametric tests because numbers were low. Data are expressed as means±standard error of the mean (s.e.m.).
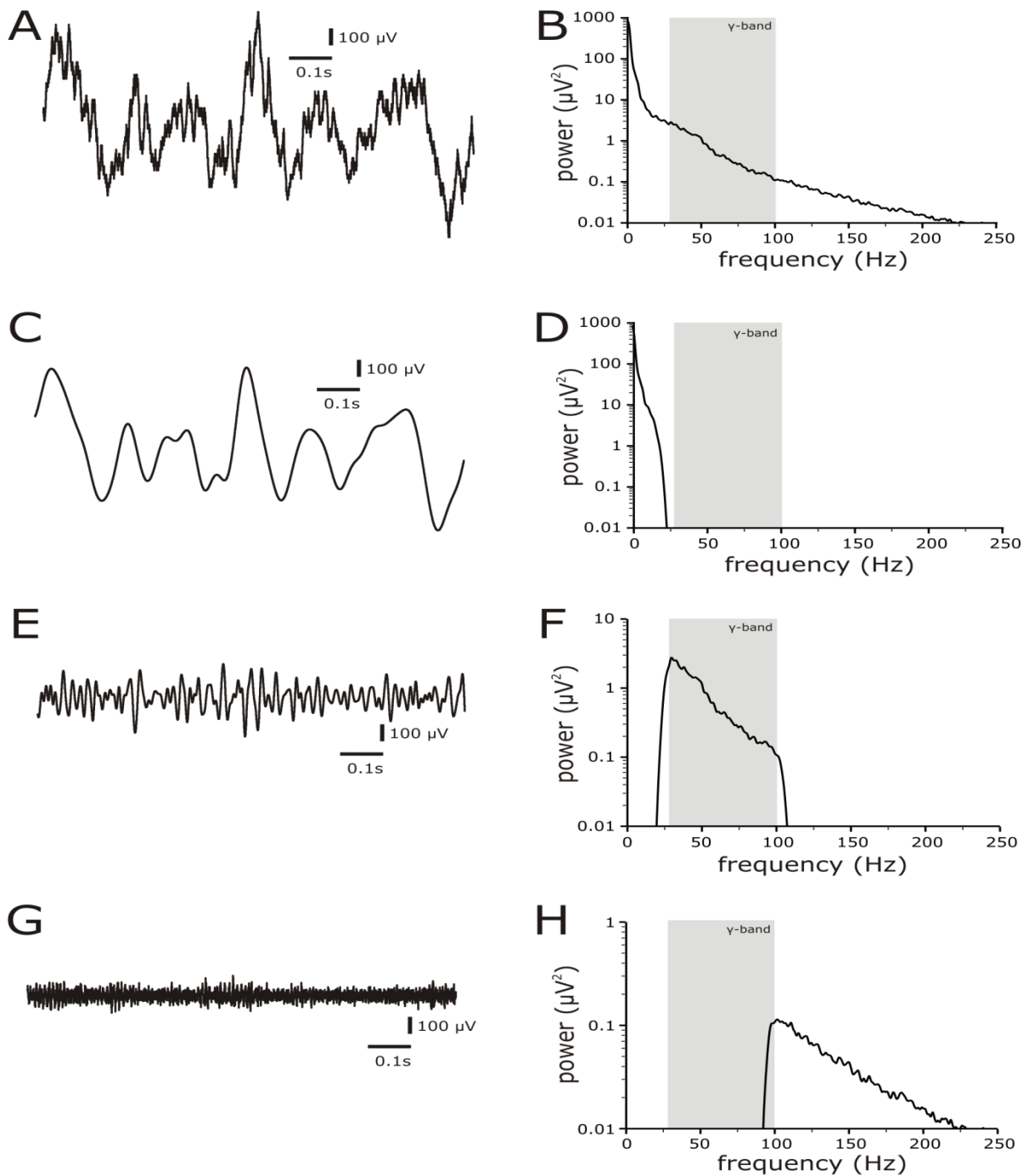
Figure 6.2. Effect of filtering data on recordings. Original data recorded from the CA3c area of the hippocampus (**A**) was filtered using a low pass (**C**, <13 Hz), band pass (**E**, 30-100 Hz) and high pass (**G**, >100 Hz) filter. The accompanying power spectra (**B, D, F, H** respectively) show the effect each type of filtering has on the recorded signal. Power spectra are shown with a logarithmic scale because the proportion of power in the lower frequencies is much higher in in vivo recordings. The gamma band is indicated by the light grey area. The filtered signals are very clean and narrow for their frequency bands indicating the right settings were used.

6.3. Results.

6.3.1. The effect of lightened anaesthetic on hippocampal gamma oscillations.

To assess whether or not a rat is experiencing pain during the experiment the standard pedal reflex test is commonly used. When a rat responds to a squeeze in the paw by pulling its leg towards it abdomen extra anaesthesia is required. In pilot experiments sometimes a quick and substantial rise in gamma oscillation strength in the hippocampus was observed that was responsive to a ketamine medetomidine mixture top-up. The increase in power within the gamma band occurs before any pedal reflex can be observed. If no additional anaesthetics were given the animal would start to respond to the pedal reflex test within the next 15 minutes. Figure 6.3 shows the effect of lightened anaesthetics on hippocampal gamma oscillations in CA3c. When anaesthetics are lighter there is an increase in synchronous activity visible in the unfiltered raw trace (Figure 6.3.A). There is an increase in power in the gamma range with a distinct hump appearing in the power spectrum (Figure 6.3.B). Within five minutes the power increased approximately 5-fold in this example (Figure 6.3.C). After a top-up of anaesthetic the power returned back to baseline within five minutes. This finding complicates the analysis of the *in vivo* recordings. Because there was no marker besides the increase in gamma activity that indicated the anaesthetic were lightened care was taken in selecting experiments for analysis to only select those experiment were the level of anaesthesia were similar. If there was doubt about the level of anaesthesia around the time measurements are taken the experiment was rejected. Consequently the numbers in this chapter are rather low. The pedal reflex test is a commonly used test to get an indication of anaesthesia depth. The pedal reflex was tested every 10 minutes though after observing the increase in gamma oscillations during lightened
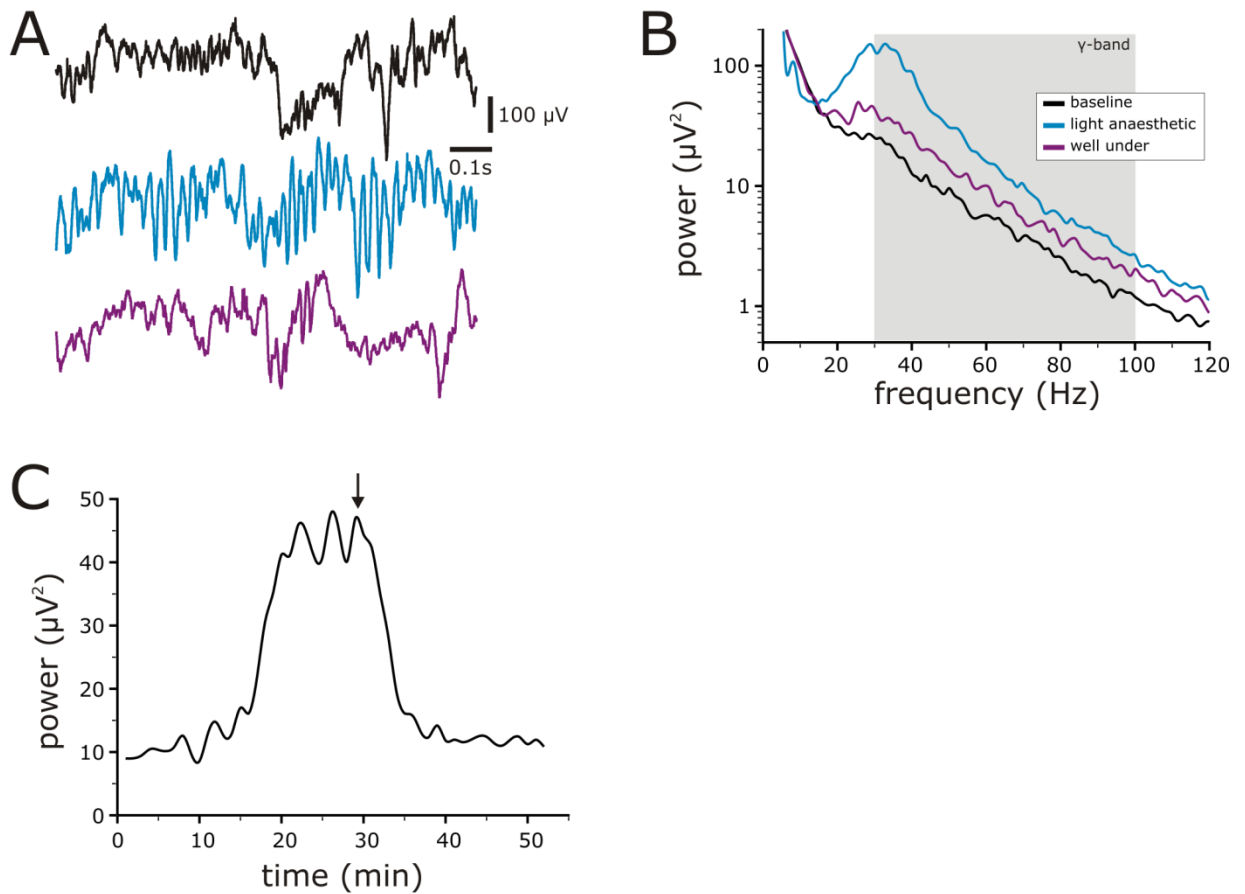
Figure 6.3. Effect of lightened anaesthetic on hippocampal gamma oscillations. **A+B.** Raw traces (**A**) and accompanying power spectrum (**B**) for the CA3c area at baseline (black), light anaesthetic (blue) and after anaesthetic top-up (purple). Lightened anaesthetic increased power in the gamma range in the CA3c area visible by the appearance of a hump in the gamma range as well as increased synchronous network activity in the raw trace. **C.** Time course of the change in average gamma power during lightened anaesthetic. There is a 5-fold increase in average gamma power within a few minutes that disappears just as fast when an anaesthetic top-up is injected (arrow).

anaesthetics, anaesthesia top-up was given as soon as an unusually large increase in gamma activity was observed.

6.3.2. Description of the in vivo gamma oscillation.

There is a distinguishable difference between the oscillation in the CA3c and the oscillation in the CA1 area of the hippocampus *in vivo* in our experiments. In most cases the power in the CA1 area decreases steadily with frequency within the gamma range. In the CA3c area there is often a shoulder at the start of the gamma range after which the power declines steadily with frequency. Figure 6.4.A shows the power of simultaneous recorded oscillations in CA3c and CA1 that nicely illustrate the difference in power distribution. To quantify this difference the gamma/beta ratio is calculated by dividing the power in gamma by the power in beta for both areas. The gamma/beta ratio is significantly greater in CA3c (0.26±0.04, n=6) than the gamma/beta ratio in CA1 (0.18±0.03, n=6, see Tables 6.2 and 6.3, Figure 6.4.B; Student's paired *t*-test, *t*=2.8, p=0.038).
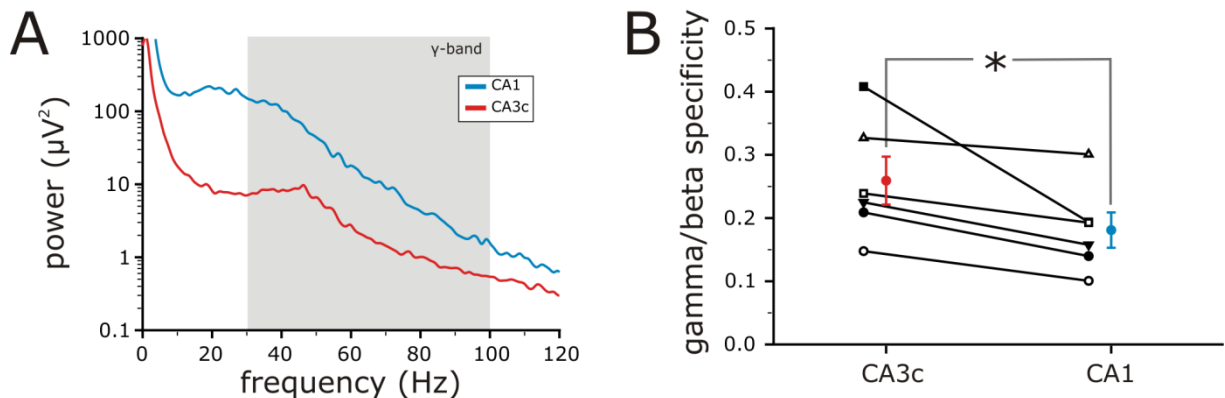
Figure 6.4. Difference in power spectrum between CA3c and CA1. **A.** Power spectrum from simultaneous recorded CA3c (red) and CA1(blue). CA1 shows a steady decline with increasing frequency within the gamma band. CA3c first has a shoulder after which power declines with increasing frequency. **B.** Gamma/beta specificity in the CA3c and CA1 area during simultaneous recordings. The specificity for each area is connected with a line. The mean±SEM are given by a dot with error bars. The specificity is significantly lower (p=0.027, n=6) in the CA1 compared to CA3c.

As recordings were made simultaneously the phase relationship between CA3c and CA1 can be investigated using cross-correlation. In most experiments there was a good phase relationship between filtered gamma of CA3c and CA1 (see Table 6.1). Figure 6.5.A shows a 1 second epoch of filtered gamma in CA3c and CA1. The peaks and troughs occur within a few milliseconds of each other on a large portion of the cycles. The cross-correlation of the same animal has a cross-correlation maximum of 0.58. The lag of the peak of the cross-correlation (Figure 6.5.B) is slightly positive indicating that the peak in the CA1 area is slightly after the peak in the CA3c area. The CA3c area leads the CA1 area in 5 out of 6 experiments (average 1.27±0.63 ms (n=6, n.s.).
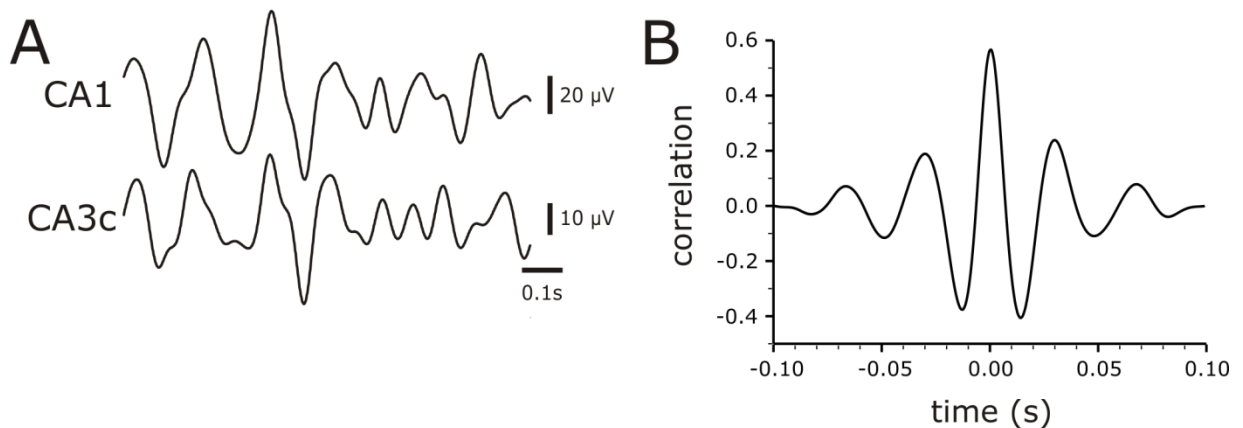
Figure 6.5. Cross correlation between CA3c and CA1. **A.** Example of one second filtered gamma traces from which cross-correlation is calculated. The peaks and troughs in both areas occur within milliseconds of each other for a large proportion of the gamma cycles. **B.** Cross-correlation between CA3c and CA1 calculated from traces band pass filtered for gamma. The peak is positive indicating that CA3c peaks earlier than and possibly leads CA1. The high peak indicates that Ca3 and Ca1 are phase coupled.

Gamma power fluctuates strongly in both CA1 and CA3c. To find out whether the power fluctuations between CA3c and CA1 is related the root mean square amplitude of the filtered gamma was calculated and then filtered with a low pass filter (FIR cut-off 13 Hz). Figure 6.6.A shows the CA3c filtered gamma waveform (I), the root mean square amplitude of the

signal (II) and the low pass filtered waveform of the root mean square amplitude modified waveform (III). The root mean square modification inverts the troughs after which a low pass filter describes the fluctuation in gamma power. A waveform correlation between CA3c and CA1 is made on the low pass filtered waveform comparing the fluctuation in power over time of the gamma oscillation in both areas (Figure 6.6.B). The power in CA3c is high at the same time the power in CA1 is high. This example shows that there is a correlation between the power in CA3c and CA1 with a cross-correlation maximum of 0.37. On average the correlation maximum is 0.24±0.07 (n=5, see Table 6.1).
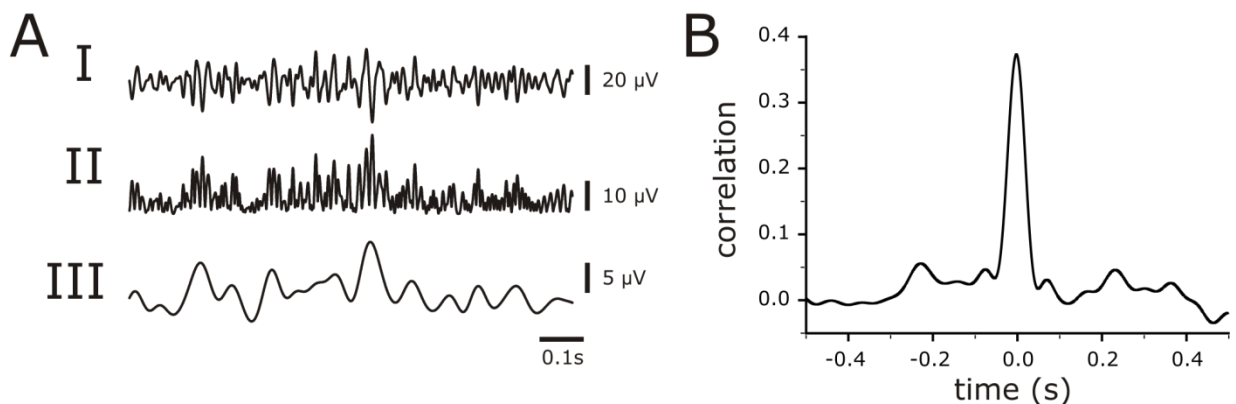
Figure 6.6. Root mean square amplitude. **A.** Traces of filtered gamma (I), the root mean square amplitude (II) and the low pass filtered waveform of the root mean square amplitude (III) recorded in the CA3c area. The root mean square amplitude modification inverts the troughs after which a low pass filtered waveform becomes an good indicator of the power fluctuation over time. **B.** Cross-correlation between the power fluctuation in CA3c and CA1. There is a sizeable correlation between the powers in both areas.

Because a wide spectrum of frequencies is recorded single units can be picked up. Recorded waveforms are high pass filtered for all frequencies above 300 Hz (Figure 6.7.A top). Any event that is bigger than three times the standard deviation (indicated with the grey line) is regarded as a single unit. The average single unit waveform in the CA3c of 1 experiment is shown in Figure 6.7.B. There is a distinctive average single unit visible showing the selected events are mostly single units. To determine if single units are related to the phase of the

gamma oscillations the timing of single units to gamma troughs (Figure 6.7.A bottom) was calculated. In four out of six experiments the intervals of single units to the gamma troughs are uniformly distributed (example in Figure 6.7.C, One sample Kolmogorov-Smirnov Test, $Z=0.6$, $p=0.881$) within the gamma oscillation. In two out of six experiments there is a non-uniform distribution of the single units (example in Figure 6.7.D, One sample Kolmogorov-Smirnov Test, $Z=1.8$, $p=0.004$). There is concentrated firing of the cells recorded just before the trough of the gamma peak in this experiment.
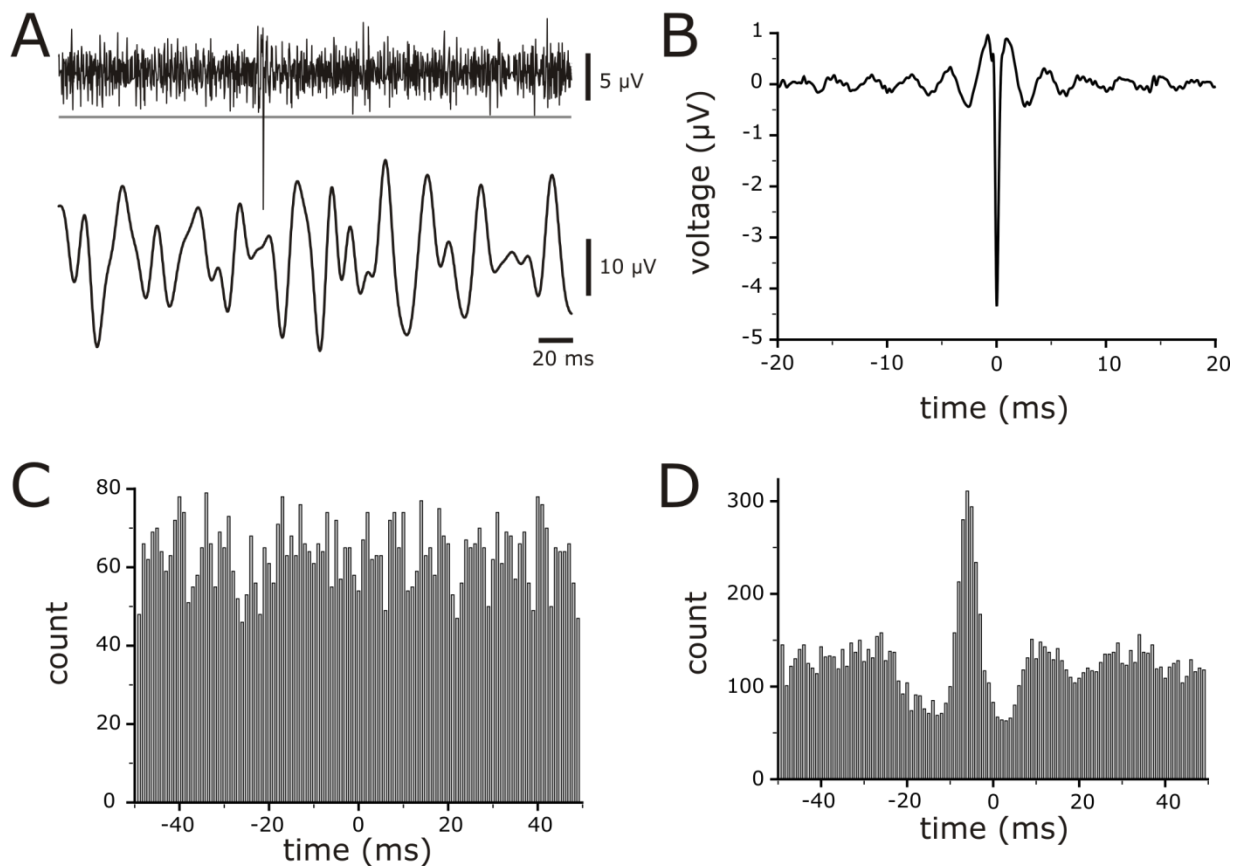
Figure 6.7. Event correlation in CA3c. **A.** Trace high pass filtered (>300 Hz, top trace) with corresponding gamma (bottom trace). Any event with an amplitude falling through three standard deviations (grey line) is taken as a single unit. **B.** Average waveform from selected events. A clear single unit is visible in the middle with little activity next to it. **C.** Spike distribution relative to the gamma trough. This example shows a uniform distribution. **D.** Example of an experiment whit a non-uniform distributed spike distribution. Spikes are concentrated just before the trough of the gamma oscillation.

6.3.3. The effects of A₁-receptor modulation on in vivo gamma oscillations.

Because A$_1$-receptors are distributed widely throughout the brain an injection into the ventricle is likely to affect other brain areas besides the hippocampus as well. Injecting the A$_1$-receptor agonist CPA into the ventricle decreases heart rate and breathing rate. Care was taken to keep the blood oxygen levels above 80%.

Due to the low numbers (n=3) in these experiments it is hard to make any definite conclusions on the effect of A$_1$-receptor modulation on *in vivo* gamma oscillations. There are some interesting observations that do provide good clues to what possible effect A$_1$-receptor modulation can have on *in vivo* gamma oscillations. Though not significant all rats injected with CPA (2 µg/kg) show a reduction of the power in all frequency bands in CA3c and CA1 30 minutes after injection (see Tables 6.2 and 6.3). Figure 6.8. A and B shows an example of the change of *in vivo* brain oscillations in CA3c and CA1 after ventricular CPA (2 µg/kg) injection. In this example there is a clear reduction of power in the CA3c area while in the CA1 area the decrease is less pronounced. The power after 8-CPT (300 µg/kg) injection has a less consistent effect compared to the effect of CPA. On average there is an increase in power in all frequency bands in both CA3c and CA1 after 8-CPT injection (see Table 6.2 and 6.3). The effect is less consistent because in one experiment both CA3c and CA1 show a reduction in power within the gamma range. In the example shown in Figure 6.8 C and D an increase in gamma power in the CA3c area (C) but a reduction in the CA1 area (D) is observed.

All the other parameters described did not show any consistent effects and thus speculation about the possible influence A$_1$-receptor modification would not be justified. The mean and

SEM of the cross-correlation, RMS-amplitude and spike distribution are summarised in Tables 6.2 and 6.3.
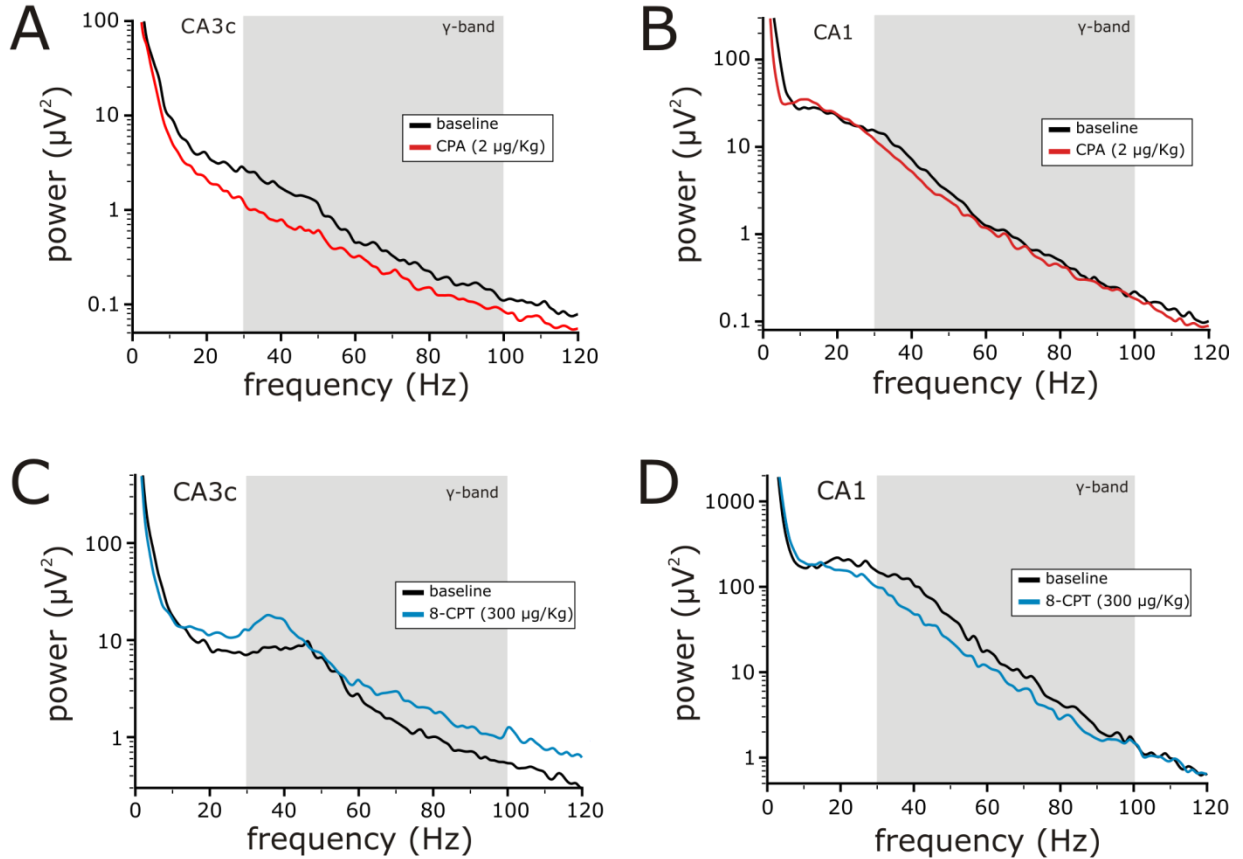
Figure 6.8. A1-receptor modulation of oscillation power in vivo. **A + B.** Brain oscillations recorded in an anesthetised animal from the CA3c (A) and CA1 (B) region of the hippocampus (black lines). CPA (2 µg/kg) consistently reduced the power in all frequency bands in both areas (red lines). The power on the y-scale is on a logarithmic scale because the power in the lower frequencies is very high. **C + D.** Brain oscillations recorded in an anesthetised animal from the CA3c (C) and CA1 (D) region of the hippocampus (black lines). 8-CPT (300 µg/kg) did not have a consistent effect on brain oscillations (blue lines). In this example the power in the CA3c area is increased in the gamma range, but reduced in the CA1 area. The power on the y-scale is on a logarithmic scale because the power in the lower frequencies is very high.

6.4. Discussion.

Compared to *in vitro* recordings the oscillation recorded *in vivo* has a lot more power in the lower frequency bands. This is probably due to projections into the hippocampus from other brain areas that are severed when cutting slices. For instance, the hypothalamus and the septum project to the hippocampus with a theta range frequency (Kirk and Mackay, 2003).

The oscillation in the CA3c area of the hippocampus measured *in vivo* has a higher gamma/beta ratio compared to the CA1 area. There is a small (not significant) phase lead of the CA3c area over the CA1 area and the power in both areas is also coupled. CA3c pyramidal neurons project to the stratum radiatum of the CA1 area while there are few projections from CA1 to CA3c. Thus it is likely that the CA3c influences the phase and possibly power of the gamma oscillation recorded in CA1. The linking of the two different areas in the hippocampus could serve as a means to transmit information between areas (Fries et al., 2007). In most experiments the timing of presumed single units was uniformly distributed compared to gamma troughs. In the few experiments that did have a non-uniform spike distribution the resulting figure (Figure 6.7.D) is what you would expect for gamma oscillations (Fries et al., 2007).

The increase in gamma band power during lightened anaesthetics was quite surprising. It could be that the type of anaesthesia used suppresses gamma oscillations and that what is recorded when the animal is deeply anaesthetised is a suppressed version of normal gamma oscillations. But if we compare the power spectrum during lightened anaesthetic with previously published *in vivo* recordings in freely moving animals (Buzsaki et al., 2003) the power in the gamma band is a lot higher. Thus it seems unlikely that the gamma recorded during lightened anaesthetic is the true gamma signal. It is more likely that it is a reaction to non-specific sensory stimuli reaching the cortex even though no pedal reflex was present.

Care was taken that in all experiments animals were anaesthetised to the standards required by the UK 'Animals (Scientific Procedures) Act 1986' and the Biomedical Ethics Review Sub-Committee. If it were the case that in the present experimental setup the gamma recorded is a suppressed version, one must be very careful in interpreting the results. Gamma oscillations in a freely moving animal might then respond in different ways that would not be picked up while looking at the suppressed version under anaesthetics.

No definite conclusions can be drawn about the influence of A_1-receptor modulation on *in vivo* gamma oscillations because the study was underpowered. The injection of A_1-receptor agonist CPA did however have a very consistent effect by reducing the power in all frequency bands in all experiments. This general suppression is quite different from the change observed *in vitro* (chapter 2) where A_1-receptor activation suppresses gamma band activity more specifically. The decrease in power in all frequency bands looks similar to a very high dose of adenosine *in vitro* which suppresses most oscillatory activity. The concentration CPA injected into the ventricle was about 100 times the receptor saturation concentration which could indicate a very high dose was used. However injections with a 5 times lower concentration did not suppress network activity in any frequency bands (not shown). Another option is that because CPA was injected into the ventricle the incoming inputs from other brain areas are also suppressed. With the widespread distribution of A_1-receptors and the ventricle being connected to the septum it is likely that activity in the septum will also be suppressed. Suppression of the septum would cause a reduction of the theta range input to the hippocampus which would reduce the power in the lower frequency bands. Thus it looks like A_1-receptor activation can also reduce gamma oscillations *in vivo* but in a less specific way.

The A_1-receptor antagonist 8-CPT did not show any consistent effect. The concentration used for 8-CPT (300 µg/kg) cannot easily be increased. 8-CPT cannot be dissolved in a higher

concentration than used which would leave as only option to increase the injection volume. Increasing the injection volume is not preferable because it will add more pressure to the brain of the rat and possibly displace all the aCSF in the ventricle. A better solution would be to use a different A_1-receptor antagonist that can be injected using a small volume. The concentration 8-CPT used is at least 100 times higher than the receptor saturation concentration used *in vitro*. The fact that there is little effect of the 8-CPT injection with such high concentrations could also indicate that adenosine levels are low under the recording conditions. If ambient adenosine levels are low during anaesthesia experiments, 8-CPT will not be able to increase gamma oscillations.

6.5. Future research.

As the study presented in this chapter was underpowered one should first increase the number of observations as to be able to draw better conclusions. Given the fact that gamma oscillations can increase substantially during lightened anaesthetics it is probably preferable to immediately investigate the effects of adenosine receptor modulation on gamma oscillations in freely moving animals. If the findings of the freely moving animal experiments are in line with previous result it would be interesting to investigate the role of A_1-receptors and gamma oscillations in behavioural tasks relating behavioural performance to gamma oscillation strength modified by adenosine receptors. Both gamma oscillations strength (Fell et al., 2001;Herrmann et al., 2004) and A_1-receptor modulation (Corodimas and Tomita, 2001;Hauber and Bareiss, 2001) have been linked to increased cognitive function but there is no research yet linking both in the same experiment.

The present study can be improved by injecting A_1-receptor acting drugs more localised. The ventricle was chosen because the whole hippocampus could then be targeted. The reduction in the low frequency bands indicates brain areas projecting to the hippocampus are also suppressed by ventricular injection. A more localised injection will remove the change in activity of brain areas that project to the hippocampus.

Parameter		Parameter value	before	CPA (2 µg/kg)	Before	8-CPT (300 µg/kg)
CA3c-CA1		*n=6*	*n=3*	*n=3*	*n=3*	*n=3*
Cross-correlation						
Peak	Mean	0.32	0.50	0.45	0.15	0.14
	SEM	0.09	0.07	0.10	0.06	0.05
Peak, time (ms)	Mean	1.27	1.45	0.10	1.09	3.30
	SEM	0.63	0.80	0.81	1.13	2.96
RMS amplitude		*n=5*	*n=3*	*n=3*	*n=2*	*n=2*
Peak	Mean	0.24	0.32	0.25	0.12	0.12
	SEM	0.07	0.08	0.13	0.03	0.03
Peak, time (ms)	Mean	1.16	2.47	1.40	-0.80	-5.8
	SEM	1.56	2.43	1.93	0.40	7.0

Table 6.1. Cross-correlation and RMS amplitude relationships between CA3c and CA1.

Parameter		Parameter value	before	CPA (2 µg/kg)	CPA normalised	Before	8-CPT (300 µg/kg)	8-CPT normalised
CA3c		*n=6*	*n=3*	*n=3*	*n=3*	*n=3*	*n=3*	*n=3*
Power								
Gamma (30-100 Hz	Mean	13.1	21.2	15.3	0.66	5.1	7.3	1.7
	SEM	7.9	15.7	11.2	0.09	1.5	1.0	0.5
Slow (3-13 Hz)	Mean	409.6	751.5	160.6	0.55	67.7	89.3	1.2
	SEM	295.5	564.8	86.4	0.24	24.7	44.8	0.3
Beta (13-30 Hz)	Mean	60.1	102.4	38.8	0.48	17.8	24.5	1.6
	SEM	35.8	67.6	21.0	0.08	8.1	6.7	0.4
Fast (100-250 Hz)	Mean	0.36	0.47	0.30	0.68	0.25	0.39	1.6
	SEM	0.15	0.31	0.18	0.04	0.04	0.00	0.2
Gamma/beta ratio	Mean	**0.26**	0.19	0.30		0.32	0.34	
	SEM	0.04	0.02	0.10		0.05	0.08	
Spike distribution								
Z-value	Mean	1.13	1.17	1.90		1.10	1.24	
	SEM	0.20	0.34	0.71		0.29	0.38	

Table 6.2. Effect of A_1-receptor modulation on *in vivo* hippocampal (CA3c) gamma oscillations. Bold numbers indicate significant differences ($p<0.05$) between CA3c and CA1 (Table 6.3).

Parameter		Parameter value	before	CPA (2 µg/kg)	CPA normalised	Before	8-CPT (300 µg/kg)	8-CPT normalised
CA1		*n=6*	*n=3*	*n=3*	*n=3*	*n=3*	*n=3*	*n=3*
Power								
Gamma (30-100 Hz	Mean	14.1	10.1	4.3	0.63	18.0	32.7	2.09
	SEM	5.8	6.6	1.5	0.16	10.4	22.4	1.37
Slow (3-13 Hz)	Mean	324.3	441.6	45.9	0.32	207.1	493.4	2.26
	SEM	169	351.2	10.7	0.17	75.7	253.4	0.98
Beta (13-30 Hz)	Mean	76.7	70.3	28.2	0.65	83.2	119.4	1.84
	SEM	30.5	39.1	3.3	0.24	55.5	59.0	1.01
Fast (100-250 Hz)	Mean	0.17	0.12	0.05	0.58	0.22	0.29	1.23
	SEM	0.05	0.06	0.01	0.17	0.08	0.12	0.22
Gamma/beta ratio	Mean	**0.18**	0.13	0.15		0.23	0.24	
	SEM	0.03	0.02	0.04		0.04	0.07	
Z-value	Mean	0.76	0.75	0.77		0.70	0.63	
	SEM	0.09	0.17	0.13		0.13	0.07	

Table 6.3. Effect of A_1-receptor modulation on *in vivo* hippocampal (CA1) gamma oscillations. Bold numbers indicate significant differences ($p<0.05$) between CA1 and CA3c (Table 6.2).

CHAPTER 7: ADENOSINERGIC MODULATION OF HIPPOCAMPAL GAMMA OSCILLATIONS: FROM SINGLE CELL TO WHOLE ANIMAL.

7.1. Can adenosine receptor modulation alter hippocampal gamma oscillations in vitro?

Applying exogenous adenosine decreases hippocampal gamma oscillations in all of the *in vitro* models used. A high dose of adenosine decreases oscillatory activity in all frequency bands while a lower dose is specific for the gamma band. Adenosine suppresses gamma oscillations through A_1-receptor activation. A_{2A}-receptor activation moderately increases gamma oscillations. Blocking A_1-receptors increases hippocampal gamma oscillations more potently than A_{2A}-receptor activation.

Fluctuating endogenous adenosine levels influence gamma oscillation strength *in vitro*. Increasing adenosine levels by blocking adenosine breakdown decreases gamma band activity specifically. Interestingly it is estimated that the increase in adenosine levels falls within the natural fluctuation observed *in vivo*. This makes a strong case that fluctuating adenosine levels can determine gamma oscillation strength *in vivo*. Decreasing adenosine levels by facilitating adenosine break-down has the opposite effect and increases gamma oscillations.

7.2. What cellular and synaptic changes underlie adenosinergic modulation of hippocampal gamma oscillations?

Adenosine decreases hippocampal gamma oscillations by hyperpolarising the resting membrane potential and inhibiting excitatory synaptic transmission through presynaptic receptors. Adenosine also increases the maximum IPSP amplitude most likely by increasing

the driving force through a shift of the IPSP reversal potential to a more negative potential. Monosynaptic inhibition is not altered by adenosine receptor modulation suggesting adenosine receptors are not present on inhibitory synapses. Increased strength of inhibitory synapses is more likely to increase gamma oscillations but adenosine has the opposite effect. Thus, the increase in driving force for inhibition is outweighed by the reduction in excitation and hyperpolarisation of the membrane potential.

Blocking A_1-receptors increases hippocampal gamma oscillations by facilitation of excitatory synapses and increasing principal cell excitability. By increasing principal cell excitability and making excitatory synapses more effective, more interneurons will be activated per gamma cycle resulting in an increase in the extracellular recorded signal.

7.3. Does adenosinergic modulation have the same effect in vivo?

Due to a small number of observations no definite conclusions can be drawn about the effect of A_1-receptor modulation on *in vivo* gamma oscillations. However, A_1-receptor activation did reduce the strength of the oscillation in all frequency bands in every experiment. This is quite different from the *in vitro* situation as there the suppression is more specific for the gamma band. This difference is most likely due to suppression of inputs from other brain regions projecting to the hippocampus. Blocking A_1-receptors did not have any consistent effect on *in vivo* hippocampal gamma oscillations.

7.4. Implications of this study.

With the very clear effects of adenosinergic modulation of hippocampal gamma oscillations *in vitro* adenosine receptors seem like a good target to alter cognitive performance related

to gamma oscillations. However, the results *in vivo* are ambiguous indicating that a lot more work has to be done to find a suitable drug. Gamma oscillations are probably still a good target for treating memory deficiency or prevent memory decline during old age. Gamma oscillation strength has been linked to cognitive performance in rodents (Fuchs et al., 2007) making it likely that adenosinergic modulation of gamma oscillations can affect cognitive function. Among the drugs currently used to treat memory related diseases are cholinesterase inhibiters that prevent the breakdown of acetylcholine. Carbachol, used to induce hippocampal gamma oscillations *in vitro*, and acetylcholine target the same metabotropic receptors which is a good indication that gamma oscillations can be a viable target for treating memory deficiency. With the widespread distribution of adenosine receptors throughout the brain and their strong homology between different brain structures (Fredholm et al., 2001) adenosine receptor acting drugs are very likely to have many side effects. However if drugs can be designed to target specific areas in the brain adenosine receptors are a good candidate to modulate brain function. Both the A_1-receptor and the A_{2A}-receptor have been shown to prevent cognitive impairment or increase cognitive function in rodents (Cognato et al., 2010;Hauber and Bareiss, 2001;Pereira et al., 2002). To maximise a drug's potential to increase gamma oscillations and possibly cognitive function using adenosine receptors, the compound used should ideally be an A_1-receptor antagonist and an A_{2A}-receptor agonist.

In the case of old age dementia preventing the increase in adenosine levels with age can be a promising strategy.

In conclusion adenosine receptors modulate gamma oscillations *in vitro* very effectively but are difficult targets for developing new treatments that have cognitive benefits because of their ambiguous effects *in vivo*. If brain areas can be targeted specifically adenosine

receptors are a good possible target to develop therapies for treating cognitive deficiencies

linked to a reduction in gamma oscillation strength.

Reference List

Alzheimer C, ten Bruggencate G. (1991) Postsynaptic inhibition by adenosine in hippocampal CA3 neurons: Co(2+)-sensitive activation of an inwardly rectifying K+ conductance. Pflugers Arch 419:288-295.

Bach ME, Barad M, Son H, Zhuo M, Lu YF, Shih R, Mansuy I, Hawkins RD, Kandel ER (1999) Age-related defects in spatial memory are correlated with defects in the late phase of hippocampal long-term potentiation in vitro and are attenuated by drugs that enhance the cAMP signaling pathway. Proc Natl Acad Sci U S A 96:5280-5285.

Ballarin M, Fredholm BB, Ambrosio S, Mahy N (1991) Extracellular levels of adenosine and its metabolites in the striatum of awake rats: inhibition of uptake and metabolism. Acta Physiol Scand 142:97-103.

Bartos M, Vida I, Jonas P (2007) Synaptic mechanisms of synchronized gamma oscillations in inhibitory interneuron networks. Nat Rev Neurosci 8:45-56.

Bauer EP, Paz R, Pare D (2007) Gamma oscillations coordinate amygdalo-rhinal interactions during learning. J Neurosci 27:9369-9379.

Boddeke HW, Best R, Boeijinga PH (1997) Synchronous 20 Hz rhythmic activity in hippocampal networks induced by activation of metabotropic glutamate receptors in vitro. Neuroscience 76:653-658.

Buzsaki G, Buhl DL, Harris KD, Csicsvari J, Czeh B, Morozov A (2003) Hippocampal network patterns of activity in the mouse. Neuroscience 116:201-211.

Capogna M, Gahwiler BH, Thompson SM (1996) Presynaptic inhibition of calcium-dependent and -independent release elicited with ionomycin, gadolinium, and alpha-latrotoxin in the hippocampus. J Neurophysiol 75:2017-2028.

Chavez-Noriega LE, Stevens CF (1994) Increased transmitter release at excitatory synapses produced by direct activation of adenylate cyclase in rat hippocampal slices. J Neurosci 14:310-317.

Chen X, Johnston D (2005) Constitutively active G-protein-gated inwardly rectifying K+ channels in dendrites of hippocampal CA1 pyramidal neurons. J Neurosci 25:3787-3792.

Cognato GP, Agostinho PM, Hockemeyer J, Muller CE, Souza DO, Cunha RA (2010) Caffeine and an adenosine A(2A) receptor antagonist prevent memory impairment and synaptotoxicity in adult rats triggered by a convulsive episode in early life. J Neurochem 112:453-462.

Corodimas KP, Tomita H (2001) Adenosine A1 receptor activation selectively impairs the acquisition of contextual fear conditioning in rats. Behav Neurosci 115:1283-1290.

Csicsvari J, Jamieson B, Wise KD, Buzsaki G (2003) Mechanisms of gamma oscillations in the hippocampus of the behaving rat. Neuron 37:311-322.

Cunha RA (2001) Adenosine as a neuromodulator and as a homeostatic regulator in the nervous system: different roles, different sources and different receptors. Neurochem Int 38:107-125.

Cunha RA, Johansson B, van dP, I, Sebastiao AM, Ribeiro JA, Fredholm BB (1994) Evidence for functionally important adenosine A2a receptors in the rat hippocampus. Brain Res 649:208-216.

Cunha RA, Ribeiro JA (2000) Adenosine A2A receptor facilitation of synaptic transmission in the CA1 area of the rat hippocampus requires protein kinase C but not protein kinase A activation. Neurosci Lett 289:127-130.

Dale N, Pearson T, Frenguelli BG (2000) Direct measurement of adenosine release during hypoxia in the CA1 region of the rat hippocampal slice. J Physiol 526 Pt 1:143-155.

Dickinson R, Awaiz S, Whittington MA, Lieb WR, Franks NP (2003) The effects of general anaesthetics on carbachol-evoked gamma oscillations in the rat hippocampus in vitro. Neuropharmacology 44:864-872.

Driver JE, Racca C, Cunningham MO, Towers SK, Davies CH, Whittington MA, Lebeau FE (2007) Impairment of hippocampal gamma-frequency oscillations in vitro in mice overexpressing human amyloid precursor protein (APP). Eur J Neurosci 26:1280-1288.

Dunwiddie TV, Diao L (1994) Extracellular adenosine concentrations in hippocampal brain slices and the tonic inhibitory modulation of evoked excitatory responses. J Pharmacol Exp Ther 268:537-545.

Dunwiddie TV, Diao L, Proctor WR (1997) Adenine nucleotides undergo rapid, quantitative conversion to adenosine in the extracellular space in rat hippocampus. J Neurosci 17:7673-7682.

Dunwiddie TV, Masino SA (2001) The role and regulation of adenosine in the central nervous system. Annu Rev Neurosci 24:31-55.

Engel AK, Singer W (2001) Temporal binding and the neural correlates of sensory awareness. Trends Cogn Sci 5:16-25.

Etherington LA, Patterson GE, Meechan L, Boison D, Irving AJ, Dale N, Frenguelli BG (2009) Astrocytic adenosine kinase regulates basal synaptic adenosine levels and seizure activity

but not activity-dependent adenosine release in the hippocampus. Neuropharmacology 56:429-437.

Fano S, Behrens CJ, Heinemann U (2007) Hypoxia suppresses kainate-induced gamma-oscillations in rat hippocampal slices. Neuroreport 18:1827-1831.

Fell J, Klaver P, Lehnertz K, Grunwald T, Schaller C, Elger CE, Fernandez G (2001) Human memory formation is accompanied by rhinal-hippocampal coupling and decoupling. Nat Neurosci 4:1259-1264.

Fisahn A (2005) Kainate receptors and rhythmic activity in neuronal networks: hippocampal gamma oscillations as a tool. J Physiol 562:65-72.

Fisahn A, Pike FG, Buhl EH, Paulsen O (1998) Cholinergic induction of network oscillations at 40 Hz in the hippocampus in vitro. Nature 394:186-189.

Foskett A, Ali A, Gant N (2009) Caffeine enhances cognitive function and skill performance during simulated soccer activity. Int J Sport Nutr Exerc Metab 19:410-423.

Fredholm BB (2010) Adenosine receptors as drug targets. Exp Cell Res 316:1284-1288.

Fredholm BB, Battig K, Holmen J, Nehlig A, Zvartau EE (1999) Actions of caffeine in the brain with special reference to factors that contribute to its widespread use. Pharmacol Rev 51:83-133.

Fredholm BB, Chen JF, Cunha RA, Svenningsson P, Vaugeois JM (2005) Adenosine and brain function. Int Rev Neurobiol 63:191-270.

Fredholm BB, IJzerman AP, Jacobson KA, Klotz KN, Linden J (2001) International Union of Pharmacology. XXV. Nomenclature and classification of adenosine receptors. Pharmacol Rev 53:527-552.

Frenguelli BG, Llaudet E, Dale N (2003) High-resolution real-time recording with microelectrode biosensors reveals novel aspects of adenosine release during hypoxia in rat hippocampal slices. J Neurochem 86:1506-1515.

Freund TF, Buzsaki G (1996) Interneurons of the hippocampus. Hippocampus 6:347-470.

Fries P, Nikolic D, Singer W (2007) The gamma cycle. Trends Neurosci 30:309-316.

Fries P, Reynolds JH, Rorie AE, Desimone R (2001) Modulation of oscillatory neuronal synchronization by selective visual attention. Science 291:1560-1563.

Fuchs EC, Zivkovic AR, Cunningham MO, Middleton S, Lebeau FE, Bannerman DM, Rozov A, Whittington MA, Traub RD, Rawlins JN, Monyer H (2007) Recruitment of parvalbumin-positive interneurons determines hippocampal function and associated behavior. Neuron 53:591-604.

Greene RW, Haas HL (1985) Adenosine actions on CA1 pyramidal neurones in rat hippocampal slices. J Physiol 366:119-127.

Guillen-Gomez E, Calbet M, Casado J, de LL, Soriano E, Pastor-Anglada M, Burgaya F (2004) Distribution of CNT2 and ENT1 transcripts in rat brain: selective decrease of CNT2 mRNA in the cerebral cortex of sleep-deprived rats. J Neurochem 90:883-893.

Haas HL, Selbach O (2000) Functions of neuronal adenosine receptors. Naunyn Schmiedebergs Arch Pharmacol 362:375-381.

Haas M, Forbush B, III (1998) The Na-K-Cl cotransporters. J Bioenerg Biomembr 30:161-172.

Hajos M, Hoffmann WE, Robinson DD, Yu JH, Hajos-Korcsok E (2003) Norepinephrine but not serotonin reuptake inhibitors enhance theta and gamma activity of the septo-hippocampal system. Neuropsychopharmacology 28:857-864.

Hajos N, Palhalmi J, Mann EO, Nemeth B, Paulsen O, Freund TF (2004) Spike timing of distinct types of GABAergic interneuron during hippocampal gamma oscillations in vitro. J Neurosci 24:9127-9137.

Hajos N, Paulsen O (2009) Network mechanisms of gamma oscillations in the CA3 region of the hippocampus. Neural Netw 22:1113-1119.

Hauber W, Bareiss A (2001) Facilitative effects of an adenosine A1/A2 receptor blockade on spatial memory performance of rats: selective enhancement of reference memory retention during the light period. Behav Brain Res 118:43-52.

Herrmann CS, Munk MH, Engel AK (2004) Cognitive functions of gamma-band activity: memory match and utilization. Trends Cogn Sci 8:347-355.

Hogervorst E, Bandelow S, Schmitt J, Jentjens R, Oliveira M, Allgrove J, Carter T, Gleeson M (2008) Caffeine improves physical and cognitive performance during exhaustive exercise. Med Sci Sports Exerc 40:1841-1851.

Hosli L, Hosli E, Uhr M, Della BG (1987) Electrophysiological evidence for adenosine receptors on astrocytes of cultured rat central nervous system. Neurosci Lett 79:108-112.

Huber A, Padrun V, Deglon N, Aebischer P, Mohler H, Boison D (2001) Grafts of adenosine-releasing cells suppress seizures in kindling epilepsy. Proc Natl Acad Sci U S A 98:7611-7616.

Huchzermeyer C, Albus K, Gabriel HJ, Otahal J, Taubenberger N, Heinemann U, Kovacs R, Kann O (2008) Gamma oscillations and spontaneous network activity in the hippocampus are highly sensitive to decreases in pO2 and concomitant changes in mitochondrial redox state. J Neurosci 28:1153-1162.

Huston JP, Haas HL, Boix F, Pfister M, Decking U, Schrader J, Schwarting RK (1996) Extracellular adenosine levels in neostriatum and hippocampus during rest and activity periods of rats. Neuroscience 73:99-107.

Jarvis MF, Schulz R, Hutchison AJ, Do UH, Sills MA, Williams M (1989) [3H]CGS 21680, a selective A2 adenosine receptor agonist directly labels A2 receptors in rat brain. J Pharmacol Exp Ther 251:888-893.

Jutras MJ, Fries P, Buffalo EA (2009) Gamma-band synchronization in the macaque hippocampus and memory formation. J Neurosci 29:12521-12531.

Kirk IJ, Mackay JC (2003) The role of theta-range oscillations in synchronising and integrating activity in distributed mnemonic networks. Cortex 39:993-1008.

Klotz KN (2000) Adenosine receptors and their ligands. Naunyn Schmiedebergs Arch Pharmacol 362:382-391.

Kopf SR, Melani A, Pedata F, Pepeu G (1999) Adenosine and memory storage: effect of A(1) and A(2) receptor antagonists. Psychopharmacology (Berl) 146:214-219.

Latini S, Bordoni F, Pedata F, Corradetti R (1999) Extracellular adenosine concentrations during in vitro ischaemia in rat hippocampal slices. Br J Pharmacol 127:729-739.

Latini S, Pedata F (2001) Adenosine in the central nervous system: release mechanisms and extracellular concentrations. J Neurochem 79:463-484.

Lei Q, Jones MB, Talley EM, Garrison JC, Bayliss DA (2003) Molecular mechanisms mediating inhibition of G protein-coupled inwardly-rectifying K+ channels. Mol Cells 15:1-9.

Li H, Henry JL (2000) Adenosine action on interneurons and synaptic transmission onto interneurons in rat hippocampus in vitro. Eur J Pharmacol 407:237-244.

Lloyd HG, Fredholm BB (1995) Involvement of adenosine deaminase and adenosine kinase in regulating extracellular adenosine concentration in rat hippocampal slices. Neurochem Int 26:387-395.

Lopes LV, Cunha RA, Ribeiro JA (1999) Cross talk between A(1) and A(2A) adenosine receptors in the hippocampus and cortex of young adult and old rats. J Neurophysiol 82:3196-3203.

Lorist MM, Tops M (2003) Caffeine, fatigue, and cognition. Brain Cogn 53:82-94.

Luscher C, Jan LY, Stoffel M, Malenka RC, Nicoll RA (1997) G protein-coupled inwardly rectifying K+ channels (GIRKs) mediate postsynaptic but not presynaptic transmitter actions in hippocampal neurons. Neuron 19:687-695.

Lynch MA (2004) Long-term potentiation and memory. Physiol Rev 84:87-136.

Mackiewicz M, Nikonova EV, Zimmermann JE, Romer MA, Cater J, Galante RJ, Pack AI (2006) Age-related changes in adenosine metabolic enzymes in sleep/wake regulatory areas of the brain. Neurobiol Aging 27:351-360.

Middleton S, Jalics J, Kispersky T, Lebeau FE, Roopun AK, Kopell NJ, Whittington MA, Cunningham MO (2008) NMDA receptor-dependent switching between different gamma rhythm-generating microcircuits in entorhinal cortex. Proc Natl Acad Sci U S A 105:18572-18577.

Mogul DJ, Adams ME, Fox AP (1993) Differential activation of adenosine receptors decreases N-type but potentiates P-type Ca2+ current in hippocampal CA3 neurons. Neuron 10:327-334.

Montgomery SM, Buzsaki G (2007) Gamma oscillations dynamically couple hippocampal CA3 and CA1 regions during memory task performance. Proc Natl Acad Sci U S A 104:14495-14500.

Montgomery SM, Sirota A, Buzsaki G (2008) Theta and gamma coordination of hippocampal networks during waking and rapid eye movement sleep. J Neurosci 28:6731-6741.

Ochiishi T, Chen L, Yukawa A, Saitoh Y, Sekino Y, Arai T, Nakata H, Miyamoto H (1999) Cellular localization of adenosine A1 receptors in rat forebrain: immunohistochemical analysis using adenosine A1 receptor-specific monoclonal antibody. J Comp Neurol 411:301-316.

Palhalmi J, Paulsen O, Freund TF, Hajos N (2004) Distinct properties of carbachol- and DHPG-induced network oscillations in hippocampal slices. Neuropharmacology 47:381-389.

Paxinos G, Watson C (1998) The rat brain in stereotaxic coordinates fourth edition.

Pereira GS, Mello e Souza, Vinade ER, Choi H, Rodrigues C, Battastini AM, Izquierdo I, Sarkis JJ, Bonan CD (2002) Blockade of adenosine A1 receptors in the posterior cingulate cortex facilitates memory in rats. Eur J Pharmacol 437:151-154.

Pietersen AN, Lancaster DM, Patel N, Hamilton JB, Vreugdenhil M (2009a) Modulation of gamma oscillations by endogenous adenosine through A1 and A2A receptors in the mouse hippocampus. Neuropharmacology 56:481-492.

Pietersen AN, Patel N, Jefferys JG, Vreugdenhil M (2009b) Comparison between spontaneous and kainate-induced gamma oscillations in the mouse hippocampus in vitro. Eur J Neurosci 29:2145-2156.

Rasmussen T, Schliemann T, Sorensen JC, Zimmer J, West MJ (1996) Memory impaired aged rats: no loss of principal hippocampal and subicular neurons. Neurobiol Aging 17:143-147.

Rebola N, Pinheiro PC, Oliveira CR, Malva JO, Cunha RA (2003) Subcellular localization of adenosine A(1) receptors in nerve terminals and synapses of the rat hippocampus. Brain Res 987:49-58.

Rosenzweig ES, Barnes CA (2003) Impact of aging on hippocampal function: plasticity, network dynamics, and cognition. Prog Neurobiol 69:143-179.

Ryan L, Hatfield C, Hofstetter M (2002) Caffeine reduces time-of-day effects on memory performance in older adults. Psychol Sci 13:68-71.

Scanziani M, Capogna M, Gahwiler BH, Thompson SM (1992) Presynaptic inhibition of miniature excitatory synaptic currents by baclofen and adenosine in the hippocampus. Neuron 9:919-927.

Sebastiao AM, Cunha RA, de MA, Ribeiro JA (2000) Modification of adenosine modulation of synaptic transmission in the hippocampus of aged rats. Br J Pharmacol 131:1629-1634.

Sebastiao AM, Ribeiro JA (1996) Adenosine A2 receptor-mediated excitatory actions on the nervous system. Prog Neurobiol 48:167-189.

Sebastiao AM, Ribeiro JA (2000) Fine-tuning neuromodulation by adenosine. Trends Pharmacol Sci 21:341-346.

Singer W (1993) Synchronization of cortical activity and its putative role in information processing and learning. Annu Rev Physiol 55:349-374.

Sperlagh B, Zsilla G, Baranyi M, Kekes-Szabo A, Vizi ES (1997) Age-dependent changes of presynaptic neuromodulation via A1-adenosine receptors in rat hippocampal slices. Int J Dev Neurosci 15:739-747.

Swanson TH, Drazba JA, Rivkees SA (1995) Adenosine A1 receptors are located predominantly on axons in the rat hippocampal formation. J Comp Neurol 363:517-531.

Tabata T, Kawakami D, Hashimoto K, Kassai H, Yoshida T, Hashimotodani Y, Fredholm BB, Sekino Y, Aiba A, Kano M (2007) G protein-independent neuromodulatory action of adenosine on metabotropic glutamate signalling in mouse cerebellar Purkinje cells. J Physiol 581:693-708.

Takigawa T, Alzheimer C (2002) Phasic and tonic attenuation of EPSPs by inward rectifier K+ channels in rat hippocampal pyramidal cells. J Physiol 539:67-75.

Thompson SM, Haas HL, Gahwiler BH (1992) Comparison of the actions of adenosine at pre- and postsynaptic receptors in the rat hippocampus in vitro. J Physiol 451:347-363.

Trevino M, Vivar C, Gutierrez R (2007) Beta/gamma oscillatory activity in the CA3 hippocampal area is depressed by aberrant GABAergic transmission from the dentate gyrus after seizures. J Neurosci 27:251-259.

Von Lubitz DK, Paul IA, Bartus RT, Jacobson KA (1993) Effects of chronic administration of adenosine A1 receptor agonist and antagonist on spatial learning and memory. Eur J Pharmacol 249:271-280.

Vreugdenhil M, Toescu EC (2005) Age-dependent reduction of gamma oscillations in the mouse hippocampus in vitro. Neuroscience 132:1151-1157.

Wall M, Dale N (2008) Activity-dependent release of adenosine: a critical re-evaluation of mechanism. Curr Neuropharmacol 6:329-337.

Wall MJ, Atterbury A, Dale N (2007) Control of basal extracellular adenosine concentration in rat cerebellum. J Physiol 582:137-151.

Wall MJ, Dale N (2007) Auto-inhibition of rat parallel fibre-Purkinje cell synapses by activity-dependent adenosine release. J Physiol 581:553-565.

Winn HR, Rubio R, Berne RM (1981) Brain adenosine concentration during hypoxia in rats. Am J Physiol 241:H235-H242.

Wu LG, Saggau P (1994) Adenosine inhibits evoked synaptic transmission primarily by reducing presynaptic calcium influx in area CA1 of hippocampus. Neuron 12:1139-1148.

Yoon KW, Rothman SM (1991) Adenosine inhibits excitatory but not inhibitory synaptic transmission in the hippocampus. J Neurosci 11:1375-1380.